AN ABSTRACT OF THE THESIS OF

Denise E. L. Giles for the degree of Master of Science in Geology presented on January 23, 2009.

Title: Dynamics of a Long-lived Magmatic System as Indicated by Variations in Amphibole Composition and Textures in Dacites Erupted over 11 M.y. at the Aucanquilcha Volcanic Cluster, Central Andes, Chile

Abstract Approved:

Anita L. Grunder

The Aucanquilcha Volcanic Cluster (AVC) is the erupted part of a magmatic system with a complex and long-lived history. The AVC lies at 21°S in the high Andes and is built on thick continental crust. The thick crust in the area combined with the prolonged magmatic activity make it an excellent natural laboratory for examining long-term evolution of a continental arc volcanic system. The eruptive products deposited over the last 11 million years of volcanic activity preserve snapshots of the developing, dominantly dacitic, magmatic system and gives indications of the processes occurring at depth. In this study, the textural and compositional diversity of amphiboles from selected dacites inform the development of the intensive magmatic parameters including pressure, temperature and volatile content, during the protracted magmatism observed at the AVC.

There are 4 dominant amphibole compositions erupted at the AVC, higher aluminum magnesiohastingsite, pargasite, and tschermakite and the relatively low aluminum magnesiohornblende, using the nomenclature of Leake et al., 1997. Amphiboles in early erupted dacites (11-8 Ma) occur in two compositionally distinct aluminum populations and have diverse textures. During voluminous dacite volcanism

between 6 and 2 Ma, amphiboles are most strongly compositionally zoned, and while still displaying textural diversity, some equilibrium textures common in the early and late stages are rare. In the youngest stage (1-0.24 Ma), amphiboles in many dacites have two compositional populations distinguished by alunimum; equilibrium crystals with thin or no reaction rim are most common in the amphiboles from this stage.

Changes in Cl, F and S and stable isotopes of the system were used as indicators of the evolution of the magmatic system. Fluorine increases in amphiboles over the 11 million year magmatic history independent of amphibole composition, implying a system-wide increase in F. Sulfur and chlorine in amphiboles correlate well with aluminum in amphibole: low aluminum amphiboles have low S (up to 40 ppm), whereas higher aluminum amphiboles had sulfur contents from 70-160 ppm. Amphiboles with lower aluminum have lower Cl contents than amphiboles with higher aluminum.

Coupled amphibole geothermometry and geobarometry are utilized in this study to investigate pressure and temperature of the magmas at the AVC. Amphiboles from the early group are consistent with eruption of dacite from discrete magma batches: some residing at shallow levels of ~1-2 kbar and ~700-800 °C and some deeper at ~4-6.5 kbar and ~750-850 °C. It is interpreted that with time, the dacitic magma reservoir becomes integrated at relatively shallow levels (1.8-3.5 kbar and ~800-900°C). In waning, increasingly silicic stage of volcanism (~1-0.24 Ma), dacite magma is erupted from a shallow and cooler system of ~0.5-1.8kbar and ~700-800 °C.

# Dynamics of a Long-lived Magmatic System as Indicated by Variations in Amphibole Composition and Textures in Dacites Erupted over 11 M.y. at the Aucanquilcha Volcanic Cluster, Central Andes, Chile

by
Denise E. L. Giles

A THESIS

submitted to

Oregon State University

in partial fulfillment of
the requirements for the
degree of

Master of Science

Presented January 23, 2009
Commencement June 2010

Master of Science thesis of Denise E. L. Giles presented on January 23, 2009

APPROVED:

---

Major Professor, representing Geology

---

Chair of the Department of Geosciences

---

Dean of the Graduate School

I understand that my thesis will become part of the permanent collection of Oregon State University libraries. My signature below authorizes release of my thesis to any reader upon request.

---

Denise E. L. Giles, Author

ACKNOWLEDGEMENTS

Thanks to all that helped.

TABLE OF CONTENTS

Page

TABLE OF CONTENTS (Continued)

Page

LIST OF FIGURES

Figure Page

LIST OF FIGURES (Continued)

Figure Page

LIST OF TABLES

LIST OF APPENDICES:

Appendix Page

# Dynamics of a Long-lived Magmatic System as Indicated by Variations in Amphibole Composition and Textures in Dacites Erupted over 11 M.y. at the Aucanquilcha Volcanic Cluster, Central Andes, Chile

**Introduction:**

The Aucanquilcha Volcanic Cluster of northern Chile has been active for the last 11 million years (Grunder et al., 2008). Eruptive products from the 11 million year lifespan of the system give snapshots of intensive parameters of the magma that inform the life-cycle of a long-lived volcanic system. Prolonged activity at a single volcanic cluster provides a natural laboratory for tracking the development and maturation of long-lived magmatic systems as sampled by successive volcanoes. Recent work in the processes related to pluton growth has led to a paradigm shift away from large pots of homogenous magma towards a model of incrementally emplaced plutons (Glazner, 2003, Paterson,1995, Coleman 2003, 2004, Lipman 2007). Some of the questions to ask with respect to long-lived silicic volcanism include: At what depth in the crust is the magma being staged? To what degree is the magma interacting with crust or is it cannibalizing its own plutonic precursors? For how long do these processes occur? How do volatile contents and compositions change over the lifespan of the system?

In this study, I will investigate amphiboles in selected dacites that span the 11 million year history of the system. I build on the major and trace element evolution of the Aucanquilcha Volcanic Cluster (AVC), a long-lived volcanic system in the Central Andes (Grunder et al., 2008) and use amphiboles in dacites as an indicator of the evolution of the entire system. The evolution in textures and composition of amphiboles in dacites from the evolving granitoid plutonic complex are used to infer the pressure,

temperature, and volatile evolution of the plutonic underpinnings as they evolve over the magmatic system's 11 million year history.

By considering the textural and compositional diversity of amphiboles over a restricted bulk composition, I aim to unravel the magmatic conditions that lead to compositional homogeneity but textural heterogeneity. Work on Pinatubo (Holtz, 2005; Scailliet and Evans, 1999), Unzen, Mt. St. Helens (Rutherford and Devine, 1988; Carroll and Wyllie, 1990), as well as studies of synthetic samples and other natural dacite/granodiorite compositions (Naney 1983), have constrained phase relations in compositions similar to the AVC. These studies have shown that amphiboles form at temperatures from 675 to 975 °C , with water contents above 3.75 wt%. An increase in pressure from 200 to 800 MPa expands the stability of amphibole and restricts the pyroxene stability field.

For this study, a temporally representative suite of amphiboles was chosen to track the 11 million year evolution of the system. Texture, composition and volatile content of amphiboles were analyzed as indicators of magmatic conditions at the time of amphibole crystallization and speak to the complex and prolonged magmatic history at the AVC.

**Geologic Setting:**

The Aucanquilcha Volcanic Cluster (AVC) includes ~20 Miocene to recent volcanoes and is located at 21ºS. In this region of northern Chile, the Nazca Plate

subducts below the South American Plate at a rate of ~8mm/yr with a dip angle of approximately 25º (Geise et al., 1998) (Figures 1 & 2). The Aucanquilcha Volcanic Cluster (AVC) is part of the Central Volcanic Zone of the Andes and has been active for ~11 million years (Grunder et al., 2008). Here the continental crust is exceptionally thick (>60km, Geise et al., 1998) and the isotopic character of the volcanic rocks of the Central Volcanic Zone indicates extensive interaction between magma and crust (e.g., Woerner 1988; Davidson, 1992; Schmitz 2001). The AVC sits at the northern boundary of the Altiplano Puna Volcanic Complex, that overlies a magma body as inferred from a seismic low velocity zone (see Zandt et al., 2003). This zone of seismic wave attenuation lies between 17 and 30 km depth and has been linked to a Miocene ignimbrite flare-up in the back-arc region.

The AVC has an areal extent of ~700-$km^2$ and is mainly composed of andesite and dacite lavas (~57 to 69 wt. % $SiO_2$) and a small ash-flow tuff. The eruptive volume of the system is ~327±20 $km^3$ (Figure 3). A majority of this volume was erupted between 6 and 2 Ma as dacite. (Figures 4 & 5) (Table 1). The AVC makes up a calc-alkaline suite, slightly enriched in potassium, but within the range reported for the Central Volcanic Zone. Forty $^{40}Ar/^{39}Ar$ ages for the AVC range from 10.97±0.35 to 0.24±0.05 Ma and define four major, 1-3 million year pulses of volcanism.

The first pulse of magmatism (~11-8 Ma, Alconcha Group) defines a crudely bimodal pyroxene andesite and dacite suite and produced 7 volcanoes (~42$km^3$) and the 4-$km^3$ Ujina Ignimbrite. After a possible two million year hiatus, the second pulse of volcanism (~6-4.2 Ma, Gordo Group) produced at least 5 volcanoes with compositions

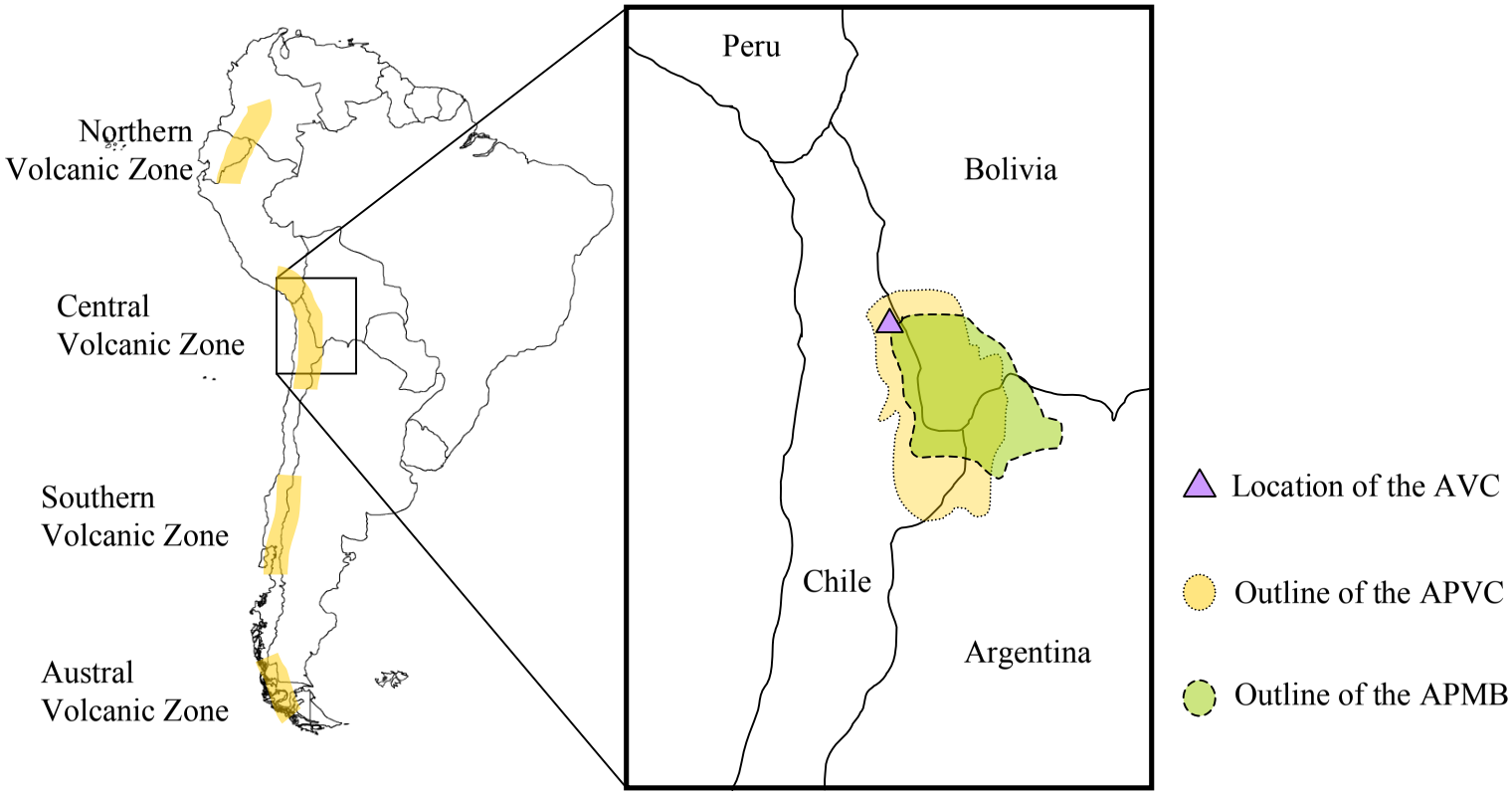


**Figure 1. Location Figure.**
The Aucanquilcha Volcanic Cluster (AVC) includes ~20 Miocene to recent volcanoes and is located at 21ºS in the Central Volcanic Zone of northern Chile. The AVC is one of the northernmost volcanoes of the Altiplano-Puna Volcanic Complex (APVC), and is just beyond the northern boundary of the Altiplano Puna Magma Body (APMB), described by Zandt et al, 2003 as a regional sill-like magma body.

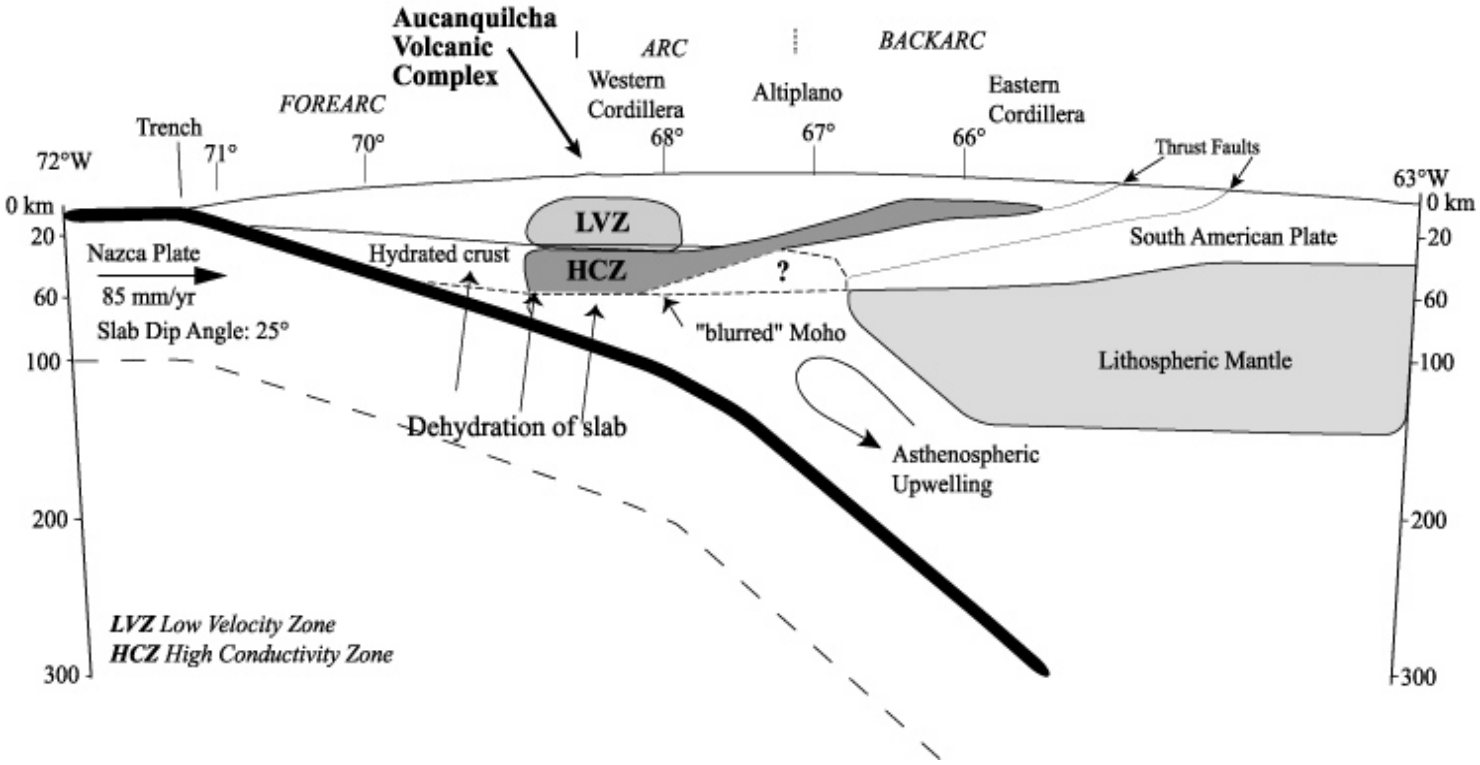


**Figure 2.**
Cross section of the Aucanquilcha Volcanic Cluster after Giese 1999, Schmitz 1999, Scheuber, 1999, Tassara, 2004. The crust in this region is exceptionally thick (>60km), the low velocity zone (LVZ) present at this section of the volcanic arc has been interpreted by others to represent a large magma body or MASH zone at the nearby Altiplano Puna Volcanic Cluster (Swenson, 1999 and deSilva, 2007).

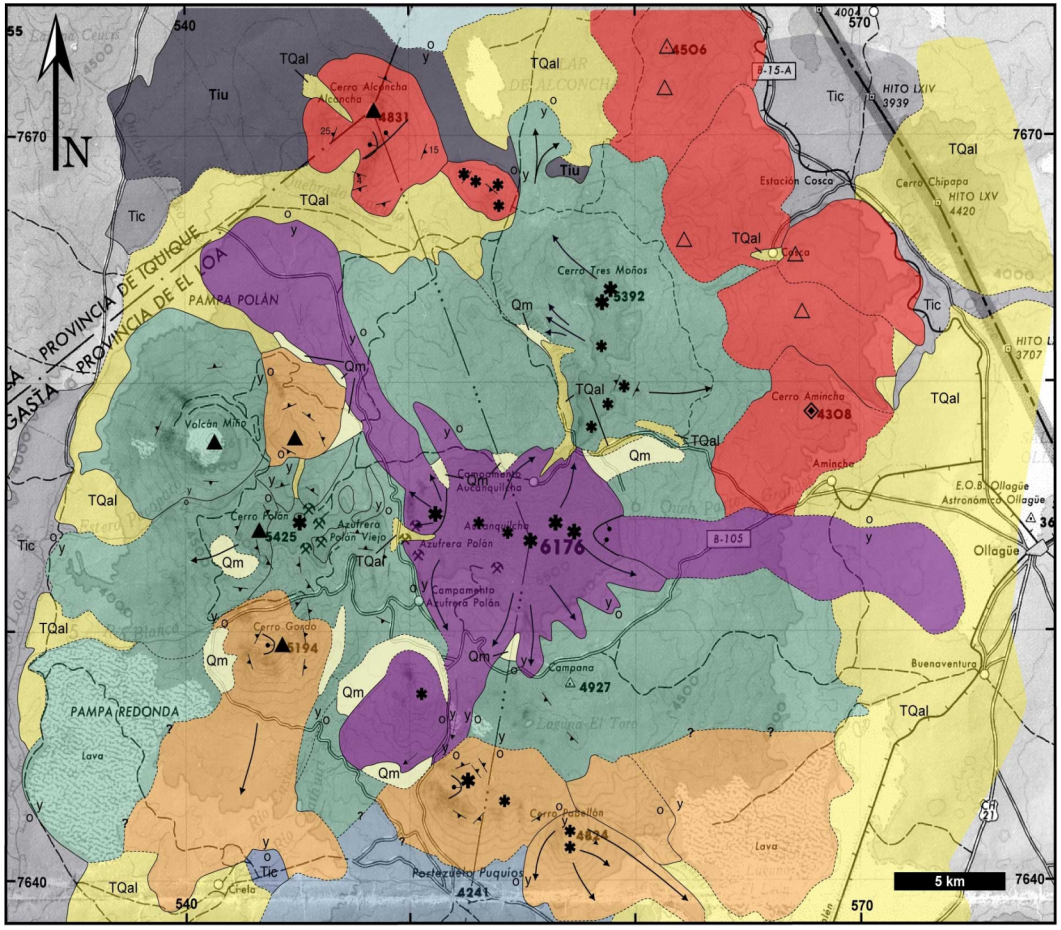


**Figure 3.**

**Map of the Aucanquilcha Volcanic Cluster.**

Simplified map of the AVC as modified from Grunder et al., 2008, by Barry Walker and adapted here. The 11 million year history of the AVC is divided into 4 eruptive stages, each one lasting ~1-4 million years. Red= Alconcha Group (~11-8 Ma), Orange=Gordo Group (~6-4 Ma), Green=Polan Group (~3.4-2Ma), and Aucanquilcha=Purple (~1Ma-recent). Note that the system erupts in a 'bulls-eye' pattern, with the oldest eruptions on the periphery, and the youngest erupted in the center of the volcanic system.

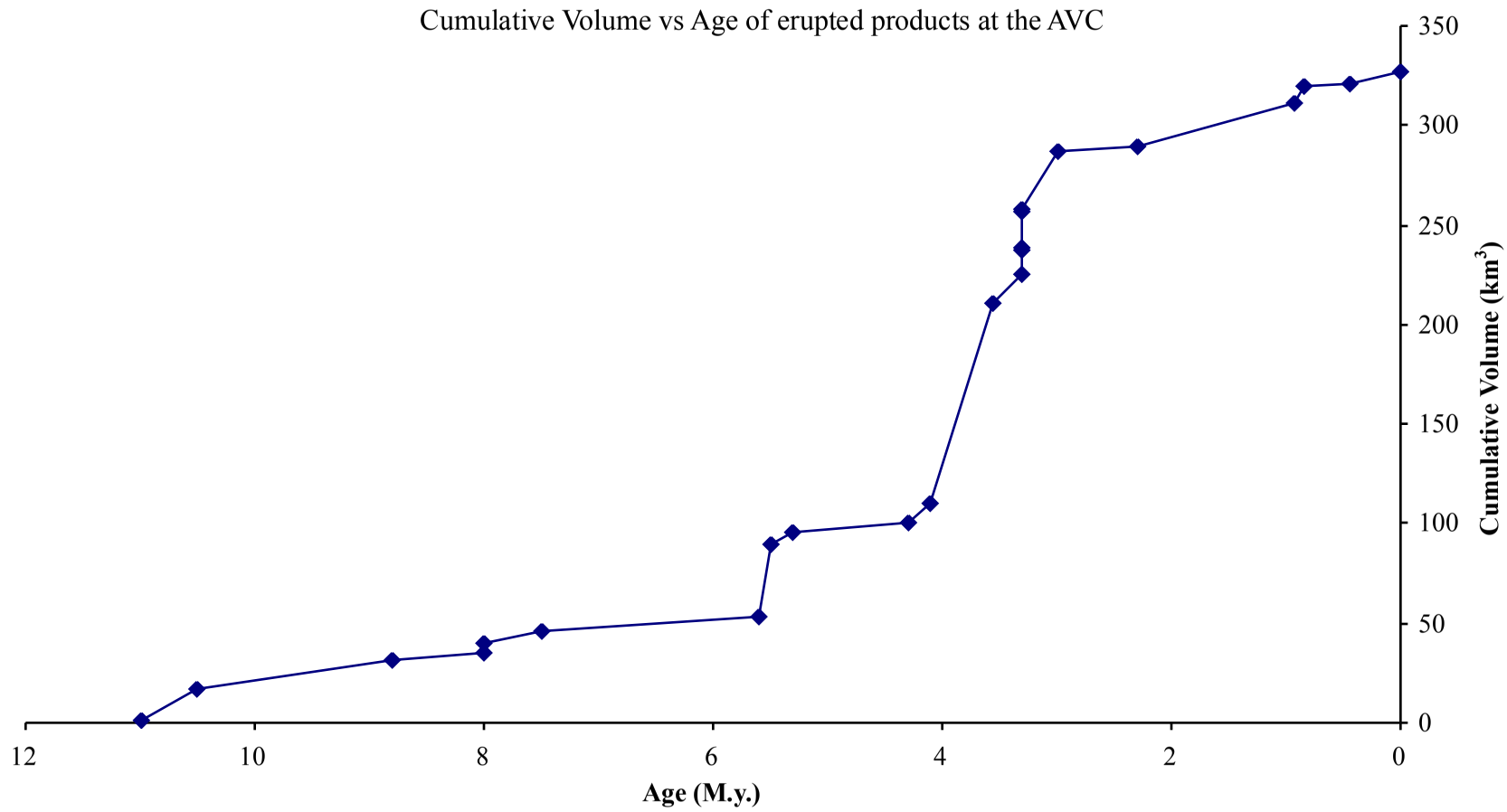


**Figure 4.**

Cumulative volume of erupted material in cubic kilometers versus the age of the erupted samples from the Aucanquilcha Volcani Cluster. The increase in volcanism at 4 million years is coincident with a shift to dominantly dacitic eruptive products with hydrous mineral assemblages.

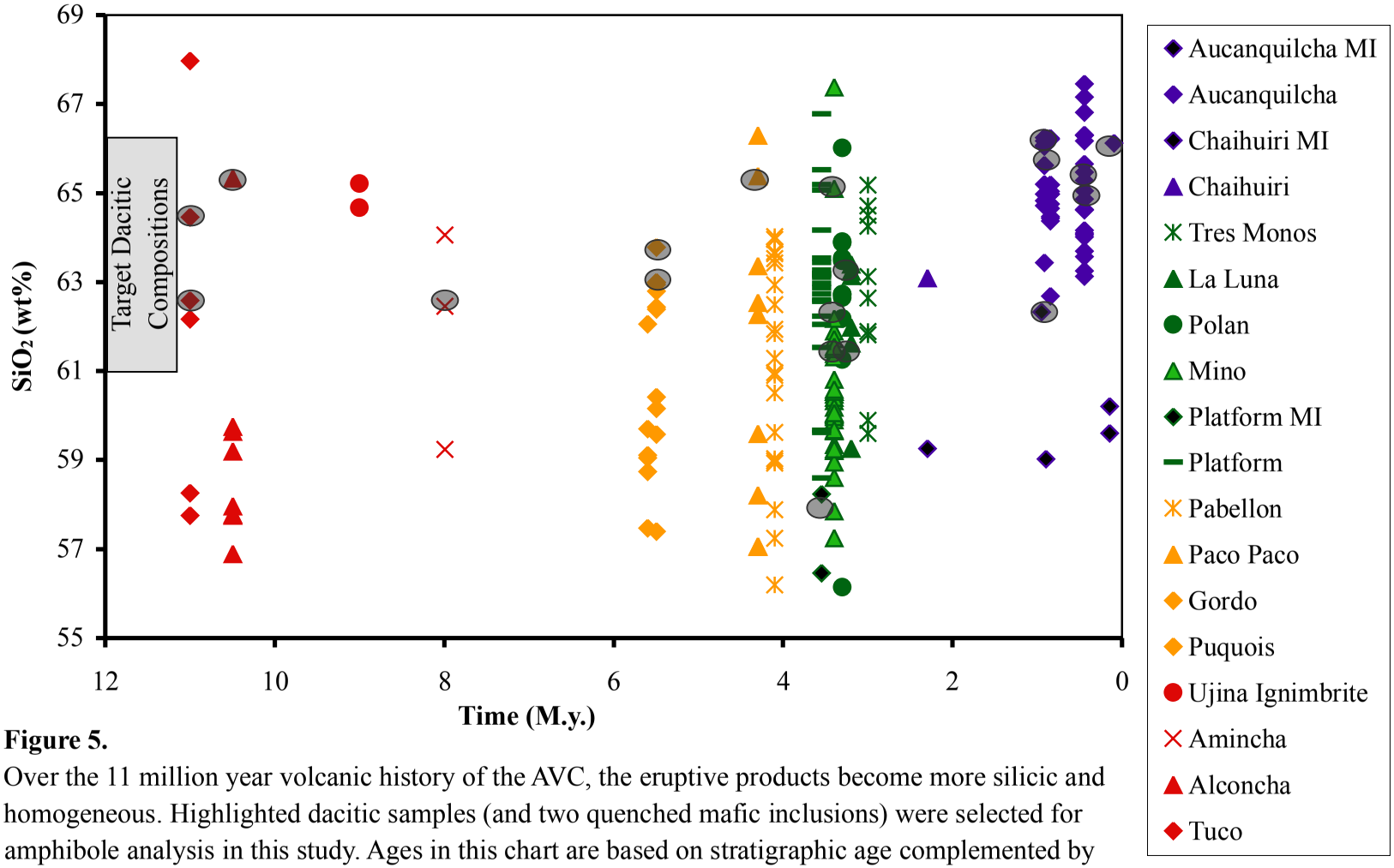


**Figure 5.**

Over the 11 million year volcanic history of the AVC, the eruptive products become more silicic and homogeneous. Highlighted dacitic samples (and two quenched mafic inclusions) were selected for amphibole analysis in this study. Ages in this chart are based on stratigraphic age complemented by $^{40}Ar/^{39}Ar$ age dates. Whole rock data and age relations from Klemetti, 2005.

**Table 1.**

| | Volcanic Center | Approximate Age (M.y.) | Volume ($km^3$) | Cumulative sum ($km^3$) |
|---|---|---|---|---|
| Alconcha Group | Tuco | 11 | 1.1 | 1.1 |
| | Alconcha | 10.5 | 15.7 | 16.8 |
| | Coscalito, Coasa | 8.8 | 14.1 | 30.9 |
| | Ujina Ignimbrite | 8 | 4.5 | 35.4 |
| | Amincha | 7.99 | 4.6 | 40 |
| | Achupella, Inca | 7.5 | 6.4 | 46.4 |
| Gordo Group | Puquois | 5.6 | 6.8 | 53.2 |
| | Gordo | 5.5 | 36.9 | 90.1 |
| | Las Bolitas | 5.3 | 5.5 | 95.6 |
| | Paco Paco | 4.3 | 5.5 | 101.1 |
| | Pabellon | 4.1 | 9.4 | 110.5 |
| Polan Group | Platform | 3.55 | 100 | 210.5 |
| | Mino | 3.3 | 14.5 | 225 |
| | Polan | 3.3 | 12.5 | 237.5 |
| | Pampas | 3.3 | 0.9 | 238.4 |
| | La Luna | 3.3 | 18.7 | 257.1 |
| | Casisca Flow | 3.3 | 0.5 | 257.6 |
| | Tres Monos | 3 | 29.2 | 286.8 |
| Aucanquilcha | Chaihuiri | 2.3 | 3.1 | 289.9 |
| | Azufrera | 0.92 | 21.1 | 311 |
| | Rodado | 0.85 | 9.1 | 320.1 |
| | Cumbre Negro | 0.45 | 0.7 | 320.8 |
| | Angulo | 0.1 | 5.8 | 326.6 |

Age relations are based on Ar/Ar age dates as well as stratigraphic relations and are taken from Grunder et al., 2008.

ranging from pyroxene-bearing andesite to dacite. The third pulse (~3.8-2.0 Ma, Polán Group) represents the most vigorous activity in the history of the AVC, with eruption of at least another 5 volcanoes, broadly distributed in the center of the AVC, and composed dominantly of biotite-amphibole dacite; andesites at this stage occur as magmatic inclusions rather than lavas. Mino, which lies at the periphery of the system is an exception and erupts dominantly andesites. The fourth pulse and most recent activity (1 Ma to recent) is in the center of the AVC at Volcán Aucanquilcha, a potentially active composite volcano made of biotite-two amphibole dacite with andesite and dacite magmatic inclusions.

Four major patterns mark the evolution of the system. 1) The oldest centers occur on the periphery and the younger centers towards the middle of the AVC, creating a bulls-eye pattern of volcanism. 2) the compositions erupted are more homogeneous in time and more silicic. 3) There is an increase in the eruptive volume of material as the system matures and becomes dominantly dacitic. 4) Over time, the mineral assemblage changes from being dominantly anhydrous, two pyroxene+/- olivine with lesser hornblende, to assemblages with abundant amphibole and biotite. (Figure 3 & 6).

Grunder et al. (2008) interpret this progression of anhydrous to hydrous, low volume to voluminous and decreasing age towards the center of the cluster to reflect the growth of an integrated and evolved middle to upper crustal granitoid magma reservoir after several million years of fitful volcanism-similar to that described by Zandt, 1999, for the nearby APVC. The evolutionary succession of the AVC is mimicked by other long-lived intermediate volcanic systems, like eastern-central Nevada (Gans et al., 1989,

**Figure 6.**
Histogram showing the compositional variability in erupted products and their volumes over the 11 million year history of the AVC. The Alconcha group erupts the least volume with greatest variability in $SiO_2$; the dominant mineral assemblage of the Alconcha Group is Ol>px>hb. Through time the mineral assemblages become more hydrous and the erupted material is dominanty dacitic in composition. Note the pulse of dacitic activity a the Polan Group, and the overall increase in wt % $SiO_2$ of the erupted prodcuts of Volcan Aucanquilcha.

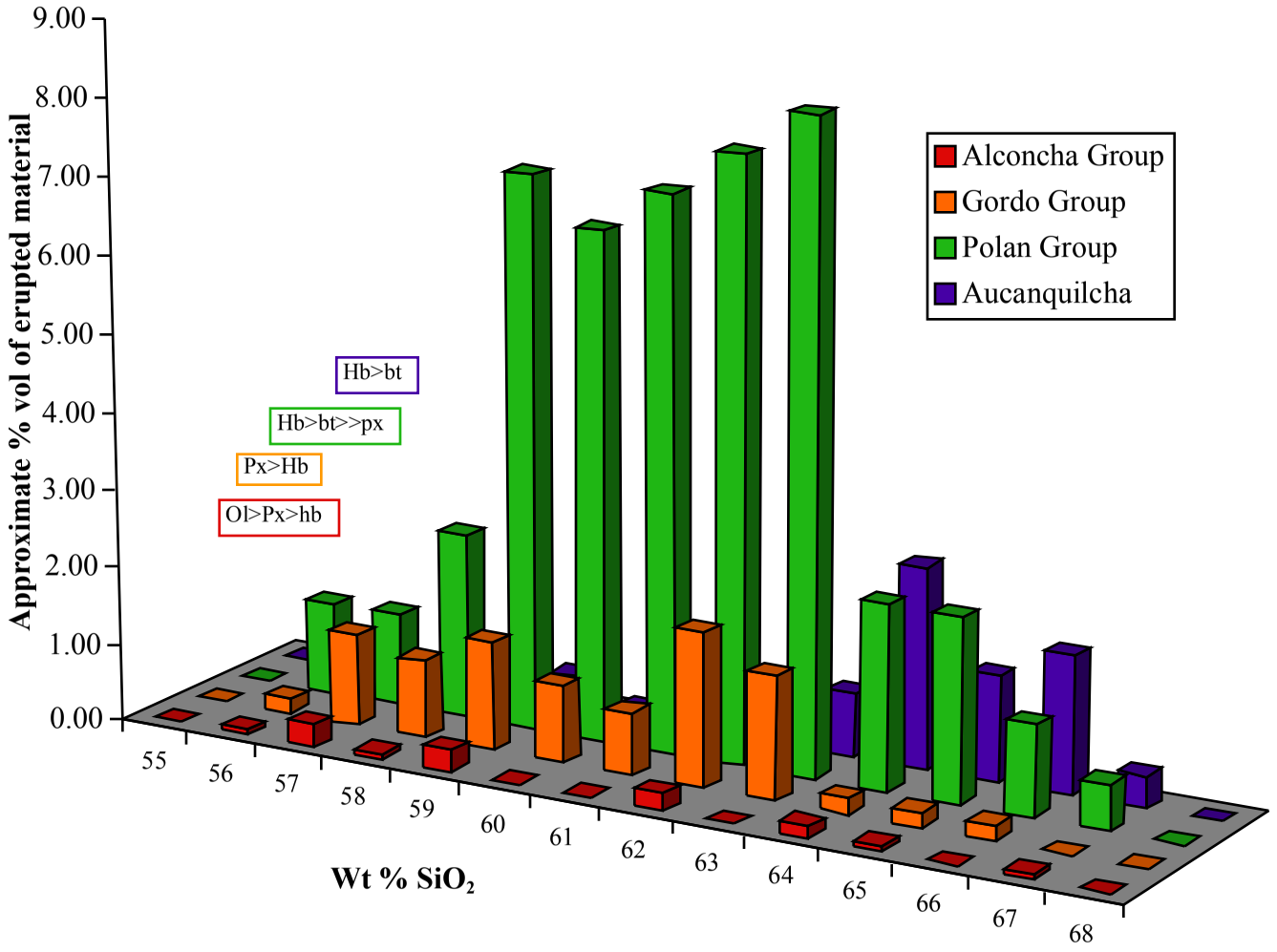

Grunder, 1995) and Yanacocha, Perú (Longo, 2005). The episodic and long-lived history of the AVC also finds an analog in the 10-m.y. history and incremental growth of the Tuolumne Intrusive Series (Coleman et al., 2004; Glazner et al., 2004) (Figures 7 & 8).

**Approaches to the problem:**

Dacitic compositions are erupted over the entire 11 million year history of the AVC, and were thus selected for investigation. In addition the onset of dominantly dacitic eruptions coincides with an increase in the volume of eruptive material. In this study I look at amphiboles at this restricted bulk composition to determine the evolution of dacite magmas over the 11 million year history of the volcanic system. Whole rock and modal variability in the volcanic systems are combined with variations in amphibole composition, texture and volatile content, to track the depth and temperature at which dacites are forming and to infer the evolution of the magmatic underpinnings of the Aucanquilcha Volcanic Cluster.

***Changes in whole rock composition and eruptive volume:***

The evolution of the dacites over time are combined with the known eruptive history of the system. Changes in bulk composition and volume of eruptive products can be correlated to the dacitic history determined in this study from amphiboles. Changes in the eruptive volume of a system can be used as a proxy for the heat budget of the system. Homogenization over time of the erupted products implies an amalgamation of magma inputs and crustal melts, or some other MASH-type process (Melting, Assimilation,

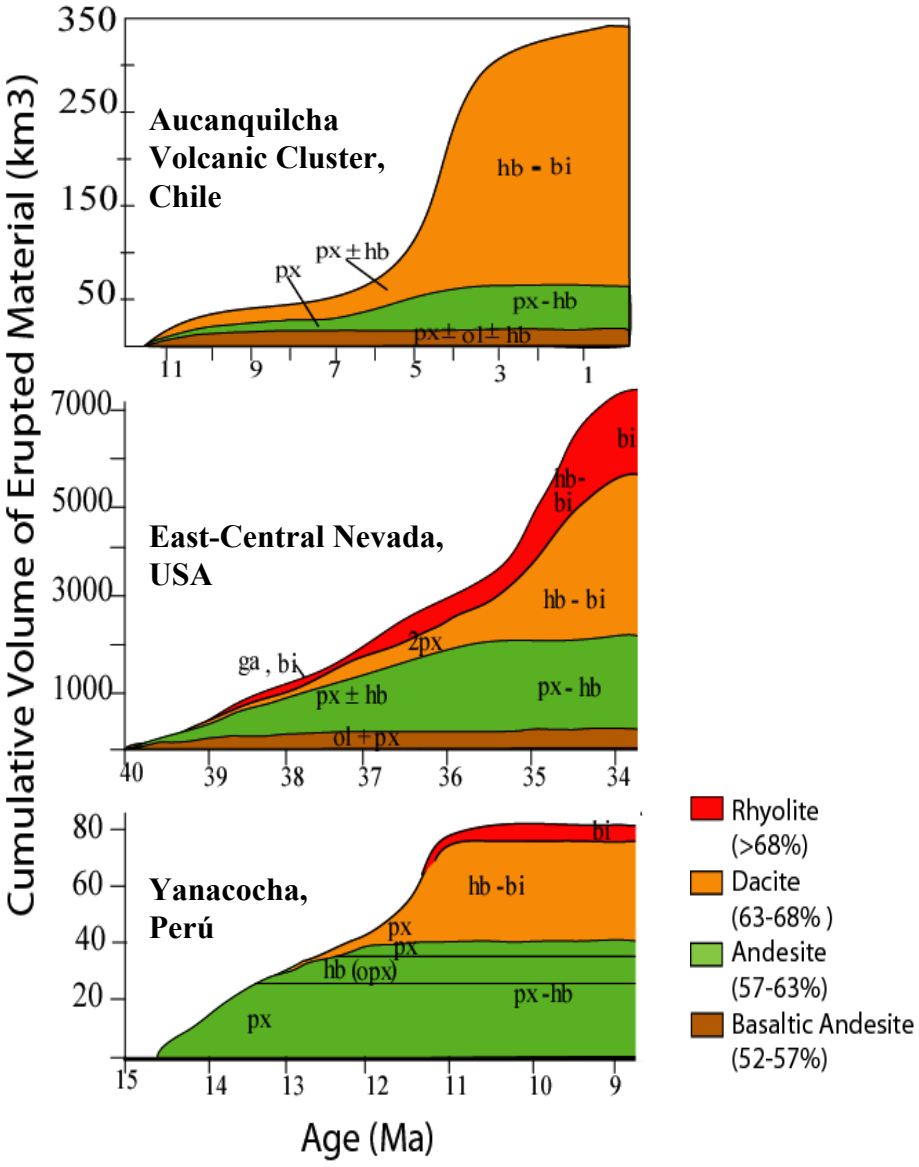


**Figure 7.**
Cumulative eruptive volume of the AVC compared to analogous intermediate volcanic systems including East-Central Nevada and Yanacocha, Peru. (Data from Grunder, 1995 & 2008, and Longo 2005.) In all three systems, the increase in eruptive volume is associated with an increase in the eruption of dacitic compositions, and a transition to a more hydrous mineral assemblage.

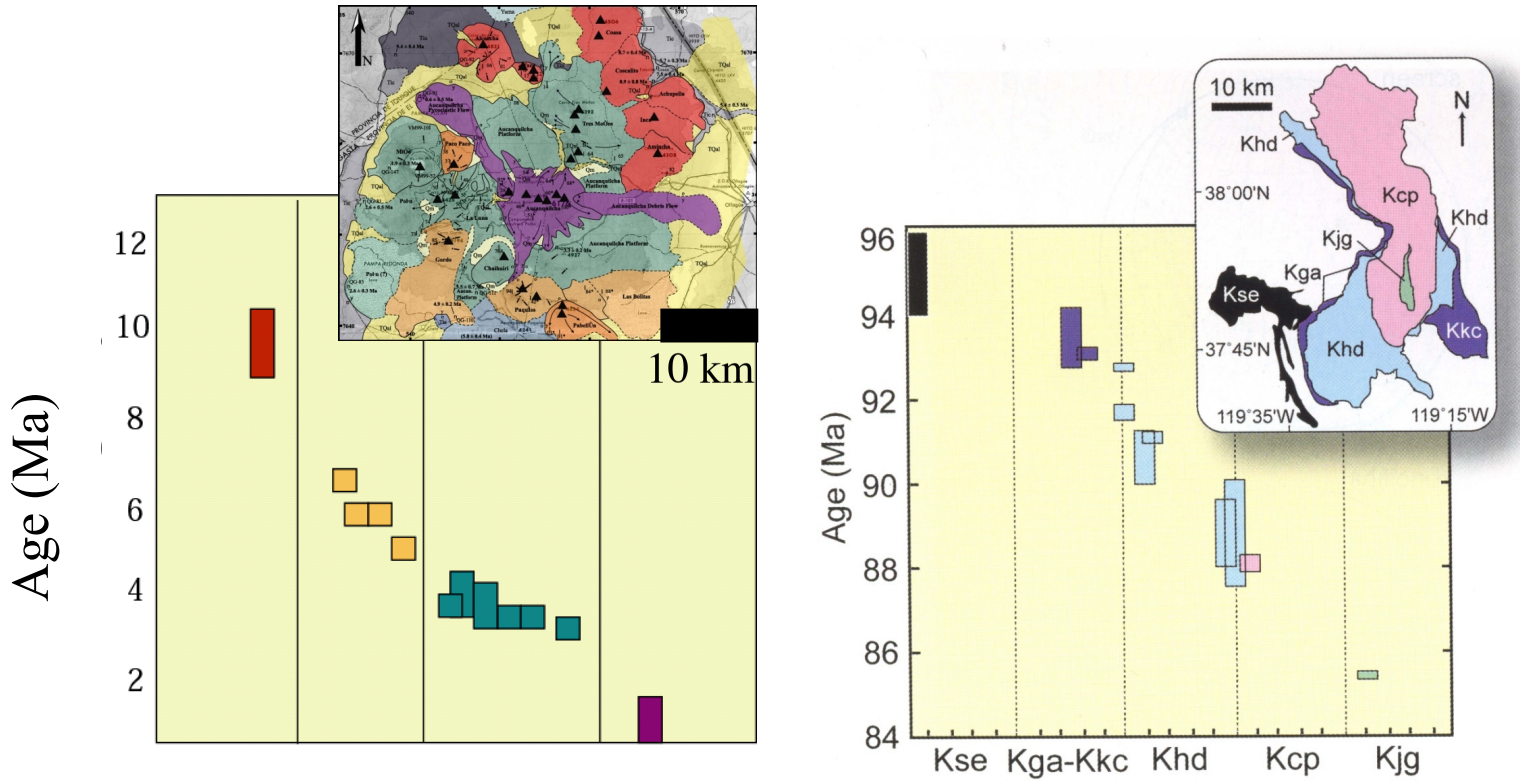


**Figure 8.**
Footprint and relative timing of the AVC compared to the Tuolemne Intrusive Series. Note the similarity in size as well as lifespan of the volcanic systems. The implication is that the AVC is showing the 'extrusive' behavior of batholith formation, whereas the TIS shows the growth and evolution of the long-lived magmatic system at depth (Glazner, 2003; Grunder, 2008).

Storage and Homogenization), which leads to the homogenization of the magma source. It remains unclear whether the apparent density cap present in the Polan Group forms as a function of repeated (but disconnected) magmatic pulses which results in an area of thermally mature and similar crust, or if there is actually a large liquid silicic reservoir.

***Amphibole compositions:***

The general formula for an amphibole is $A_{(0-2)}B_2C_5T_8O_{22}(OH, F, Cl)_2$. Common cations for each site are listed below.

A site: empty, Na, K

B site: Ca, Na

C site: $Al^{VI}$, Ti, Cr, $Fe^{2+3+}$, Mn, Mg

T site: Si, $Al^{IV}$

Variations in the complex structure of amphibole can be taken as indicators of the pressure, temperature, composition and $fO_2$. Zoned amphiboles most likely record convecting or pulsing within a chamber with amphibole stable conditions (Femenias, 2006). Compositionally diverse amphiboles within a sample imply stalling or mixing of magmas within the magmatic plumbing system. Variations in amphibole composition from the core to rim may indicate the effects of degassing, crystallization or mixing of magmas.

### *Amphibole textures, mode size and habit:*

**Texture:**

Variations in the presence and thicknesses of reaction rims on amphiboles, as well as the presence of completely reacted amphiboles can be used as indicators of the time that the amphibole-bearing dacitic magmas experienced in or out of equilibrium (Browne, 2006). Abundant disequilibrium textures imply changes in pressure, temperature and water content of the magma after the crystallization of amphibole. Work on amphiboles from Mt. St. Helens has shown the amount of time needed to form rims on amphiboles is on the order of days to weeks (Rutherford and Devine, 1988). Abundant equilibrium textures will imply that amphibole-bearing dacites travel quickly to the surface and experience less time out of equilibrium. Textural heterogeneity implies mixing and/or stalling of magmas.

**Mode:**

Phase equilibrium of granodioritic compositions similar to the AVC have been constrained by Naney (Figure 9). Observed mineral assemblages can be compared to these phase diagrams to estimate ranges of temperatures and water content of the parent magmas.

**Size and habit:**

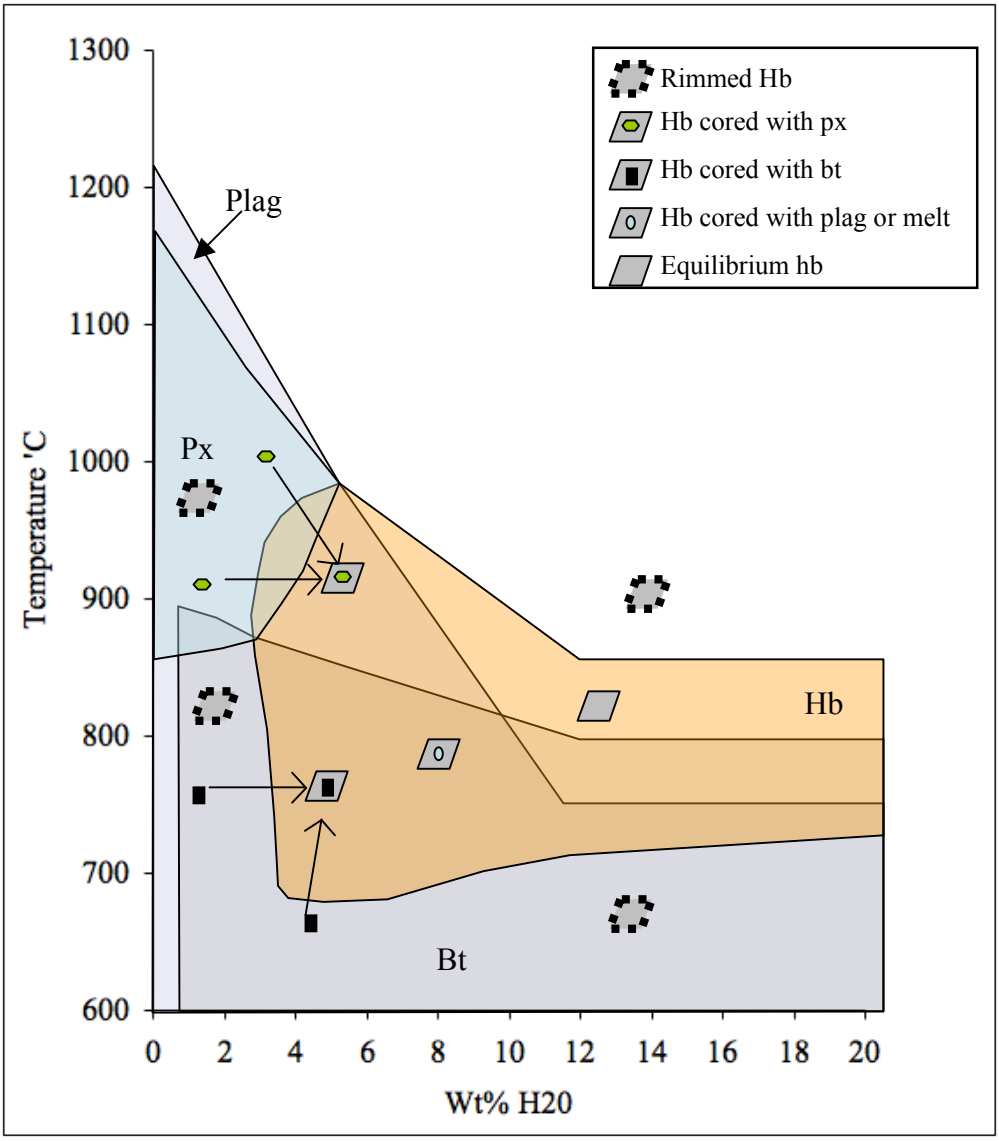


**Figure 9. Simplified phase stability diagram of a granodiorite composition at 800MPa after Naney, 1983.**
Px=pyroxene, Plag=Plagioclase, Hb=Hornblende (amphibole) and Bt=Biotite. Equilibrium amphiboles form within the amphibole stability range. Amphiboles cored with pyroxene may form by either a decrease in temperature or an increase in water. Hornblendes cored with biotite may form with increases in water or temperature. Amphiboles cored with plagioclase or melt may form over a wide range of magmatic conditions. Rimmed amphiboles form in various magmatic conditions; the composition of the rim is important in determining the magmatic conditions which contributed to rim formation which could include, increases or decreases in temperature, or decreases in water content.

Mineral size and crystal habit can be indicators of magmatic conditions. Rapidly cooled magmas will host many small crystals, whereas thermally stable magmas generally form fewer, larger crystals.

***Amphibole volatiles:***

Volatiles in amphiboles can be used as a proxy for the volatile composition of the melt at the time of amphibole crystallization (Sato, 2004).

Fluorine can be used as an indicator cannibalism of magmatic precursors--fluorine is left in the magma as other Cl and water more readily fractionate into the vapor phase. Increases in the fluorine content might then be related to differentiation to F-rich magma or to the assimilation of hydrothermally altered crust.

Changes in water, chlorine and sulfur between samples may be related to changes in the magmatic system. Changes within individual mineral grains from core to rim, and variations within a sample of these volatiles could be particularly helpful to determine if the crystals have experienced degassing, mixing or assimilation of distinct volatile sources. If the variations of Cl from core to rim in amphiboles correspond to changes in the ratio of [Mg/(Mg+Fe)] (the Mg#), then we could relate these changes to fractional crystallization, (and or mixing). Decoupling of Mg# and Cl in amphibole may simply indicate that a Cl-rich fluid phase was not lost during amphibole crystallization.

### *Amphibole Thermometry and Barometry*

Plagioclase-amphibole geobarometer and thermometer can be utilized to determine the pressure and temperature of amphibole formation. Investigation of amphibole-bearing dacitic magmas over the lifespan of the volcanic system will provide snapshots through time of the formation of dacitic magmas at a long-lived volcanic system and how (if at all) the system varies over time.

**Methods:**

Amphibole-bearing dacites (and some silicic andesites) were chosen for this study to track the evolution of the system.

Over the life of the AVC, the eruptive products range in $SiO_2$ from 57-69 wt %. (Figures 5 & 6). Because dacites are common throughout the volcanic history of the AVC, they were chosen as a monitor of the evolution of the system.

Whole rock major element and trace element data were compiled from Klemetti, 2005 and McKee, 2002 (Table 2).

Dacites spanning the 11 million year history of the AVC were examined petrographically. Amphiboles in thin sections were counted and categorized texturally (by core and rim types) using a petrographic microscope at 2x magnification.

Amphibole-bearing samples were selected for amphibole mineral analysis. Microprobe analyses of thin sections and grain mounts were performed on the Cameca SX-100 at Oregon State University. The mineral phases targeted included, amphibole,

**Table 2. WHOLE ROCK and TRACE ELEMENT DATA FOR Selected samples from the AVC (from Klemetti, 2005 and McKee 2002)**

| | Volcanic Center | Alconcha | Amincha | Tuco | Tuco | Gordo | Paco Paco | Paco Paco | Paco Paco | Paco Paco |
|---|---|---|---|---|---|---|---|---|---|---|
| | Sample # | AP 00 03 | AP 00 82 | AP 00 17 | AP 00 16 | AP 00 86 | AP 00 37 | AP 00 31 | AP 00 33 | AP 00 34 |
| Unnormalized whole rock data | SiO2 | 65.08 | 62.38 | 62.65 | 67.80 | 63.35 | 61.87 | 61.71 | 57.91 | 65.17 |
| | Al2O3 | 17.21 | 17.53 | 17.96 | 16.35 | 16.55 | 16.73 | 17.14 | 16.94 | 15.85 |
| | TiO2 | 0.480 | 0.797 | 0.563 | 0.354 | 0.642 | 0.851 | 0.675 | 1.044 | 0.682 |
| | FeO* | 3.72 | 5.01 | 4.65 | 3.15 | 4.47 | 4.89 | 4.56 | 6.61 | 4.37 |
| | MnO | 0.086 | 0.103 | 0.102 | 0.080 | 0.071 | 0.082 | 0.076 | 0.106 | 0.076 |
| | CaO | 4.10 | 5.30 | 5.24 | 3.59 | 4.78 | 5.07 | 4.99 | 6.45 | 3.97 |
| | MgO | 1.33 | 1.69 | 2.35 | 1.16 | 2.74 | 2.81 | 2.53 | 4.15 | 2.07 |
| | K2O | 2.95 | 2.91 | 2.22 | 2.90 | 2.73 | 2.77 | 2.67 | 2.07 | 3.25 |
| | Na2O | 4.44 | 3.92 | 4.15 | 4.21 | 3.79 | 4.07 | 4.11 | 3.92 | 4.05 |
| | P2O5 | 0.215 | 0.244 | 0.214 | 0.147 | 0.182 | 0.207 | 0.215 | 0.279 | 0.176 |
| | Total | 99.61 | 99.89 | 100.10 | 99.74 | 99.31 | 99.35 | 98.68 | 99.48 | 99.67 |
| | Method | XRF | XRF | XRF | XRF | XRF | XRF | XRF | XRF | XRF |
| | Ni | 2 | 9 | 14 | 4 | 23 | 17 | 18 | 31 | 16 |
| | Cr | 3 | 13 | 19 | 4 | 63 | 44 | 44 | 82 | 38 |
| | Sc | 11 | 16 | 7 | 9 | 14 | 8 | 13 | 20 | 5 |
| | V | 67 | 109 | 99 | 55 | 114 | 137 | 112 | 165 | 103 |
| | Ba | 915 | 776 | 807 | 953 | 758 | 807 | 858 | 696 | 822 |
| | Rb | 81 | 95 | 52 | 82 | 85 | 80 | 62 | 48 | 105 |
| | Sr | 530 | 552 | 568 | 476 | 557 | 521 | 617 | 602 | 415 |
| | Zr | 175 | 148 | 139 | 122 | 139 | 161 | 140 | 151 | 171 |
| | Y | 17 | 17 | 15 | 13 | 13 | 15 | 12 | 21 | 17 |
| | Nb | 7.9 | 11.5 | 8.0 | 8.1 | 5.9 | 8.8 | 6.6 | 7.9 | 8.5 |
| | Ga | 15 | 18 | 19 | 16 | 19 | 21 | 21 | 20 | 19 |
| | Cu | 18 | 46 | 45 | 10 | 52 | 30 | 46 | 67 | 42 |
| | Zn | 66 | 82 | 68 | 53 | 70 | 79 | 75 | 94 | 71 |
| | Pb | 16 | 10 | 8 | 13 | 13 | 10 | 12 | 6 | 10 |
| | La | 37 | 33 | 18 | 32 | 27 | 47 | 38 | 21 | 43 |
| | Ce | 44 | 54 | 40 | 44 | 39 | 51 | 44 | 55 | 45 |
| | Th | 5 | 14 | 6 | 8 | 8 | 7 | 5 | 6 | 13 |
| | Method | N/D | ICP-MS | ICP-MS | N/D | N/D | ICP-MS | N/D | N/D | N/D |
| UNNORMALIZED TRACE ELEMENTS: | U | | 4.1 | 2.04 | | | 2.4 | | | |
| | Nd | | 23.19 | 19 | | | 21.67 | | | |
| | Sm | | 4.75 | 4.06 | | | 4.59 | | | |
| | Eu | | 1.22 | 1.05 | | | 1.16 | | | |
| | Gd | | 4.01 | 3.32 | | | 3.74 | | | |
| | Tb | | 0.6 | 0.52 | | | 0.55 | | | |
| | Dy | | 3.28 | 3 | | | 3.08 | | | |
| | Ho | | 0.64 | 0.6 | | | 0.57 | | | |
| | Er | | 1.72 | 1.59 | | | 1.41 | | | |
| | Tm | | 0.24 | 0.23 | | | 0.2 | | | |
| | Yb | | 1.59 | 1.47 | | | 1.25 | | | |
| | Lu | | 0.24 | 0.24 | | | 0.19 | | | |
| | Co | | | | | | | | | |
| | Cs | | | | | | | | | |
| | Hf | | | | | | | | | |
| | Ta | | | | | | | | | |

**Table 2 (cont). WHOLE ROCK and TRACE ELEMENT DATA FOR Selected samples from the AVC**

| | Volcanic Center | La Luna | Mino | Mino | Platform | Polan | Polan |
|---|---|---|---|---|---|---|---|
| | Sample # | AP 00 52 | VM99-52 | VM99-8 | AP 00 61B | AP 00 48 | AP 00 51 |
| | | | | | QMI | | |
| Unnormalized whole rock data | SiO2 | 61.68 | 64.98 | 60.00 | 55.71 | 61.92 | 63.31 |
| | Al2O3 | 18.20 | 17.04 | 17.67 | 17.99 | 16.46 | 16.80 |
| | TiO2 | 0.707 | 0.570 | 0.816 | 1.098 | 0.771 | 0.745 |
| | FeO* | 4.53 | 3.99 | 5.65 | 6.969 | 5.26 | 4.25 |
| | MnO | 0.073 | 0.06 | 0.09 | 0.102 | 0.097 | 0.069 |
| | CaO | 4.79 | 4.54 | 6.10 | 7.39 | 5.06 | 4.68 |
| | MgO | 2.43 | 2.19 | 2.97 | 3.91 | 2.42 | 2.43 |
| | K2O | 2.62 | 1.77 | 1.93 | 1.55 | 2.55 | 2.46 |
| | Na2O | 4.24 | 4.63 | 4.53 | 3.7 | 3.97 | 4.15 |
| | P2O5 | 0.238 | 0.197 | 0.239 | 0.245 | 0.204 | 0.208 |
| | Total | 99.51 | 96.43 | 99.43 | 98.664 | 98.71 | 99.10 |
| | | | | | UNNORMALIZED TRACE ELEMENTS: | | |
| | Method | XRF | INAA | INAA | XRF | XRF | XRF |
| | Ni | 14 | 17 | 24 | 19 | 25 | 18 |
| | Cr | 43 | 39 | 55 | 33 | 68 | 42 |
| | Sc | 21 | 6 | 8 | 16 | 16 | 12 |
| | V | 125 | - | - | 174 | 113 | 114 |
| | Ba | 751 | 845 | 810 | 610 | 752 | 795 |
| | Rb | 78 | 45 | 45 | 35 | 73 | 78 |
| | Sr | 553 | 593 | 694 | 609 | 553 | 551 |
| | Zr | 142 | 133 | 140 | 134 | 147 | 151 |
| | Y | 20 | 11 | 15 | 17 | 16 | 17 |
| | Nb | 8.8 | 8 | 8 | 7.2 | 7.8 | 7.3 |
| | Ga | 21 | 19 | 22 | 22 | 18 | 20 |
| | Cu | 19 | 37 | 74 | 83 | 53 | 30 |
| | Zn | 75 | 62 | 76 | 101 | 97 | 113 |
| | Pb | 17 | 9 | 11 | 20 | 8 | 10 |
| | La | 19 | 23 | 21 | 21 | 24 | 31 |
| | Ce | 55 | 38 | 47 | 47 | 52 | 36 |
| | Th | 12 | - | - | 4 | 8 | 6 |
| | Method | ICP-MS | INAA | INAA | N/D | N/D | N/D |
| UNNORMALIZED TRACE ELEMENTS: | U | 1.55 | - | - | | | |
| | Nd | 22.55 | 18 | 22 | | | |
| | Sm | 4.7 | 4 | 5 | | | |
| | Eu | 1.21 | 0.97 | 1.19 | | | |
| | Gd | 3.76 | - | - | | | |
| | Tb | 0.53 | 0.36 | 0.44 | | | |
| | Dy | 2.87 | - | - | | | |
| | Ho | 0.53 | - | - | | | |
| | Er | 1.37 | - | - | | | |
| | Tm | 0.19 | - | - | | | |
| | Yb | 1.12 | 0.87 | 0.99 | | | |
| | Lu | 0.17 | 0.12 | 0.15 | | | |
| | Co | | 9 | 15 | | | |
| | Cs | | 1.38 | 0.78 | | | |
| | Hf | | 4 | 4 | | | |
| | Ta | | 0.4 | 0.4 | | | |

**Table 2 (cont). WHOLE ROCK and TRACE ELEMENT DATA FOR Selected samples from the AVC**

| | Volcanic Center | Aucanquilcha | Aucanquilcha | Aucanquilcha | Aucanquilcha | Aucanquilcha | Aucanquilcha |
|---|---|---|---|---|---|---|---|
| | Sample # | AP2-98 | AP2-93 | AP2-92 | AP2-77 | AP2-60 | AP2-61 |
| | | Stage 2 | Stage 3 | Stage 3 | Stage 4 QMI | Stage 4 | Stage 4 |
| Unnormalized whole rock data | SiO2 | 64.99 | 66.61 | 66.84 | 59.61 | 63.72 | 67.62 |
| | Al2O3 | 17.11 | 16.37 | 16.35 | 16.97 | 16.53 | 16.39 |
| | TiO2 | 0.607 | 0.559 | 0.532 | 1.016 | 0.614 | 0.486 |
| | FeO* | 3.702 | 3.174 | 3.108 | 5.662 | 3.93 | 3.187 |
| | MnO | 0.08 | 0.051 | 0.05 | 0.083 | 0.067 | 0.052 |
| | CaO | 3.91 | 3.59 | 3.47 | 5.98 | 4.40 | 3.48 |
| | MgO | 1.35 | 1.54 | 1.49 | 3.33 | 1.70 | 1.4 |
| | K2O | 3.18 | 2.97 | 2.92 | 2.18 | 2.74 | 2.97 |
| | Na2O | 4.48 | 4.65 | 4.61 | 3.92 | 4.35 | 4.53 |
| | P2O5 | 0.272 | 0.174 | 0.157 | 0.246 | 0.170 | 0.116 |
| | Total | 99.681 | 99.688 | 99.527 | 98.997 | 98.22 | 100.231 |
| | Method | XRF | XRF | XRF | XRF | XRF | XRF |
| UNNORMALIZED TRACE ELEMENTS: | Ni | 0 | 6 | 7 | 11 | 5 | 8 |
| | Cr | 0 | 16 | 12 | 50 | 7 | 14 |
| | Sc | 8 | 11 | 6 | 11 | 11 | 4 |
| | V | 56 | 64 | 71 | 145 | 89 | 68 |
| | Ba | 1047 | 1069 | 1025 | 889 | 956 | 993 |
| | Rb | 97 | 80 | 81 | 54 | 78 | 89 |
| | Sr | 530 | 573 | 577 | 628 | 577 | 543 |
| | Zr | 214 | 149 | 148 | 169 | 158 | 140 |
| | Y | 16 | 10 | 9 | 15 | 12 | 8 |
| | Nb | 10.4 | 6.4 | 6.8 | 9.0 | 7.7 | 7.3 |
| | Ga | 19 | 19 | 22 | 21 | 19 | 19 |
| | Cu | 0 | 42 | 42 | 44 | 5 | 18 |
| | Zn | 80 | 71 | 64 | 106 | 69 | 66 |
| | Pb | 8 | 13 | 16 | 13 | 12 | 16 |
| | La | 47 | 23 | 21 | 55 | 29 | 24 |
| | Ce | 62 | 49 | 56 | 63 | 43 | 48 |
| | Th | 5 | 6 | 4 | 5 | 6 | 9 |
| | Method | ICP-MS | N/D | ICP-MS | ICP-MS | ICP-MS | ICP-MS |
| | U | 2.25 | | 1.49 | 1.12 | 1.64 | 1.92 |
| | Nd | 27.76 | | 18.23 | 24.14 | 20.95 | 16.71 |
| | Sm | 5.28 | | 3.55 | 5.45 | 4.21 | 3.4 |
| | Eu | 1.30 | | 0.89 | 1.45 | 1.06 | 0.86 |
| | Gd | 4.01 | | 2.49 | 4.62 | 3.30 | 2.59 |
| | Tb | 0.58 | | 0.34 | 0.65 | 0.46 | 0.34 |
| | Dy | 3.19 | | 1.73 | 3.35 | 2.44 | 1.81 |
| | Ho | 0.59 | | 0.31 | 0.58 | 0.44 | 0.31 |
| | Er | 1.54 | | 0.77 | 1.38 | 1.10 | 0.8 |
| | Tm | 0.22 | | 0.11 | 0.18 | 0.15 | 0.11 |
| | Yb | 1.32 | | 0.62 | 1.06 | 0.93 | 0.71 |
| | Lu | 0.21 | | 0.1 | 0.16 | 0.14 | 0.11 |
| | Co | | | | | | |
| | Cs | | | | | | |
| | Hf | | | | | | |
| | Ta | | | | | | |

plagioclase and minor biotite and pyroxene. (See appendix for complete data.) Back scatter electron (BSE) images of some amphibole and plagioclase crystals were also taken (See appendix for a catalog of all BSE images). Co-existing textural amphibole-plagioclase pairs were identified and selected for analysis and use for geobarometry and geothermometry after Holland Blundy, 1994, and Anderson and Smith, 1995.

Volatiles including Cl, F, S and $CO_2$ , as well as hydrogen isotope data on selected amphibole grains were acquired using the SIMS housed at the Department of Terrestrial Magnetism, Carnegie Institute of Washington in D.C., where amphibole mineral separates from selected dacites (and one mafic inclusion) were mounted on indium, polished and coated with a thin film of gold. Standards of glass, and amphibole were run throughout the analyses and used to standardize and correct the data (Table 3). (See appendix for details on data correction procedure for SIMS data.)

To measure the stable isotopes of hydrogen and oxygen in mineral phases, 0.2-0.4 microgram aliquots of hornblende and amphibole were wrapped in silver packets ablated in the stable isotope line housed at Oregon State University, Wilkinson Hall, Room119B modeled after Sharp, 2001. The isotope values of the resultant gases were measured on the TCEA housed at Oregon State University, College of Oceanic and Atmospheric Sciences Burt Hall (Table 4). Water values were not reported in this study as the laser treatment does not liberate all water in the mineral, only that which is contained at the hydroxyl site (Sharp 2001). Algorithms for the conversion of oxygen stable isotopes in hydroxyl groups to stable isotope values in the mineral are reported in Zheng 1993. (Values used for hydroxyl correction are reported in the stable isotope discussion, Table

Table 3.
Volatile and stable isotope data collected on amphiboles from the AVC using SIMS.
(See text for details about collection and correction of D/H data.)

| | | Sample # | H2O wt% | CO2 ppm | F ppm | S ppm | Cl ppm | D/H |
|---|---|---|---|---|---|---|---|---|
| | Tuco | AP17#2 | 1.28 | 2.78 | 1259 | 40.5 | 528 | -148 |
| | | AP17#3 | 0.72 | 2.93 | 1493 | 93.6 | 266 | -72 |
| | Mino | VM10#1 | 1.24 | 3.06 | 1981 | 77.2 | 188 | |
| | | VM10#2 | 0.91 | 4.16 | 2392 | 97.3 | 209 | |
| | | VM10#3 | 0.99 | 4.33 | 1909 | 114.3 | 260 | -143 |
| | | VM10#4 | 1.04 | 3.06 | 2192 | 99.2 | 217 | |
| | | VM10#5 | 1.20 | 5.74 | 2251 | 90.4 | 199 | -168 |
| Aucanquilcha | Stage 2 | AP2-98#1 | 1.65 | 4.19 | 2875 | 99.2 | 312 | |
| | | AP2-98#2 | 1.56 | 3.53 | 2795 | 90.4 | 319 | -118 |
| | Stage 3 | AP2-93#1 | 1.54 | 10.16 | 3256 | 13.9 | 247 | -145 |
| | | AP2-93#2 | 2.49 | 33.58 | 7022 | 162.7 | 627 | -123 |
| | | AP2-92#1b | 1.53 | 1130.09 | 3450 | 19.4 | 367 | |
| | | AP2-92#2 | 1.53 | 3.61 | 3544 | 11.5 | 318 | -119 |
| | Stage 4 | AP2-77#2 | 1.52 | 2.82 | 2803 | 11.9 | 815 | -119 |
| | | AP2-77#3 | 1.64 | 2.20 | 3609 | 14.1 | 549 | |
| | | AP2-61#1 | 2.17 | 2.01 | 4184 | 17.7 | 574 | -73 |
| | | AP2-61#2 | 2.12 | 2.74 | 4051 | 18.6 | 610 | -41 |
| | | AP2-61#3 | 2.11 | 2.38 | 4134 | 17.8 | 595 | |
| | | AP2-61#4 | 2.12 | 2358.50 | 4079 | 24.6 | 565 | |
| | | AP2-60#1 | 1.56 | 5.10 | 3783 | 101.1 | 203 | -164 |
| | | AP2-60#2 | 1.58 | 15.41 | 3536 | 166.4 | 448 | |
| | | AP2-60#3 | 1.66 | 4.18 | 3451 | 98.6 | 505 | -147 |
| | | AP2-60#4 | 1.68 | 5.86 | 3361 | 99.2 | 209 | |
| | | AP2-60#5 | 1.43 | 4.65 | 3480 | 86.0 | 394 | |

**TABLE 4.**
**Stable Isotopes from amphibole, biotite and plagioclase from the AVC**

Volcan Aucanquilcha samples are divided here into 4 eruptive stages after Klemetti, 2005
*Corrected TCEA Oxygen isotope values are reported in Table 6, and treated in the discussion.
**Plagioclase oxygen values are reported and discussed in Klemetti 2005.

| Sample # | | Center | D/H ‰ (TCEA) | Oxygen ‰ (TCEA) * | Mineral |
|---|---|---|---|---|---|
| AP2 | 61 | Stage 4 | -60.5 | -3.72 | Bt |
| AP2 | 61 | Stage 4 | -53.4 | -3.82 | Bt |
| AP2 | 93 | Stage 3 | -47.6 | -2.11 | Bt |
| AP2 | 93 | Stage 3 | -12.5 | -2.89 | Bt |
| AP2 | 25 | Stage 1 | -22.1 | 0.04 | Bt |
| AP | 39 | Stage 1 | -70.1 | -2.32 | Bt |
| AP | 39 | Stage 1 | -76.5 | -0.11 | Bt |
| AP | 8 | Platform | -67.1 | 2.14 | Bt |
| AP | 37 | Paco Paco | -61.7 | 1.23 | Bt |
| AP | 37 | Paco Paco | -69.0 | -0.71 | Bt |

| Sample # | | Center | D/H ‰ (TCEA) | Oxygen ‰ (TCEA) * | Mineral |
|---|---|---|---|---|---|
| AP2 | 61 | Stage 4 | -56.3 | 1.14 | Hb |
| AP2 | 93 | Stage 3 | -70.7 | -1.60 | Hb |
| VM99 | 10 | Mino | -53.3 | 0.56 | Hb |
| AP | 17 | Tuco | -38.9 | -1.75 | Hb |

| Sample # | | Center | D/H ‰ (SIMS) | Mineral |
|---|---|---|---|---|
| VM10#3 | | Mino | -143 | Hb |
| VM10#5 | | Mino | -168 | Hb |
| AP17#2 | | Tuco | -148 | Hb |
| AP17#3 | | Tuco | -72 | Hb |
| AP2-98#2 | | Stage | -118 | Hb |
| AP2-93#1 | | Stage 3 | -145 | Hb |
| AP2-93#2 | | Stage 3 | -123 | Hb |
| AP2-60#1 | | Stage 4 | -164 | Hb |
| AP2-60#3 | | Stage 4 | -147 | Hb |
| AP2-92#2 | | Stage 3 | -119 | Hb |
| AP2-77#2 | | Stage 4 | -119 | Hb |
| AP2-61#1 | | Stage 4 | -73 | Hb |
| AP2-61#2 | | Stage 4 | -41 | Hb |

| Sample # | | Center | Oxygen ‰ (WSU)** | Mineral |
|---|---|---|---|---|
| AP2-47 | | Stage 1 | 5.73 | plag |
| AP2-96 | | Stage 2 | 6.23 | plag |
| AP2-100 | | Stage 2 | 6.02 | plag |
| AP2-92 | | Stage 3 | 6.47 | plag |
| AP2-77 (qmi) | | Stage 4 | 6.66 | plag |
| AP2-61 | | Stage 4 | 6.57 | plag |

5.) Reported oxygen isotope values of plagioclase from Klemetti are also treated in the discussion.

## RESULTS:

### *Amphibole Textures and Textural Abundance:*

Amphiboles in dacites at the AVC can be categorized by the textural variations among cores and rims, and help to define the thermal and magmatic history of the AVC (Figure 10). There are three major types of rims: 1) euhedral crystals without reaction rims, which we refer to as plain or equilibrium rims; 2) thin reaction rim (< 25 μ); 3) thick reaction rims (>25 μ). There is a 4$^{th}$ type of rim that is not common, but when present is abundant (ex. AP-00-61B)—this rim texture consists of euhedral small amphibole, pyroxene and oxide crystals along the rim of larger amphibole phenocrysts, similar to the "gabbroic rims" described by McKee. This texture is most common in the two quenched mafic inclusions (QMI), and in the andesites of Mino. There are three types of cores in the AVC amphiboles: 1) equilibrium; 2) hollow or glass in the center; 3) cored by other, usually mafic, phases- commonly biotite or pyroxene. Nearly all rim types are found associated with all core types (Figure 11). Of course as petrographic thin sections are a two-dimension rendering of a three-dimensional system, some textures, (particularly hollow-cores) may be under-represented in the textural categories. Additionally, some rim thicknesses may have been over-estimated.

In the Alconcha Group (11-8 Ma), all core types are observed (Figure 12). Most rims are thin or thick. AP-00-17-Tuco has two major textural populations the first with

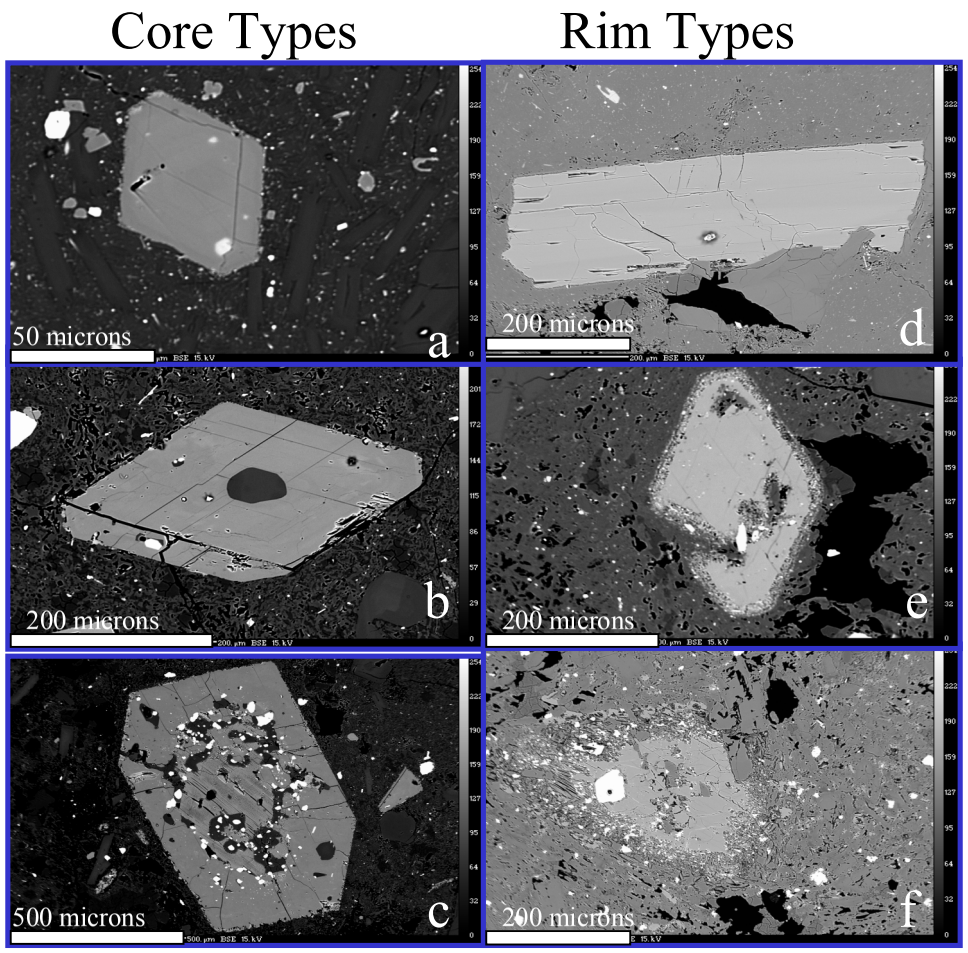


**Figure 10.**
Back-scatter electron (BSE) images of amphiboles showing different textural types observed at the AVC, classified by core and rim types. Core types on the left from top to bottom include a)plain; b) melt in core and c) mafic and other phases in the core. Rim types, (on the right) include d) no rim-equilibrium; e) thin rim and f) thick rim. The volcano, sample number and mineral number of the mineral grains are as follows: a)Volcan Aucanquilcha Stage 4, AP2-98-4; b)Volcan Aucanquilcha-Stage 4, AP2-61- 5; c) Volcan Aucanquilcha,-Stage 4, AP2-61-1 ; d) Tuco, AP-00-16-5; e) Volcan Mino, VM-52-2 ; f.)Amincha, AP-00-82-1

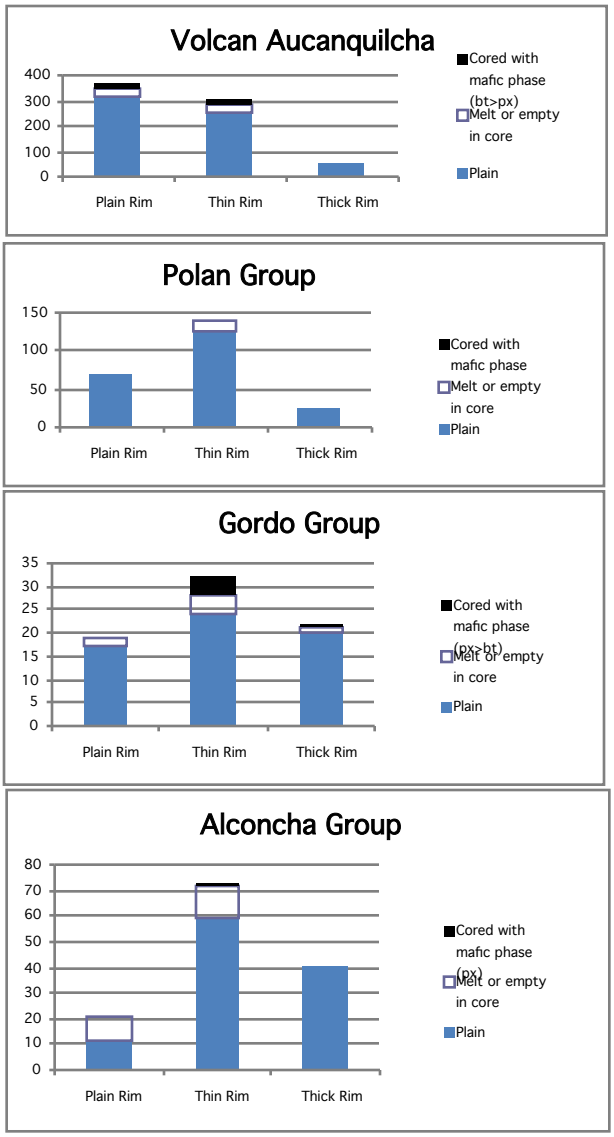


**Figure 11.**
**Summary of textural variability of amphiboles in dacites at the AVC.**
ɔred amphiboles are most common in the Gordo and Aucanquilcha groups, however in ɔrdo the amphiboles are most commonly cored with pyroxene (px), whereas at Aucanquilcha ɔtite (bt) is more common in the cores. Older samples overall have more thick rims, and a ater distribution of textural types than the younger samples. In Polan, where amphibole ɔmes a dominant phase, the textural variety of amphibole decreases. At Aucanquilcha phibole is common, but overall is smaller and makes up a smaller modal percentage than ther groups.

| AP 00 03-Alconcha | Plain rim | Thin Rim | Thick Rim |
|---|---|---|---|
| Plain | 10 | 39 | 0 |
| Melt or empty in core | 8 | 11 | 0 |
| Cored with mafic phase | 0 | 0 | 0 |

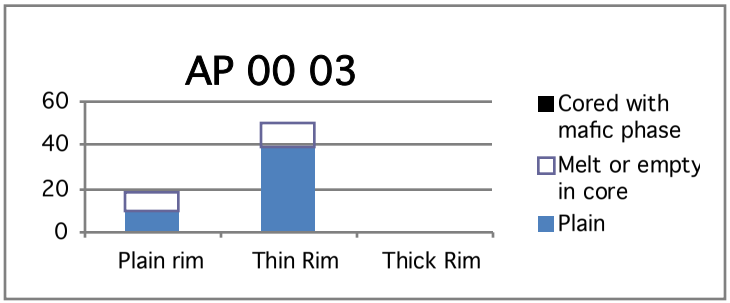


| AP 00 82-Amincha | Plainrim | Thin Rim | Thick Rim |
|---|---|---|---|
| Plain | 1 | 2 | 0 |
| Melt or empty in core | 2 | 0 | 0 |
| Cored with mafic phase | 0 | 0 | 0 |

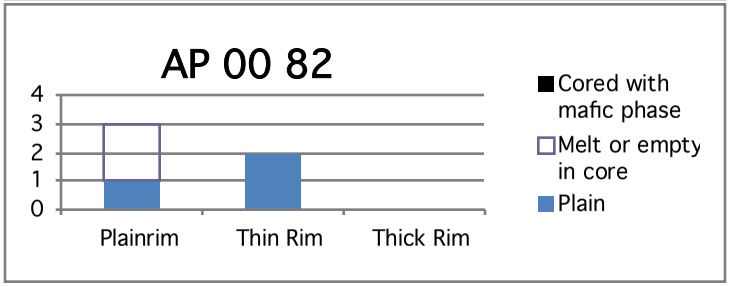


| AP 00 17-Tuco | Plain rim | Thin Rim | Thick Rim |
|---|---|---|---|
| Plain | 0 | 18 | 41 |
| Melt or empty in core | 0 | 2 | 0 |
| Cored with mafic phase | 0 | 1 | 0 |

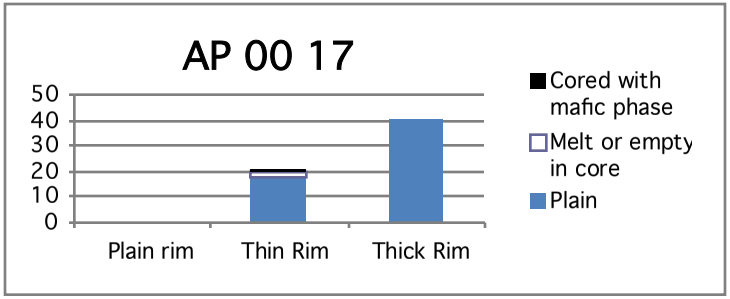


**Figure 12.**
**Summary of textural variation of amphiboles in the Alconcha Group.**
ımphiboles were classified by core and rim types for the 11-8 Ma Alconcha Group. Amphiboles from this stage show a ide range of textural types both in core and rim types. Cored amphiboles however are common, but when present, the nphiboles are cored with pyroxene.

plain cores and thin and thick rims: only a few amphiboles were noted to have melt or hollow cores in this sample. The second population of larger amphiboles is less abundant and commonly cored by pyroxene ± plagioclase. AP-00-82-Amincha, had only 5 amphiboles in the section (although there is more amphibole in the groundmass, these were not detectable at the scale of these observations.) The amphibole phenocrysts present had either plain or hollow cores with thin or no rim. In AP-00-03 there are no amphiboles with thick rims, most have thin rims with plain or hollow cores.

In the Gordo Group amphiboles (6-4.2 Ma), textural diversity is maintained (Figure 13). Amphiboles from the Gordo Group are most commonly cored with pyroxene and sometimes olivine. Amphiboles with thin or thick rims are more common than plain-rimmed amphiboles. Those grains cored with mafic phases always have thin or thick rims. Both AP-00-37 and AP-00-31, from Paco Paco, possess very few amphibole phenocyrsts that are cored with mafic phases; this volcanic center is dominated by plain amphiboles with thin or thick rims. AP-00-86-Gordo displays greater textural variety than Paco Paco.

By the time of the Polan Group (3.6-2.4 Ma), the textural diversity has diminished (Figure 14). Amphiboles cored with mafic phases, or hollow, are uncommon; most amphiboles have thin or no rims. An exception to the textural homogeneity observed in the Polan Group is the andesite center, Volcan Mino, which lies at the periphery of the AVC. Volcano Mino's amphiboles generally have thin or thick rims and exhibit all core types. Pyroxene is the most common mafic phase found in the core of the Mino

| AP 00 37-Paco Paco | No rim | Thin Rim | Thick Rim |
|---|---|---|---|
| Plain | 2 | 3 | 1 |
| Melt or empty in core | 0 | 0 | 0 |
| Cored with mafic phase | 0 | 0 | 0 |

| AP 00 31-Paco Paco | No rim | Thin Rim | Thick Rim |
|---|---|---|---|
| Plain | 0 | 1 | 13 |
| Melt or empty in core | 0 | 2 | 1 |
| Cored with mafic phase (px) | 0 | 0 | 1 |

| AP 00 86-Gordo | No rim | Thin Rim | Thick Rim |
|---|---|---|---|
| Plain | 15 | 20 | 6 |
| Melt or empty in core | 2 | 2 | 0 |
| Cored with mafic phase (px) | 0 | 4 | 0 |

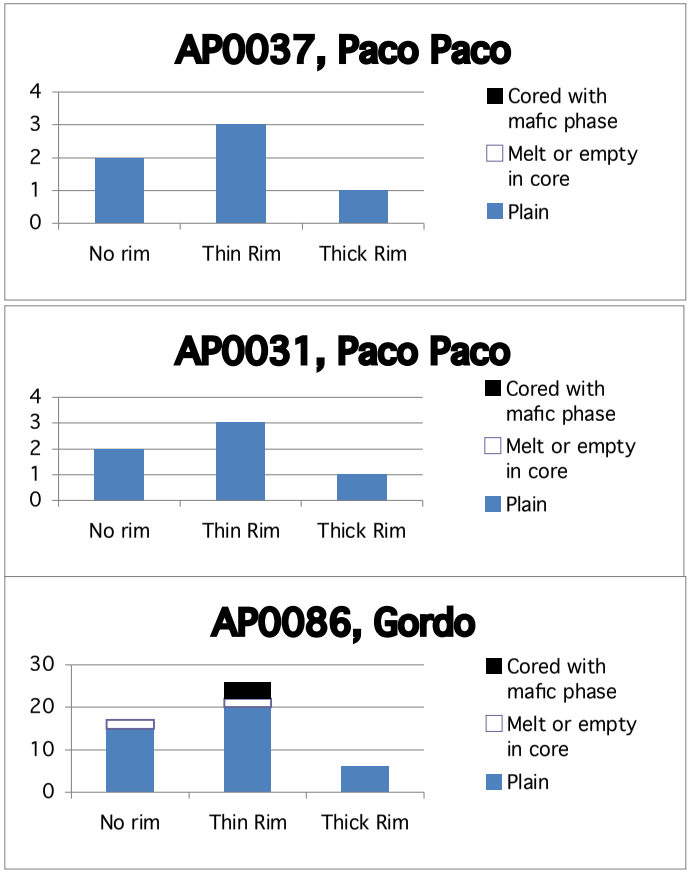


**Figure 13.**
**Summary of textural variation of amphiboles in the Gordo Group.**
Amphiboles were classified by core and rim types for the ~6-4 Ma Gordo Group. Overall amphiboles are less abundant, amphiboles with thick rims are common as are amphiboles which have been completely reacted to pyroxene +/- oxides.

| AP 00 52 | Plain Rim | Thin Rim | Thick Rim |
|---|---|---|---|
| Plain | 0 | 2 | 1 |
| Melt or empty in core | 0 | 1 | 0 |
| Cored with mafic phase | 0 | 0 | 0 |

| AP 00 51 | Plain Rim | Thin Rim | Thick Rim |
|---|---|---|---|
| Plain | 51 | 74 | 0 |
| Melt or empty in core | 0 | 0 | 0 |
| Cored with mafic phase | 0 | 0 | 0 |

| AP 00 60 | Plain Rim | Thin Rim | Thick Rim |
|---|---|---|---|
| Plain | 0 | 47 | 19 |
| Melt or empty in core | 0 | 10 | 0 |
| Cored with mafic phase | 0 | 0 | 0 |

| AP 00 90 | Plain Rim | Thin Rim | Thick Rim |
|---|---|---|---|
| Plain | 19 | 4 | 5 |
| Melt or empty in core | 0 | 0 | 0 |
| Cored with mafic phase | 0 | 0 | 0 |

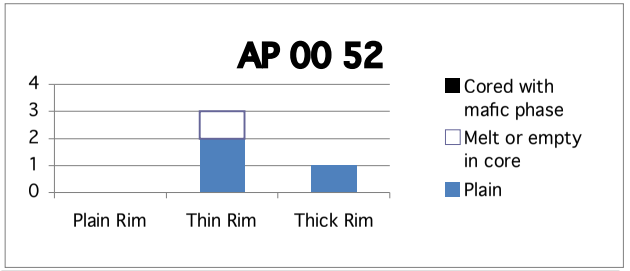


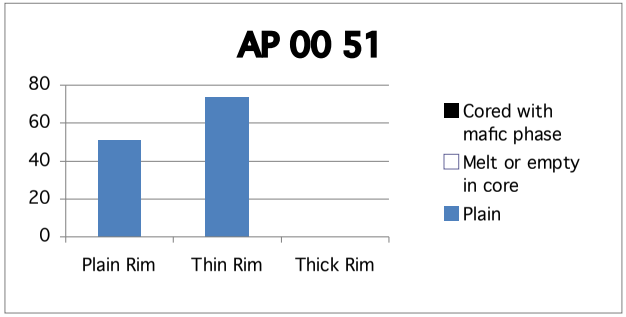


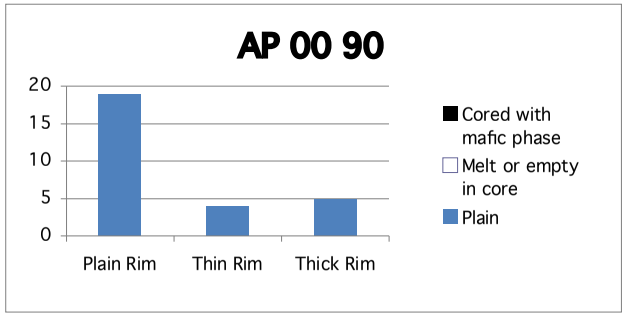


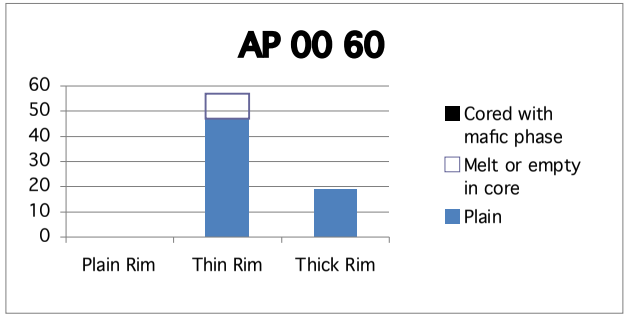


**Figure 14.**
**Summary of textural variations of Polan Group amphiboles.**
Amphiboles were classified by core and rim types for the Polan Group (~3.4-2 Ma). Cored amphiboles are not common in this group. As a whole, the Polan Group shows the least textural diversity, particularly in core types.

amphiboles. Amphiboles that are hollow or have melt in the core when present at Mino always have thin or thick rims (this study and McKee, 2002) (Figure 15).

In the youngest phase of volcanism, the Aucanquilcha Group, the amphiboles are texturally diverse (Figure 16). At Volcan Aucanquilcha amphibole is more abundant than in most of the earlier dacites and all core and rim types are represented; amphiboles with normal or hollow cores are the most abundant. Many Volcan Aucanquilcha samples contain two textural populations, one of larger reacted amphibole phenocrysts with thin to thick rims and another, more numerous population with hollow or normal cores, which have thin or plain rims. Volcan Aucanquilcha is divided into four eruptive stages. The second stage, (sample AP2-98), is dominated by normal cores with plain rims. Samples from the third stage, (AP2-93 and AP2-92) have dominantly normal core types with thin rims. In the third stage, amphiboles with melt or hollow cores are more common than in the previous stages. In samples AP2-60 and AP2-61-, from the final stage of Volcan Aucanquilcha, the majority of amphiboles display plain rims, and have all core types represented with plain rims. Only 4 of the >250 amphiboles counted in these samples have thick rims.

Two quenched andesitic inclusions from the AVC were analyzed for textural variability; one from the Platform (AP-00-61B), and another from the final stage of Volcan Aucanquilcha (AP2-77). In these samples, the matrix consisted of interlocking needles of amphibole and plagioclase as well as euhedral oxides. The matrix was not counted in this study, however ground mass amphiboles were all noted to have plain or very thin rims with plain and sometimes hollow cores. The larger phenocrysts in the

**VM-10**

| | Plain Rim | Thin Rim | Thick Rim |
|---|---|---|---|
| Plain | 0 | 23 | 19 |
| Melt or empty in core | 0 | 9 | 0 |
| Cored with mafic phase | 0 | 0 | 0 |

**VM-52**

| | Plain Rim | Thin Rim | Thick Rim |
|---|---|---|---|
| Plain | 0 | 23 | 45 |
| Melt or empty in core | 0 | 3 | 0 |
| Cored with mafic phase | 0 | 0 | 2 |

| Cobmined Mino Data | Plain Rim | Thin Rim | Thick Rim |
|---|---|---|---|
| Plain | 0 | 46 | 64 |
| Melt or empty in core | 0 | 12 | 0 |
| Cored with mafic phase | 0 | 0 | 2 |

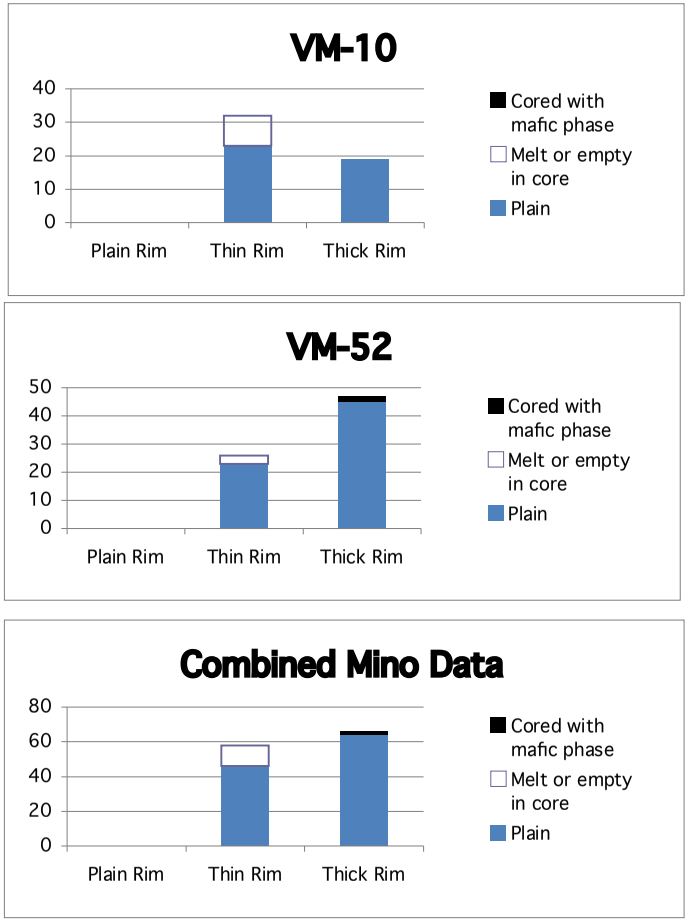


**Figure 15.**
**Summary of textural variation at Volcan Mino.**
Volcan Mino, ~3.3Ma, erupts on the periphery of the AVC during the time of the Polan Group. Its location on the periphery and its more andesitic composition set it apart from the rest of the Polan Group. Amphibole textures in this stage are often complex, and completely reacted amphiboles are common, along with amphiboles with thick rims.

| AP2-61-Stage 4 | Plain Rim | Thin Rim | Thick Rim |
|---|---|---|---|
| Plain | 69 | 2 | 0 |
| Melt or empty in core | 8 | 0 | 0 |
| Cored with mafic phase | 12 | 0 | 0 |

| AP2-60-Stage 4 | Plain Rim | Thin Rim | Thick Rim |
|---|---|---|---|
| Plain | 156 | 8 | 4 |
| Melt or empty in core | 16 | 0 | 0 |
| Cored with mafic phase | 16 | 16 | 0 |

| AP2-92-Stage 3 | Plain Rim | Thin Rim | Thick Rim |
|---|---|---|---|
| Plain | 21 | 140 | 30 |
| Melt or empty in core | 0 | 23 | 0 |
| Cored with mafic phase | 0 | 0 | 0 |

| AP2-93-Stage 3 | Plain Rim | Thin Rim | Thick Rim |
|---|---|---|---|
| Plain | 0 | 82 | 9 |
| Melt or empty in core | 0 | 14 | 0 |
| Cored with mafic phase | 0 | 2 | 0 |

| AP2-98-Stage 2 | Plain Rim | Thin Rim | Thick Rim |
|---|---|---|---|
| Plain | 72 | 18 | 6 |
| Melt or empty in core | 2 | 0 | 0 |
| Cored with mafic phase | 0 | 1 | 3 |

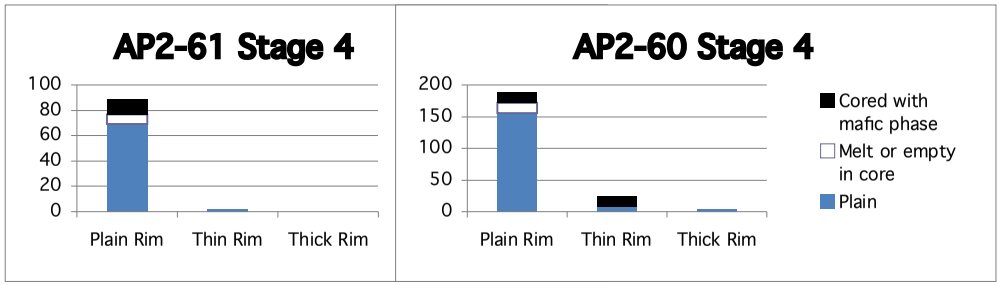





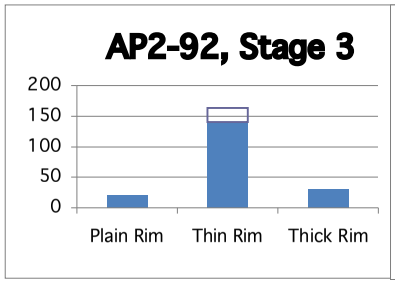


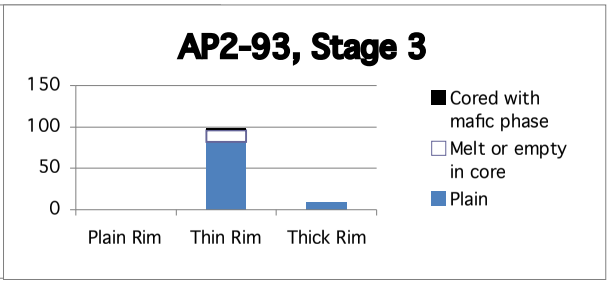


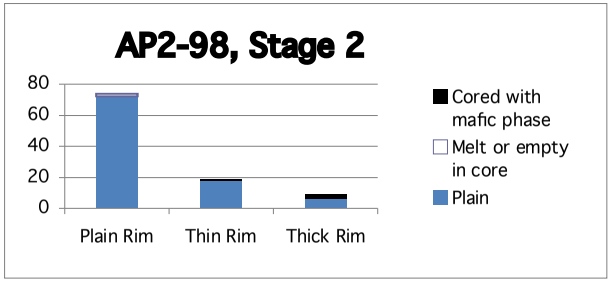


**Figure 16.**
**Summary of textural variation of amphiboles from Volcan Aucanquilcha.**
Amphiboles from Volcan Aucanquilcha were classified by core and rim type. Amphiboles at Volcan Aucanquilcha are more abundant than in previous stages, however they are overall smaller. Equilibrium textures are the most common amphibole at this stage, with most amphiboles have plain or thin rims. Amphiboles that are cored with a mafic phase are most commonly cred with biotite. Amphiboles with melt or hollow cores are also very common at this stage of volcanism indicating that do not expereience long periods of disequilibrium after crystallization and before eruption.

samples displayed a variety of both core and rim types-and most do not appear to be in equilibrium with the matrix (Figure 17).

**Textural Summary:**

Overall at the AVC amphiboles are most texturally diverse early and late in the history of the system. The least textural variability is in the Polan Group (with the exception of Volcan Mino which lies at the periphery of the cluster).

The distribution of textural type varies with time. In the Alconcha Group, amphiboles with thin to thick rims and normal cores are most abundant; when amphiboles are cored with a mafic phase it is most often pyroxene. In the Gordo Group, there is a peak in the distribution at thin-rimmed amphiboles with plain cores, and variability is limited to variations in rim types. Amphiboles at this stage, are cored with pyroxene. In the Polan Group, amphiboles cored with mafic phases are not observed, and amphiboles that are hollow or have melt quenched in the cores are proportionally less represented than in other stages. Volcan Aucanquilcha has a greater proportion of hollow/equilibrium amphiboles than any other stage. At Volcan Aucanquilcha, amphiboles with plain rims dominate and hollow amphiboles are more common than in earlier stages; amphiboles when cored are most commonly cored with biotite as a mafic phase.

***Amphibole size and mode:***

In addition to the texture of the amphiboles, the approximate size of the amphiboles, as well as the mineral assemblage of the host dacite were investigated. In the

**Aucanquilcha**
**QMI-AP2-77-Stage 4**

| | Plain Rim | Thin Rim | Thick Rim |
|---|---|---|---|
| Equilibrium | 1 | 6 | 3 |
| Melt or empty in core | 0 | 0 | 2 |
| Cored with mafic phase | 0 | 0 | 2 |

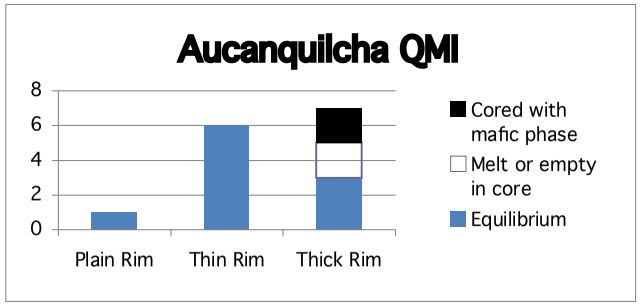


**Polan Group-Platform**
**QMI-AP 00 61 B**

| | Plain Rim | Thin Rim | Thick Rim |
|---|---|---|---|
| Equilibrium | 3 | 4 | 0 |
| Melt or empty in core | 8 | 0 | 0 |
| Cored with mafic phase | 0 | 0 | 0 |

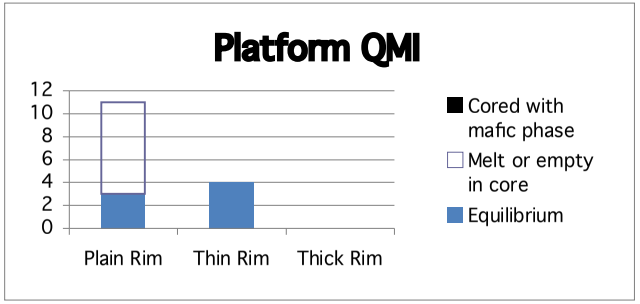


**Figure 17.**
**Summary of textural variation of quenched mafic inclusions (QMI) from the AVC.**
Amphiboles in two quenched mafic inclusions of silicic andesite were classified by core and rim types. In the QMI, amphiboles with melt in the core are common. Amphiboles with thick rims from the Aucanquilcha inclusion displayed all core types. Both inclusions also had amphibole in the groundmass that most commonly had plain with plain (or sometimes melt in the) cores.

earliest stages of volcanism, (Alconcha and Gordo Groups) amphiboles are overall less abundant and when present compose <5 modal percent in andesites-dacites. In this age group, andesites and dacites mainly contain a two-pyroxene mineralogy with olivine and or amphibole less common. As noted previously these amphiboles generally display an array of textures and compositions indicating variable conditions at a restricted whole rock composition.

During the time of the Polan group, more hydrous and shallower mineral assemblages are found, and a compositionally homogenous dacite becomes the dominant erupted composition. At this time large zoned amphiboles become abundant and overall phenocryst content increases in these lavas, with amphiboles>>than pyroxene and usually >5 modal percent when present. These amphibole phenocrysts are also some of the largest observed at the AVC. Mino, like the rest of Polan has large amphibole phenocrysts, however it is equally common to find large "amphibole" phenocrysts that have been completely replaced with with pyroxene, opaque oxides and plagioclase. Unlike the Polan Group-which is not commonly cored with mafic phases, Mino amphiboles are commonly cored with pyroxene.

During the Aucanquilcha stage, amphiboles are very common, though due to their small size, they tend to make up a smaller overall modal percentage of phenocrysts. Biotite at this stage becomes abundant (and sometimes dominant) over amphibole as a mafic phase. Amphiboles in this stage are often smaller than in previous stages, and most commonly display equilibrium and hollow core textures with very thin or plain rims.

***Amphibole Composition:***

Just as textures in amphiboles vary throughout the evolution of the AVC, so do the compositions of the amphiboles in dacites. Magnesiohastingsite is the most common amphibole, at the AVC followed by tschermakite, magnesiohornblende, paragsite and edenite (Figure 18). For this classification, stoichiometry was determined using the method and nomenclature described in Leake *et al.,* 1997. (A discussion of this process and a sample calculation are included in the Amphibole Appendix.) All amphibole compositional types are found over the range of dacite compositions selected for this study, so that on a first order, the variations in amphibole composition are not solely tied to whole-rock compositional variability (Figure 19).

**Aluminum:**

The aluminum content in the amphiboles range from $Al_{Tot}$ 1.0-2.4 (Figure 20). In the Alconcha and Aucanquilcha groups, the total aluminum range in the amphiboles is greater than in the Gordo and Polan groups. Additionally, the Alconcha and Aucanquilcha groups have multiple populations of amphiboles each with a limited $Al_{Tot}$ range: individual amphibole grains do not span a large compositional range. The large range in $Al_{Tot}$ in these groups results from the existence of compositionally distinct amphiboles, which collectively span a large compositional range that is also mimicked in alkalis and Ti.

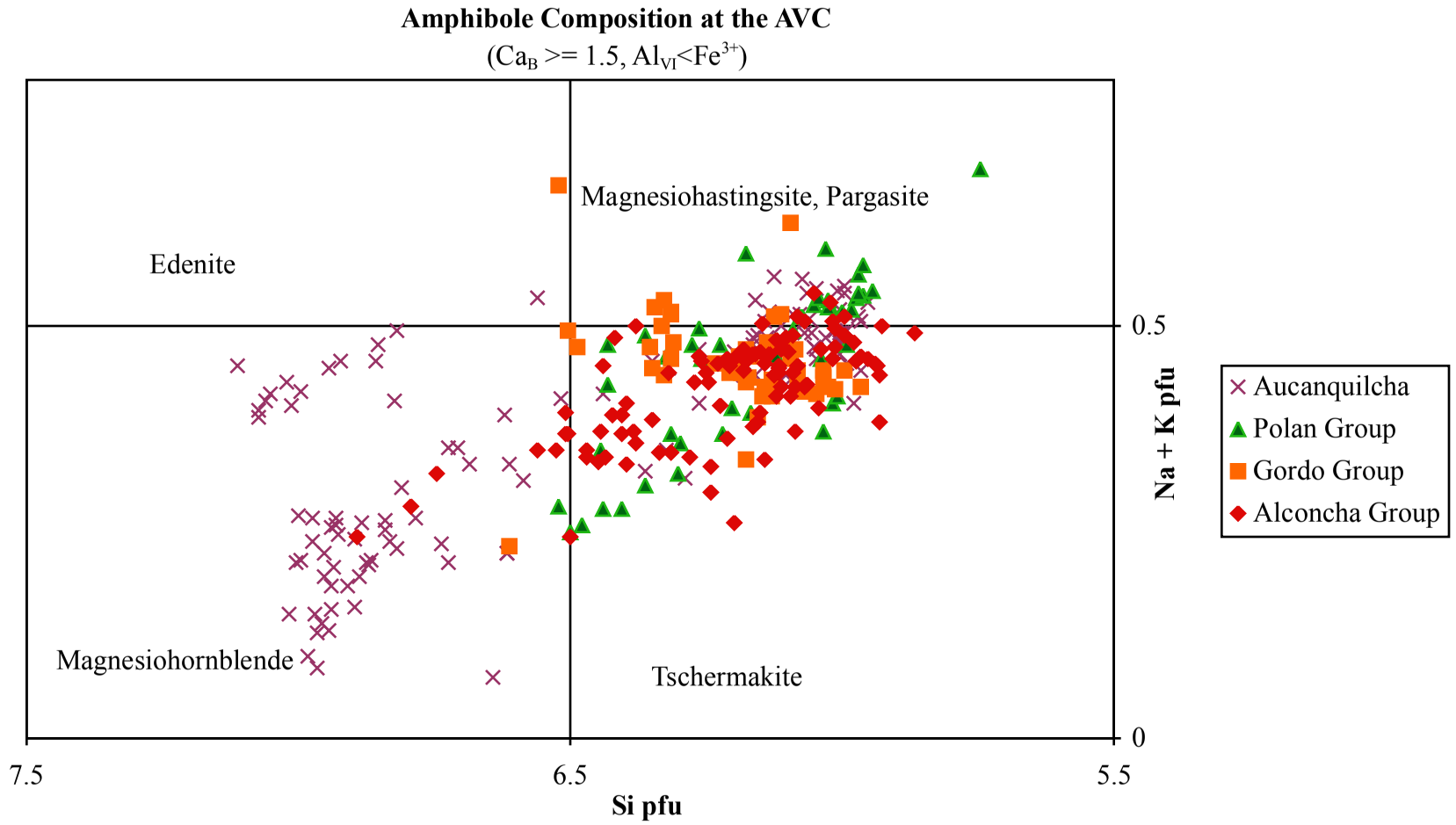


**Figure 18.**
Amphiboles named after the nomenclature of Leake et al., 1997. Amphibole compositions vary over the life of the volcanic system. Both eary and late in the system amphibole compositions are most diverse. In the Polan and Gordo Groups, amphibole compositions are more restricted, and most amphiboles classify as tschermakite.

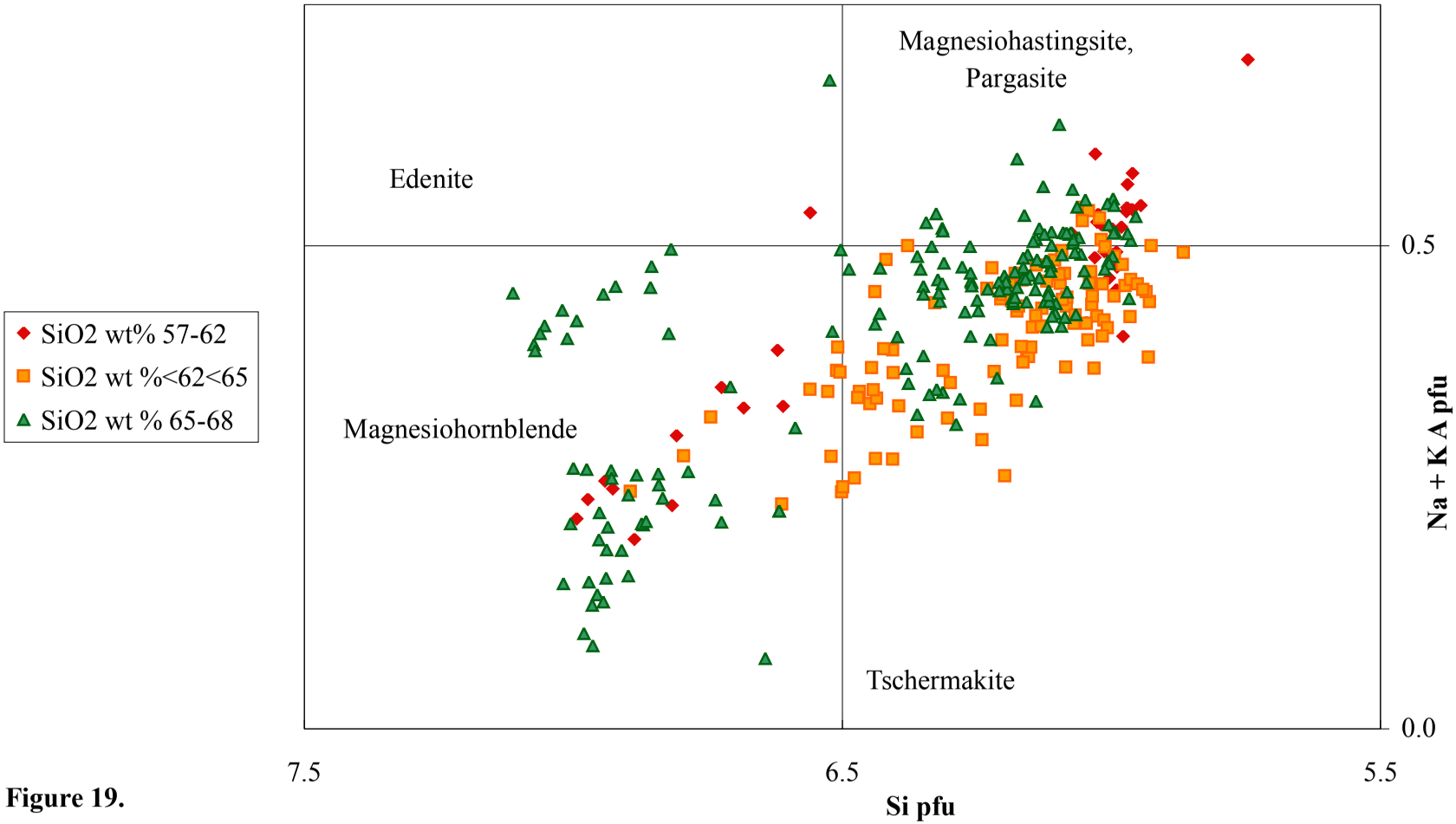


**Figure 19.**

**Amphibole classified by host whole rock composition.**

Amphiboles are classified here by host rock composition in wt% SiO2, and by the composition of the amphibole. All amphibole compositions are found hosted in all compositions of host rock.

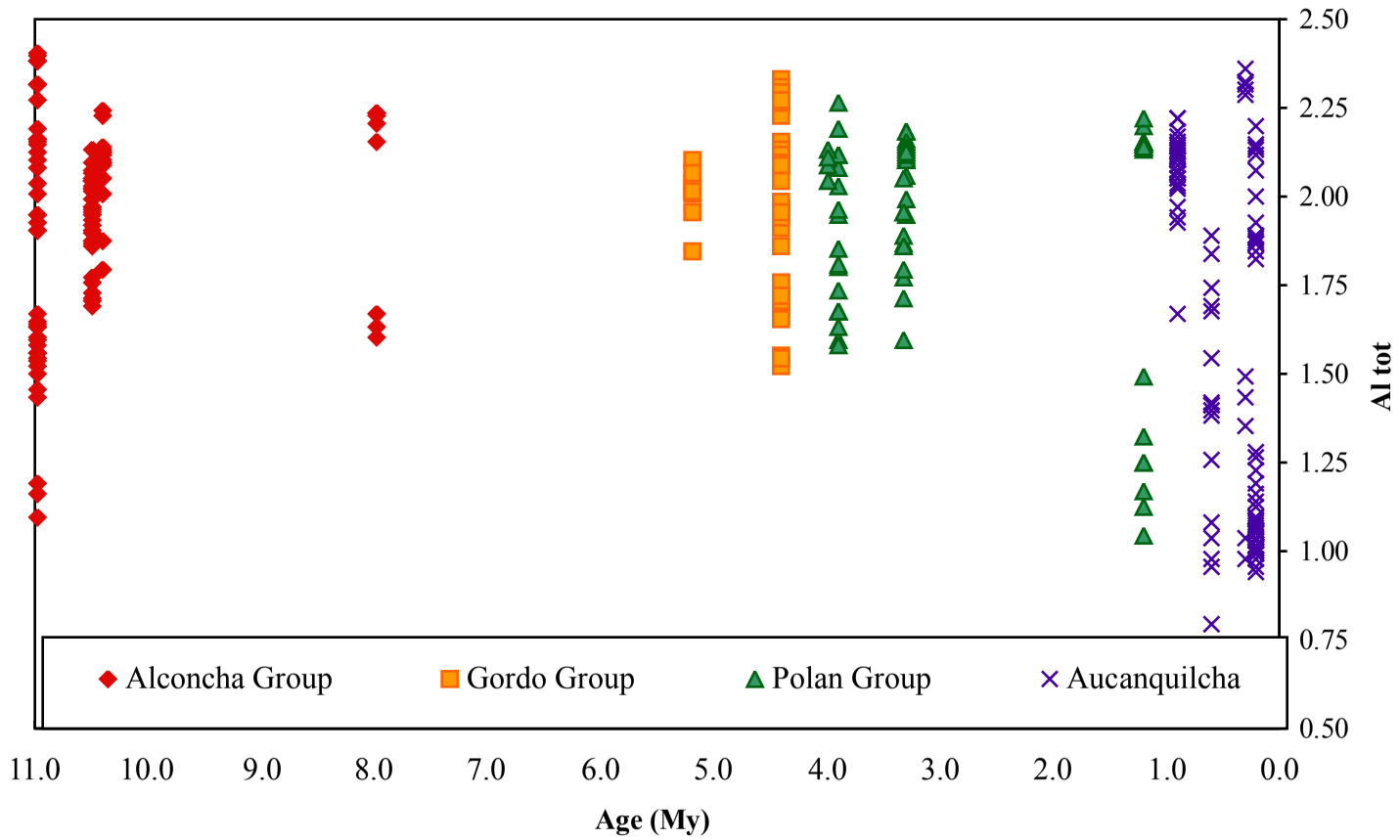


**Figure 20.**

Stratigraphic age of amphiboles from the AVC combined with aluminum total pfu. Early and late in the system the heterogeneity of the system is defined by many amphiboles which individually have a small compositional range, but when taken together, create a heterogeneous population. In the Polan Group (and less so in the Gordo Group,) single amphibole grains span the entire compositional range observed for the group.

In contrast, to the Alconcha and the Aucanquilcha Groups, whose individual grains are restricted in composition, the range in $Al_{Tot}$ of the Polan group (and less so in the Gordo group) is reflected in individual grains that make up a single population. In other words, in the Polan Group, individual amphiboles reflect the entire $Al_{Tot}$ range—and together, amphiboles define a single variable population.

**Alkalis:**

In the Alconcha, Polan and Aucanquilcha Group, $(Na+K)_A$ increases with $Al_{Tot}$. In the Gordo Group alkalis remain constant independent of changes in total Al, however there are variations from core to rim in alkalis particularly in (AP-00-34 Paco Paco) (Figure 21).

**Titanium:**

$Al_{Tot}$ generally covaries with Ti though less steeply in the Alconcha group. The steepness of the variation between Al and Ti in amphiboles has been used as a proxy for the influence of temperature and $fO_2$ changes on amphiboles (Selles, 2006; Bachmann, 2002). (Figure 22). An exception to the covariation of $Al_{Tot}$ and Ti is seen in the sodic amphiboles from sample AP2-61 from the last eruption of Volcan Aucanquilcha. In this study, AP2-61 is the only sample with sodic, rather than sodic-calcic amphiboles that is erupted from the AVC.

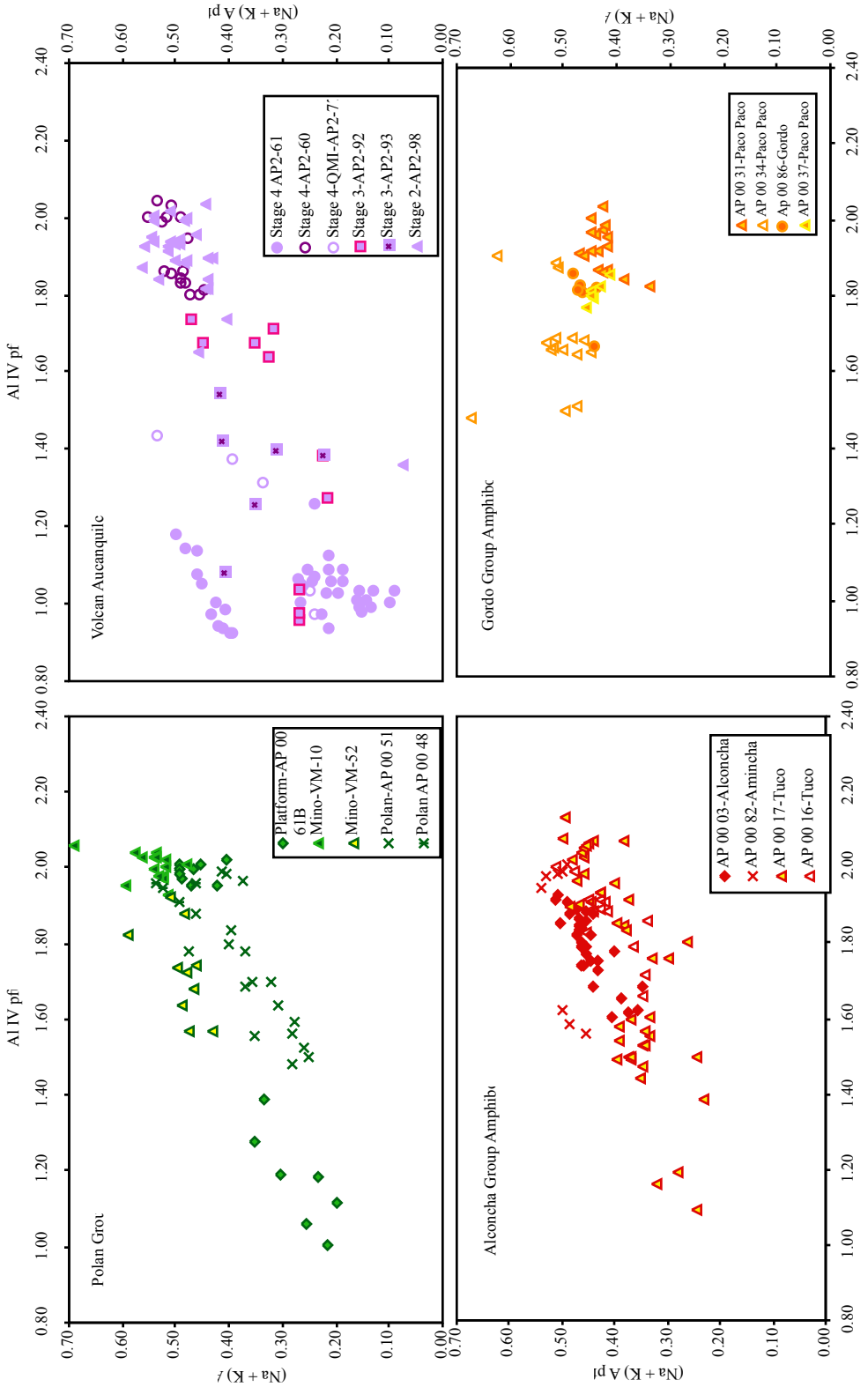


**Figure 21.**
Over the 11 million year history of the AVC, A-site occupancy in amphiboles varies from 0.08 pfu up to .70pfu.

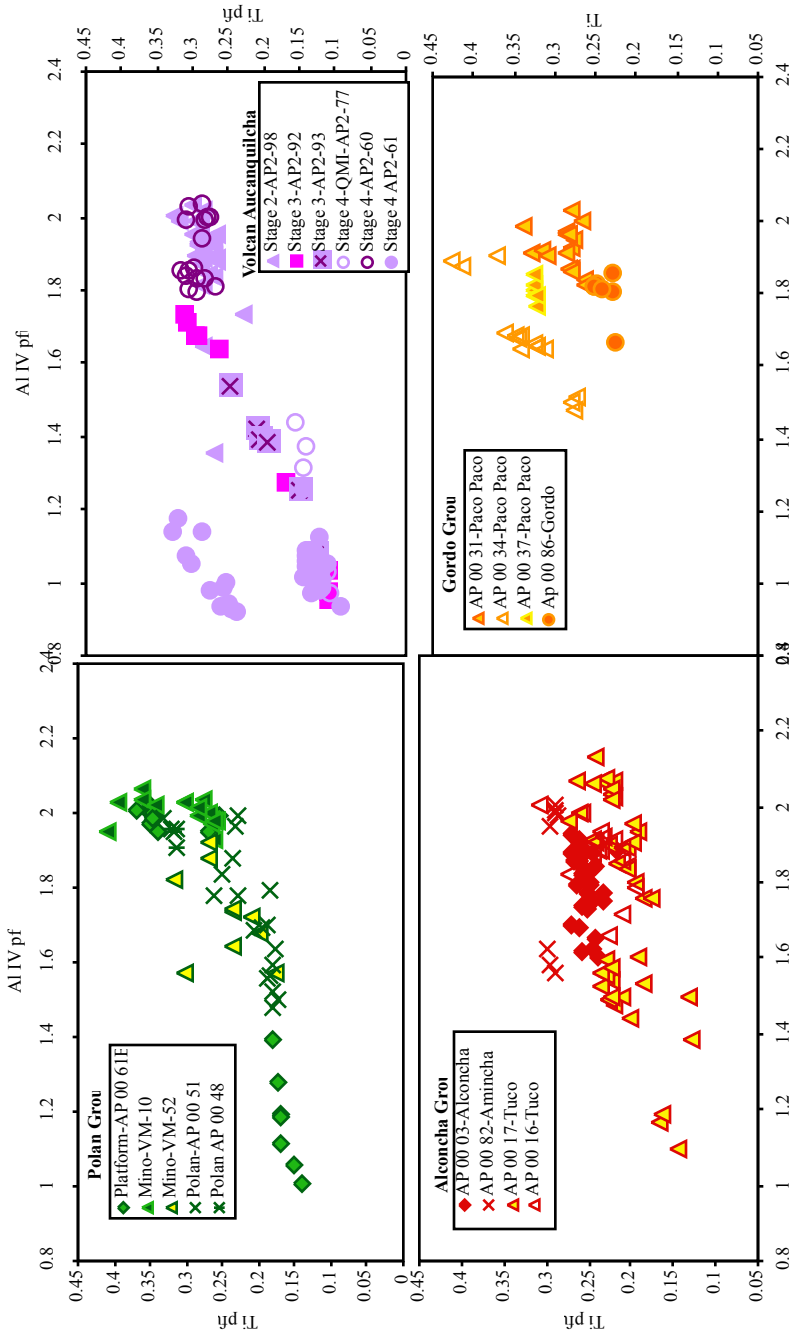


**Figure 22.**
Aluminum in amphiboles generally covaries with Ti pfu--higher aluminum amphiboles generally display higher
im. Variations in titanium has been used as an indcator of the influenceof temperatures, with steeper covariation indicating
ence of temperature changes.

### *Volatiles in amphibole:*

#### Sulfur:

Sulfur measured using SIMS ranges from 11 to 168 ppm. High and low S populations correlate to high and low Al populations. Samples with low $Al_{IV}$ have S<60ppm, and samples with high $Al_{IV}$ have S>80ppm. (Figure 23)

#### Fluorine:

There is a significant increase in the proportion of F in amphibole over the 11 million year history of the system independent of amphibole composition (Figures 24 & 25). F increases from 1250 to 1500 ppm from early groups, 1900 to 2400 ppm at Polán time and increases further to 2800 to 4200 ppm at Aucanquilcha.

#### Chlorine:

Cl in amphiboles ranges from 200 to 1800 ppm. Low aluminum amphiboles show a range of Cl from 300-1800ppm whereas higher aluminum amphiboles have more restricted and overall lower Cl (200-500 ppm) (Figure 26).

Both low and high aluminum amphiboles show both increases and decreases in chlorine from the core to rim. Low aluminum amphiboles often (but not always) show decreasing Cl towards the rim (AP-00-17-3). Higher aluminum amphiboles are also variable with no systematic chlorine correlations from core to rim; with some increasing (AP-00-16-6), some decreasing (AP-00-82-4) and some remaining more or less constant

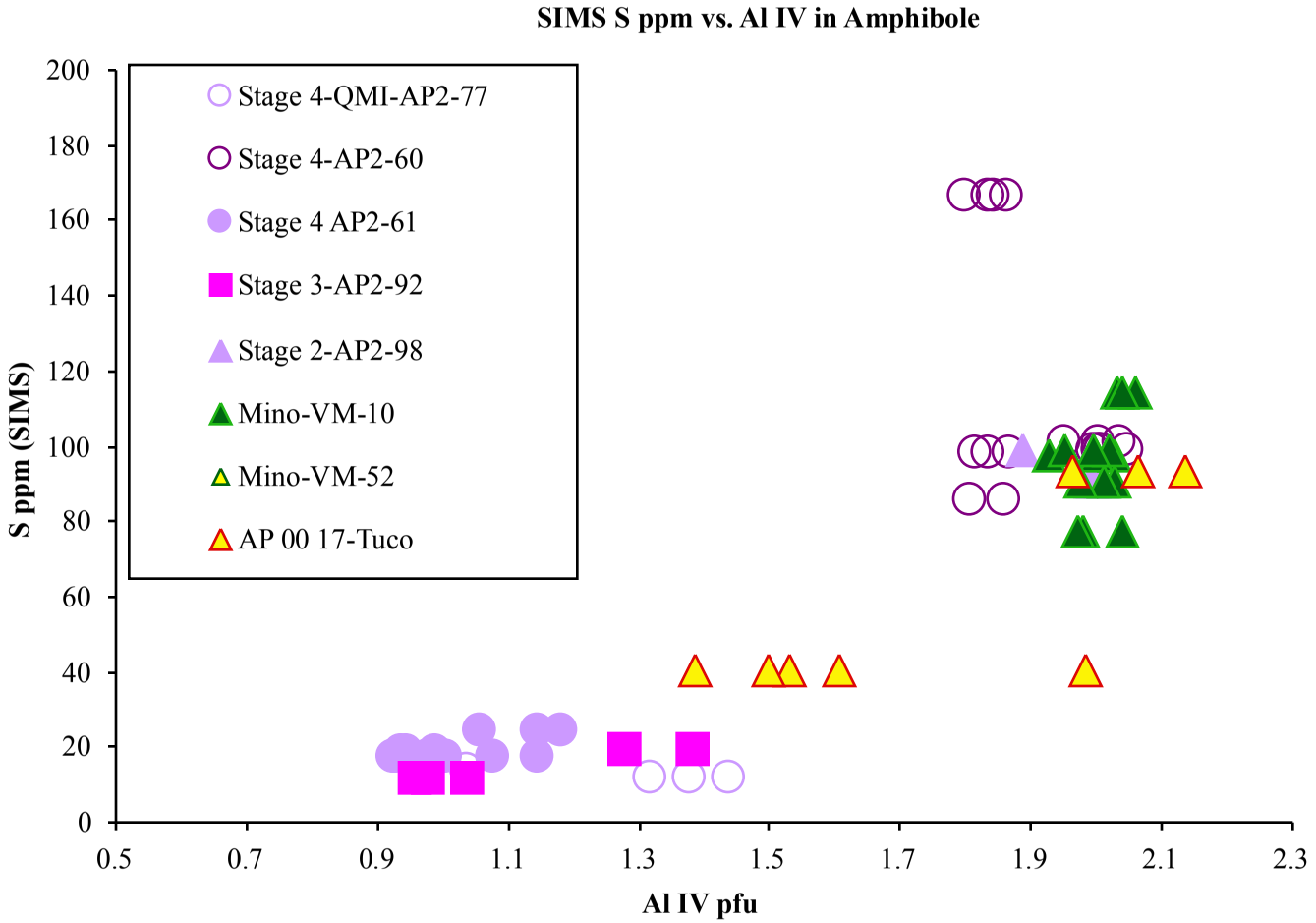


**Figure 23.**
**Aluminum in amphibole vs. sulfur in amphibole as measured by SIMS.**
ıminum amphiboles have lower sulfur than higher aluminum amphiboles.

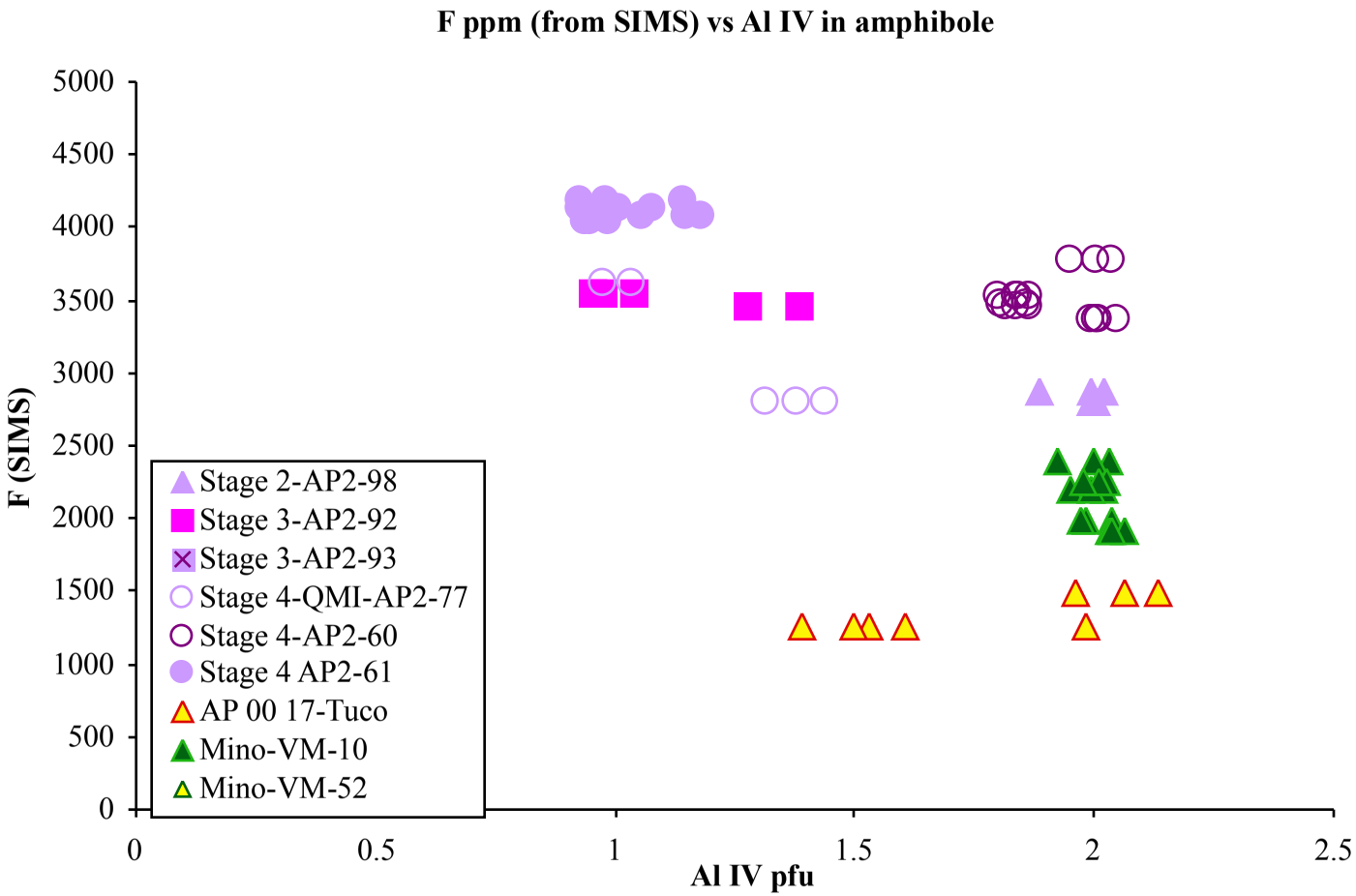


**Figure 24.**
**Amphibole vs Aluminum.**
Unlike sulfur, fluorine in amphibole and aluminum in amphibole are decoupled.

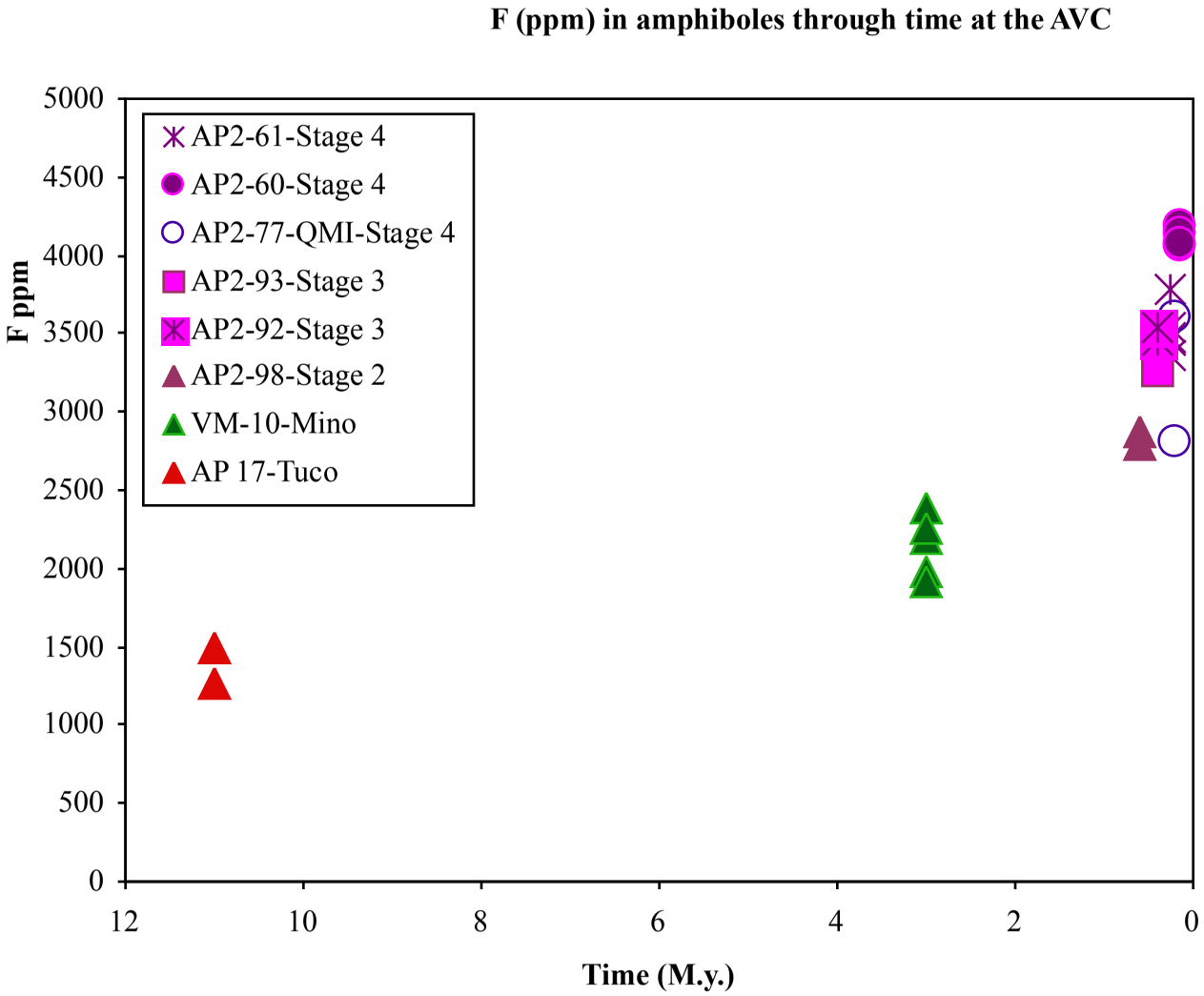


**Figure 25.**
**Fluorine through time.** Fluorine in amphiboles at the AVC increase in time independent of amphibole composition. Increases in F over the life of the magmatic system indicate the consumption of hydrothermally altered crust, as well as the the assimilation of plutonic precursors of the long-lived system.

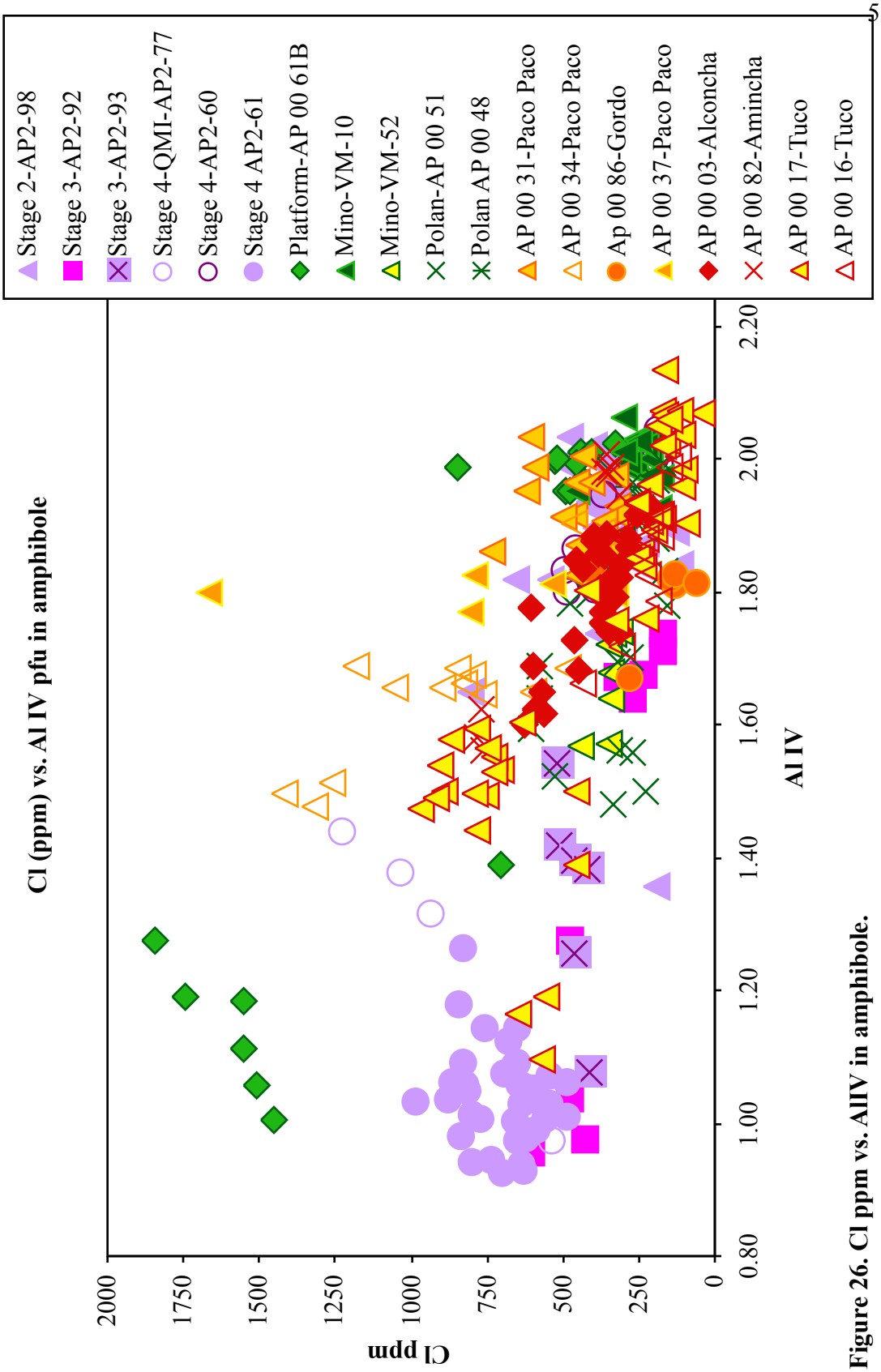


**Figure 26. Cl ppm vs. AlIV in amphibole.**

in Cl from core to rim (AP-00-04-4). In the Polan Group, Cl concentrations oscillate from core to rim, however the overall range of Cl variation in a single grain is small. The Polan Group overall has the lowest and most restricted chlorine of amphiboles in dacites. (The two QMI have the highest Cl concentrations measured for this study.)

**Water:**

The water concentration in amphiboles (measured using SIMS) varies from 0.6-1.5 wt% $H_2O$ in the early groups to 1.5-2.5 wt% at Volcan Aucanquilcha. Amphiboles with >2wt % $H_2O$ have the lowest aluminum and samples with <1wt% $H_2O$ had high aluminum (Figure 27).

***SIMS stable isotope data:***

$\Delta D$ values on amphiboles throughout the history of the system range from –168 ‰ to –41 ‰ (± 8 ‰). Correlation to aluminum in amphibole overall is poor but on the whole, low aluminum amphiboles have less depleted (less negative) $\delta D$ values than the high aluminum amphiboles (Table 3, Figure 28).

**Other Stable isotopes--amphibole, biotite and plagioclase:**

Oxygen isotope values reported by Klemetti 2005 in plagioclase range from 6.1 to 6.4, some of the lowest reported in the literature for the area.

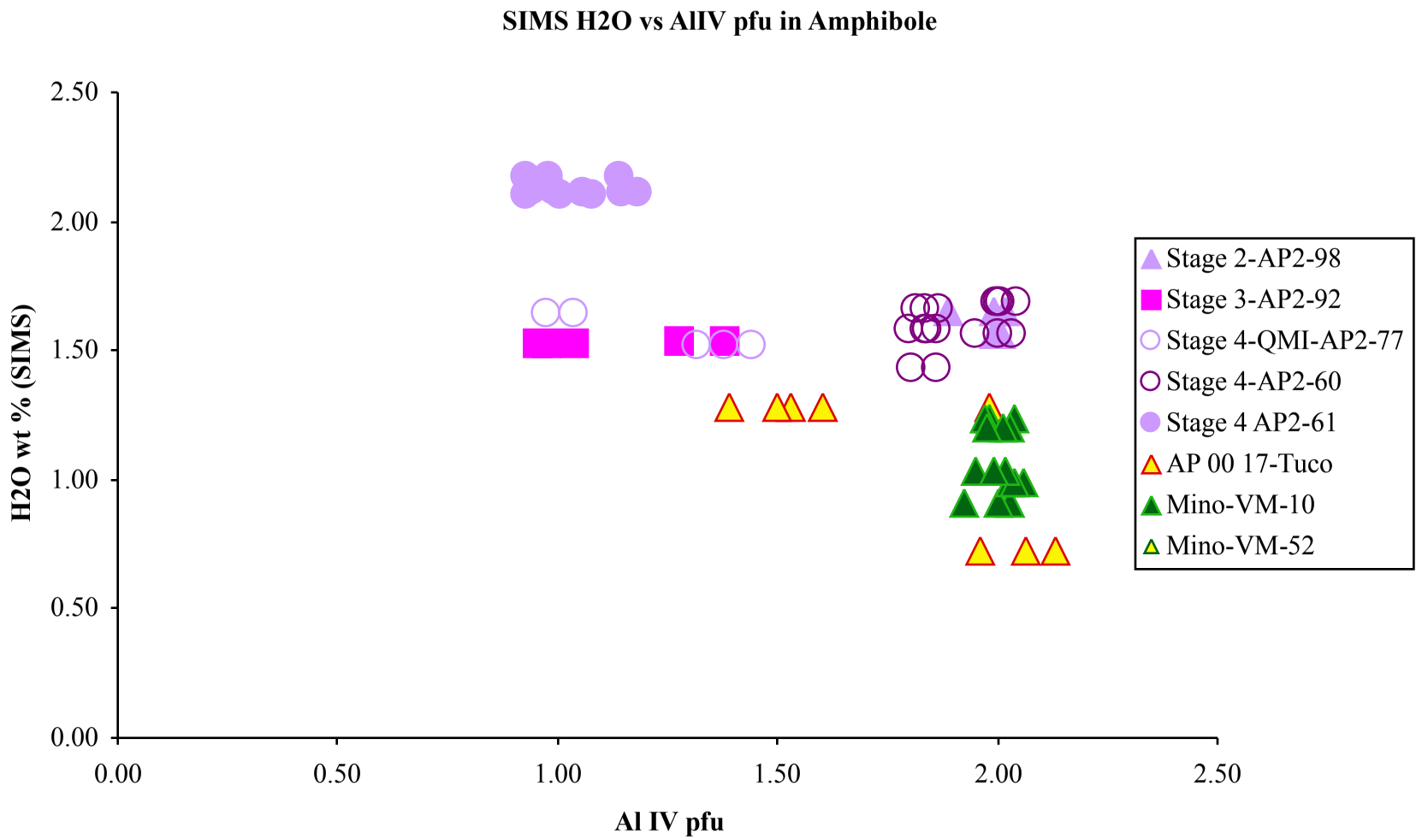


**Figure 27. Water in Amphibole vs Al IV.**

Low aluminum samples tend to have high water vaules, higher aluminum amphiboles have an intermediate to low water contents.

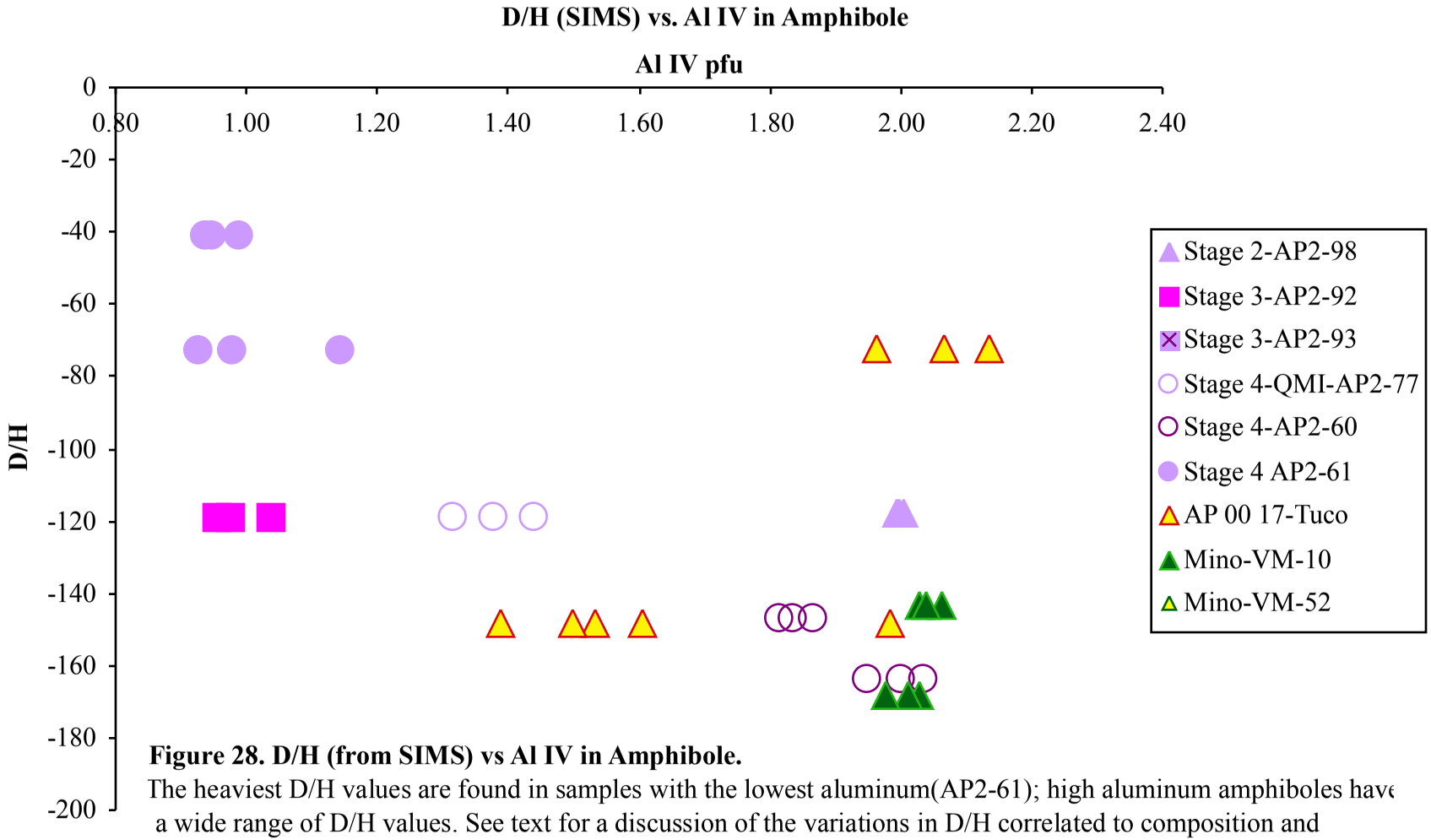


**Figure 28. D/H (from SIMS) vs Al IV in Amphibole.**
The heaviest D/H values are found in samples with the lowest aluminum(AP2-61); high aluminum amphiboles have a wide range of D/H values. See text for a discussion of the variations in D/H correlated to composition and volatiles in amphibole.

In this study, oxygen and hydrogen isotopes were measured on selected samples and their values are reported in the discussion. The isotopic value of fluids in equilibrium with the measured oxygen and hydrogen isotopes in amphibole, biotite and plagioclase were calculated at different temperatures based on the fractionation constants list in Table 5. The results of these calculations are reported in Table 6.

***Plagioclase Compositions:***

Plagioclase in the Alconcha Group range from $An_{20}$-$An_{80}$. (Figure 29). Plagioclase in the Gordo group span a similar but more restricted range, as determined by petrography and microprobe analyses by Layne Bennett (unpublished undergraduate research project, Oregon State University). Plagioclase from the Polan Group (excluding Mino which is more variable) range from $An_{38}$-$An_{78}$. Plagioclase compositions at Volcan Aucanquilcha have been reported to range from $An_{21}$-$An_{70}$ (Klemetti, 2005). This is not a comprehensive assessment of plagioclase variation at the AVC as most points for this study were selected as textural pairs to amphibole for geothermometry and geobarometry, (Table 7). For a more detailed reporting of plagioclase at the AVC see McKee, 2002, Klemetti 2005, and Plag data in appendix.

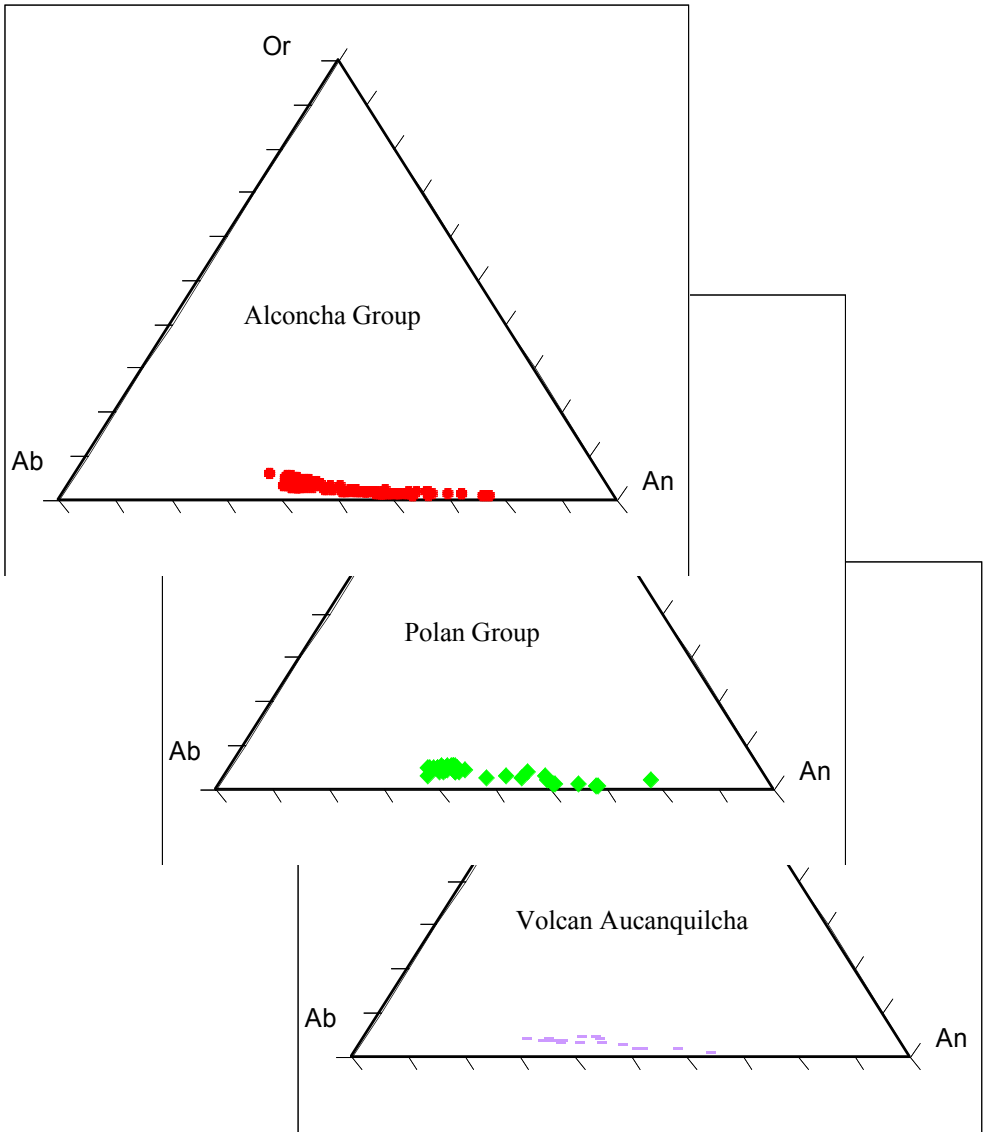


**Figure 29.**
Plagioclase ternary diagrams show selected plagioclase compositions from the AVC. As most plagioclase were selected as textural pairs to amphiboles, they do not necessarily encompass the entire compositional range of plagioclase for each age group. For a more detailed discussion of plagioclase compositions at Volcan Aucanquilcha and Mino see Klemetti, 2005 and McKee, 2002.

**Table Mineral-Water Oxygen isotope fractionations. where $10^3 \ln \alpha_{(mineral\text{-}water)} = A + B(10^6/T^2)$. An is mole fraction of anorthite in feldspar. For Zheng, $10^3 \ln \alpha_{(mineral\text{-}water)} = A^* 10^6/T^2 + B^*10^3/T + C$.**

| Mineral | Experimental Range | A | B | C | Reference |
|---|---|---|---|---|---|
| Plagioclase | 350-800 | (-3.41-.014An) | 2.91-.76An | | O'Neil and Taylor, 1967 |
| Feldspar | 500-800 | -3.7 | 3.13-1.04An | | Bottinga and Javoy, 1973 |
| Hornblende | 0-1200 | 3.89 | -8.56 | 2.43 | Zheng, 1993 |
| Pargasite | 0-1200 | 3.77 | -8.99 | 2.51 | Zheng, 1993 |
| Biotite | 0-1200 | 3.84 | -8.76 | 2.46 | Zheng, 1993 |

**Table Oxygen isotope fractionation between the whole mineral and the hydroxyl group where 10^3 ln $\alpha = A \times 10^6/T^2 + (B \times 10^3/T) + C$.**

| Mineral | Experimental Range | A | B | C | Reference: |
|---|---|---|---|---|---|
| Biotite | 0-1200 | 1.14 | 4.89 | -2.08 | Zheng, 1993 |
| Hornblende | 0-1200 | 1.22 | 5.21 | -2.22 | Zheng, 1993 |

**Table Constants for the fractionation of hydrogen isotopes between minerals and water according to the equation $10^3 \ln \alpha_{(mineral\text{-}water)} = A + B(10^6/T^2)$ .**

| **Mineral** | **Experimental Range** | **A** | **B** | **Reference:** |
|---|---|---|---|---|
| Biotite | 450-800 | -2.8 | -21.3 | Suzuoki and Epstein, 1976 |
| Hornblende | 450-800 | 7.9 | -23.9 | Suzuoki and Epstein, 1976 |
| All minerals | $1000 \ln \alpha_{(mineral\text{-}water)} = 28.2\text{-}22.4(10^6/T^2) + (2X_{Al} - 4X_{Mg} - 68X_{Fe})$ Where X is mole fraction of element in mineral | | | Suzuoki and Epstein, 1976 |
| Ferroan Pargasitic Hornblende | 350-850 | -23.1 +/- 2.5 | | Graham et al, 1984 |
| Ferroan Pargasitic Hornblende | 850-950 | 1.1 | -31 | Graham et al, 1984 |

Fractionation constants used for the calculation of fluids in equilbrium with mineral phases, sources cited in tables.

**Table 6. Calculated Plagioclase Oxygen Data**
**Calculated Oxygen composition in equilibrium with plagioclase phenocrysts**

| | | Temp (K) | 773 | 823 | 873 | 923 | 973 | 1023 | 1073 | 1123 | 1173 | 1223 | 1273 | 1323 |
|---|---|---|---|---|---|---|---|---|---|---|---|---|---|---|
| | | **Temp C** | **500** | **550** | **600** | **650** | **700** | **750** | **800** | **850** | **900** | **950** | **1000** | **1050** |
| | | **1000 ln alpha** | **-0.82** | **-0.72** | **-0.64** | **-0.58** | **-0.52** | **-0.47** | **-0.43** | **-0.39** | **-0.36** | **-0.33** | **-0.30** | **-0.28** |
| | | | | | | | | | | | | | | |
| | | **Oxygen ‰ (WSU)** | **Calculated Oxygen composition in equilibrium with plagioclase phenocrysts** | | | | | | | | | | | |
| AP2-47 | Stage 1 | 5.73 | 6.55 | 6.45 | 6.37 | 6.31 | 6.25 | 6.20 | 6.16 | 6.12 | 6.09 | 6.06 | 6.03 | 6.01 |
| AP2-96 | Stage 2 | 6.23 | 7.05 | 6.95 | 6.87 | 6.81 | 6.75 | 6.70 | 6.66 | 6.62 | 6.59 | 6.56 | 6.53 | 6.51 |
| AP2-100 | Stage 2 | 6.02 | 6.84 | 6.74 | 6.66 | 6.60 | 6.54 | 6.49 | 6.45 | 6.41 | 6.38 | 6.35 | 6.32 | 6.30 |
| AP2-92 | Stage 3 | 6.47 | 7.29 | 7.19 | 7.11 | 7.05 | 6.99 | 6.94 | 6.90 | 6.86 | 6.83 | 6.80 | 6.77 | 6.75 |
| AP2-77 (qmi) | Stage 4 | 6.66 | 7.48 | 7.38 | 7.30 | 7.24 | 7.18 | 7.13 | 7.09 | 7.05 | 7.02 | 6.99 | 6.96 | 6.94 |
| AP2-61 | Stage 4 | 6.57 | 7.39 | 7.29 | 7.21 | 7.15 | 7.09 | 7.04 | 7.00 | 6.96 | 6.93 | 6.90 | 6.87 | 6.85 |

$$1000 \ln \alpha = D\frac{(10^6)}{T^2} + E\frac{(10^3)}{T} + F$$

**D: -0.490; E: 0.00; F: 0.00**

Zhao, Z. F., & Zheng, Y. F. (2003). Calculation of oxygen isotope fractionation in magmatic rocks, Chemical Geology, v. 193, 59-80.

**Table 7. Selected Plagioclase amphibole pairs**

| Sample # | Aucanquilcha Stage 4 AP2-61 | Aucanquilcha Stage 4 AP2-60 | Aucanquilcha Stage 2 AP2-98 | Aucanquilcha Stage 2 Ap2-98 | Polan AP0051 | Polan AP0051 | Polan AP0051 | Polan AP0048 | Mino VM-52 | Mino Vm-99-8 | Mino Vm-99-8 | Mino VM99-26 | Alconcha AP0003 | Tuco AP00 17 | Tuco AP 00 17 | Tuco AP00 17 | Tuco AP00 17 |
|---|---|---|---|---|---|---|---|---|---|---|---|---|---|---|---|---|---|
| **Age** | 0.01 | 0.1 | 0.4 | 0.4 | 4 | 4 | 4 | 4.5 | 5 | 5.5 | 5.5 | 6 | 9 | 11 | 11 | 11 | 11 |
| **Plag** | plag 13 rim | core plag 2 | rim | core plag | plag pt 2 | plag pt 2 | c1rim | | Rim plag 1 | 417-inclusion in blac type | 389-in breakdow | Line 464 | | rim | core | Inclusion | amph 8, plag |
| **XAb** | 0.598 | 0.479 | 0.575 | 0.55 | 0.65 | 0.55 | 0.47 | 0.5 | 0.56 | 0.278 | 0.483 | 0.38 | 0.542 | 0.69 | 0.65 | 0.55 | 0.47 |
| **X An** | 0.366 | 0.502 | 0.378 | 0.403 | 0.28 | 0.41 | 0.51 | 0.47 | 0.4 | 0.705 | 0.45 | 0.604 | 0.43 | 0.27 | 0.31 | 0.43 | 0.5 |
| **T (+/- 30)** | **751** | **864** | **862** | **762** | **777** | **849** | **873** | **890** | **857** | **857** | **816** | **851** | **857** | **786** | **792** | **748** | **848** |
| **P (kbar) (+/- 0.6 kbar)** | **1.16** | **1.79** | **1.37** | **1.53** | **3.34** | **3.24** | **1.76** | **1.30** | **1.71** | **3.06** | **4.46** | **2.44** | **1.25** | **5.13** | **5.54** | **1.75** | **2.32** |
| **SiO2** | 50.07 | 41.62 | 42.85 | 46.58 | 44.93 | 41.95 | 43.30 | 42.65 | 43.73 | 43.91 | 42.80 | 43.68 | 44.35 | 42.51 | 42.79 | 48.29 | 44.53 |
| **TiO2** | 1.15 | 2.94 | 2.56 | 1.27 | 1.73 | 2.15 | 2.33 | 2.97 | 2.18 | 2.48 | 2.57 | 2.06 | 2.26 | 2.10 | 2.10 | 1.57 | 1.86 |
| **Al2O3** | 6.35 | 11.42 | 10.64 | 6.77 | 9.94 | 12.91 | 12.07 | 12.47 | 11.05 | 13.22 | 13.00 | 11.58 | 10.25 | 13.14 | 14.08 | 7.07 | 11.74 |
| **FeO** | 11.24 | 14.31 | 11.62 | 12.12 | 11.78 | 14.02 | 12.53 | 11.35 | 12.77 | 7.75 | 7.94 | 6.36 | 12.34 | 12.37 | 12.35 | 12.06 | 12.73 |
| **MgO** | 16.49 | 14.50 | 15.37 | 14.50 | 15.19 | 13.25 | 14.20 | 14.97 | 14.44 | 16.04 | 14.79 | 15.98 | 14.82 | 15.52 | 14.56 | 16.70 | 15.22 |
| **MnO** | 0.42 | 0.12 | 0.15 | 0.37 | 0.23 | 0.16 | 0.29 | 0.15 | 0.20 | 0.15 | 0.12 | 0.07 | 0.32 | 0.14 | 0.14 | 0.34 | 0.36 |
| **CaO** | 11.48 | 10.92 | 11.14 | 11.61 | 11.14 | 10.68 | 10.95 | 11.48 | 11.37 | 10.13 | 11.17 | 11.00 | 11.15 | 11.32 | 11.85 | 11.59 | 11.09 |
| **Na2O** | 1.27 | 2.27 | 2.18 | 1.13 | 2.01 | 2.28 | 2.31 | 2.46 | 2.38 | 2.05 | 2.54 | 2.57 | 2.00 | 2.25 | 2.23 | 1.49 | 1.94 |
| **K2O** | 0.46 | 0.60 | 0.52 | 0.56 | 0.44 | 0.51 | 0.48 | 0.58 | 0.51 | 0.20 | 0.53 | 0.44 | 0.67 | 0.44 | 0.46 | 0.53 | 0.49 |
| **Sum** | 99.01 | 98.70 | 97.04 | 94.91 | 97.42 | 97.93 | 98.48 | 99.26 | 98.67 | 96.07 | 95.61 | 93.97 | 98.21 | 99.81 | 100.58 | 99.71 | 99.99 |
| **Formula per Holland and Blundy, 1994** | | | | | | | | | | | | | | | | | |
| **Si** | 7.06 | 6.06 | 6.24 | 6.92 | 6.50 | 6.10 | 6.23 | 6.09 | 6.29 | 6.33 | 6.26 | 6.45 | 6.40 | 6.02 | 6.01 | 6.84 | 6.29 |
| **Aliv** | 0.94 | 1.94 | 1.76 | 1.08 | 1.50 | 1.90 | 1.77 | 1.91 | 1.71 | 1.67 | 1.74 | 1.55 | 1.60 | 1.98 | 1.99 | 1.16 | 1.71 |
| **Alvi** | 0.12 | 0.02 | 0.07 | 0.11 | 0.19 | 0.31 | 0.28 | 0.19 | 0.17 | 0.58 | 0.50 | 0.46 | 0.14 | 0.21 | 0.34 | 0.03 | 0.24 |
| **Ti** | 0.12 | 0.32 | 0.28 | 0.14 | 0.19 | 0.23 | 0.25 | 0.32 | 0.24 | 0.27 | 0.28 | 0.23 | 0.25 | 0.22 | 0.22 | 0.17 | 0.20 |
| **A site** | | | | | | | | | | | | | | | | | |
| **Na** | 0.17 | 0.60 | 0.48 | 0.19 | 0.39 | 0.45 | 0.45 | 0.52 | 0.48 | 0.39 | 0.47 | 0.47 | 0.37 | 0.53 | 0.48 | 0.36 | 0.40 |
| **K** | 0.08 | 0.11 | 0.10 | 0.11 | 0.08 | 0.09 | 0.09 | 0.10 | 0.09 | 0.04 | 0.10 | 0.08 | 0.12 | 0.08 | 0.08 | 0.10 | 0.09 |

**Plagioclase-Amphibole Geobarometry and Geothermometry:**

Coexisting pairs of plagioclase and amphibole were analyzed on the microprobe and barometry and thermometry of the magmatic system were determined after Holland and Blundy 1994 and Anderson 1995 (Figure 30) (Table 7). Pairs were selected to have textural relationships reflecting likely equilibrium. These textures include a) plagioclase inclusion in amphibole, b) intergrown plagioclase amphibole pairs and in a few cases, c) groundmass plagioclase were paired with the rims of equilibrium amphiboles.

The following equations were used to iteratively calculate pressure and temperature for plagioclase amphibole pairs reported (Table 7).

***Temperature iteration:***

$$Temperature\ (+/-\ 30) = (78.44+Y_{Ab\text{-}An}-33.6X^{M4}_{Na}-(66.8-2.92P)*X^{M2}_{Al} +78.5X^{T1}_{Al}+9.4X^{A}_{Na})/(0.0721-R*ln((27X^{M4}_{Na}*X^{T1}_{Si}*X^{Plag}_{An}/64X^{M4}_{Ca}*X^{T1}_{Al}*X^{Plag}_{Ab})))$$

Where $Y_{Ab\text{-}An}$ is given by: $X_{Ab}>0.5$ then $Y_{Ab\text{-}An}=3.0$ kJ, otherwise, $Y_{Ab\text{-}An}=12.0(2.0\ X_{Ab}-1)+3.0$ kJ: and where T is temperature in Kelvin, P is the pressure in kbar and X* denotes the molar fraction of species in the crystallographic site. (Holland and Blundy, 1994)

***Pressure iteration:***

$$P(kbar)(+/-\ 0.6\ kbar) = 4.76\ Al(total) - 3.01 - \{[T-675]/85\}*\{0.53\ Al(total) + 0.005294\ [T-675]\}$$

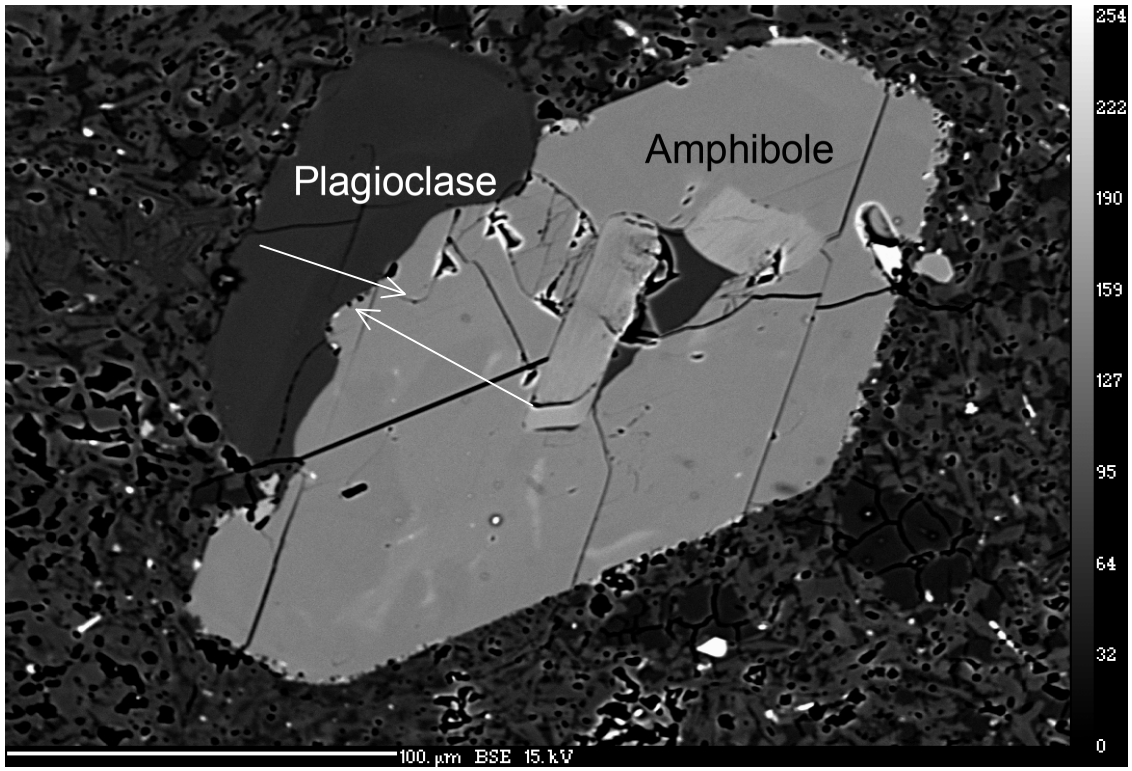


**Figure 30.**

**Representative Plagioclase-Amphibole Pair**

Amphibole-plagioclase selected from geothermometry and barometry from Volcan Aucanquilcha, Stage 4. Calculated P/T for this pair are 756 C (+/-30), and 1.15 kbar (+/- 0.4) (after Blundy and Holland, 1994 and Anderson and Smith 1995). Microprobe transects are noted with white arrows.

Where T is in C and Al(total) is the stoichiometric total of all Al in amphibole (Anderson and Smith 1995).

***Summary of barometry and thermometry results:***

Overall the amphiboles in dacites form anywhere from 0.7 kbar to 6.4 kbar, over a range of temperature from 715-915 °C. This represents a depth in the crust of ~2 to 20 kilometers. In the Alconcha Group, there are two amphibole pressure populations, the first a shallower amphibole with low temperatures (750-800 °C) and a higher pressure amphibole population of similar temperatures. These distinct amphibole populations imply that amphiboles crystallize in two distinct P/T regimes and thus either mixing of distinct magmas or stalling and differentiation in the crust is required (Figure 31).

In the Polan Group, calculated pressures for amphiboles range from ~1-3 kbar and ~ 775-875 °C. (At Mino this value is 1.5-4.7 kbar with temperatures from 800-875°C).

At Aucanquilcha amphiboles in dacites (not QMI) range in temperature from ~725-875 °C (similar to the earliest stages of volcanism). However, unlike the earliest eruptions, the calculated pressures are shallower (~0.5-3 kbar) and in general more restricted than the Alconcha and Gordo Group. The highest calculated temperatures come from amphiboles in the quenched mafic inclusion AP-00-61B, (and less so AP2-77.)

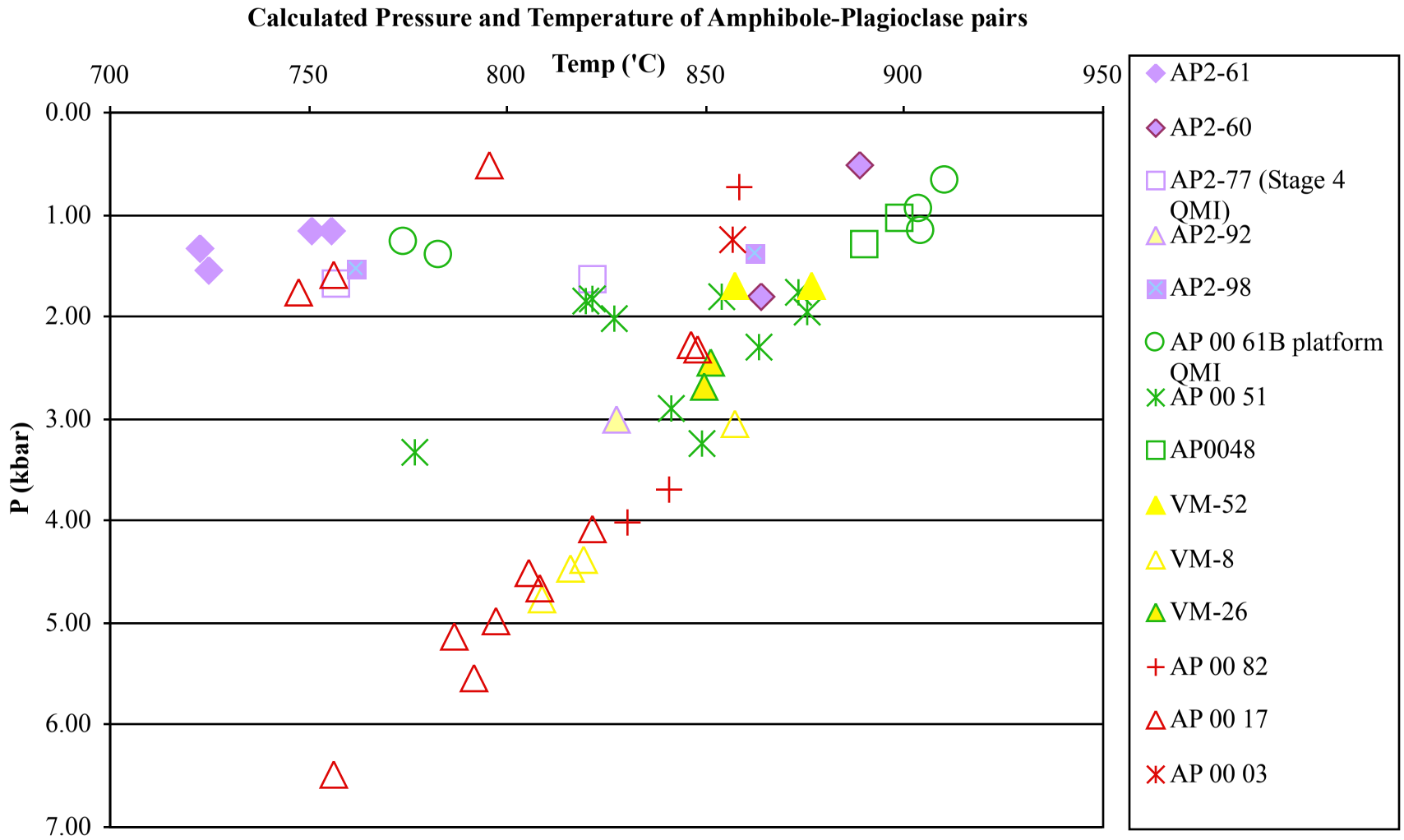


**Figure 31. Calculated Pressure and Temperature of Amphiboles in dacites at the AVC.**

## DISCUSSION:

### *Amphibole Pressure, Temperature and Composition:*

The variation of calculated pressure and temperature of amphiboles in dacites from the volcanic cluster inform the development of the magmatic plumbing at the long-lived AVC. In the Alconcha Group, the magma is staged over a wide range of pressure and temperatures. The thermal, barometric and compositional heterogeneity observed early in the system in erupted dacites imply greater variability in the staging of the magmatic system. Pyroxene cored amphiboles common in the early stages of the system indicate that warmer, more mafic magmas were flushed by cooler or more hydrous magmas.

As the system matured into the Polan Group amphiboles indicate crystallization over a more restricted pressure range in an overall thermally coherent area in the crust. Concentric zoning of amphiboles from the Polan Group indicate stirring, convection and /or differentiation of a host silicate liquid. This thermal, barometric and compositional coherence also coincides with centralizing of volcanic vents towards the heart of the system, and an increase in the volume of erupted material. At this stage, dacite is the dominant eruptive product, and andesites become present only as inclusions in dacites. Cored amphiboles at this stage are uncommon. Only at Mino, (on the periphery of the system) do we find cored amphiboles, and andesites erupting as lavas during this dominantly dacitic eruptive period.

The spatial distribution of eruptive products as well as the dominance of dacitic eruptions implies the presence of a density filter, or lid of material, which prevents less

differentiated material from escaping. This could be due to, 1) the presence of a dacitic magma body or, 2) a zone of 'thermally matured crust' or crystal mush. This thermally mature crust would have been processed by repeated injections of material (and heat) over at least 7 million years of protracted volcanism and while not forming a coherent liquid body, may form a heated crustal zone that is similar compositionally and physically. This crustal zone when heated by subsequent injections could provide material and pathways for future eruptions. Whether the AVC supports a zone of crystal mush or a coherent magma body, the textural, thermal and compositional data on amphiboles indicate that at the time of the Polan Group, erupted mineral grains experienced prolonged equilibrium in a silicate liquid. At Aucanquilcha, the system becomes increasingly silicic and dacites erupt only from shallower areas in the crust. Texturally these young amphiboles are diverse and reacted amphiboles are commonly found in the same sample with rapidly crystallized hopper-textured amphiboles, implying that an amphibole-bearing reservoir is being flushed. At this stage, amphiboles are most commonly cored with biotite implying that the system has cooled, or lost water due to degassing, and it is the flushing of the system with warmer or more hydrous pulses of magma which prompt eruption.

The amphibole pressure and temperature data combined with the amphibole textural data from dacites indicate a transition of magmatic depths and physical regimes. Initially the dacitic magmas are sourced from variable depths as well as variable temperature regimes within the crust. Overtime the system becomes more thermally coherent, and the magmas are sourced over a relatively restricted depth. Most amphiboles from this stage

indicate periods of stagnation or stewing at or near equilibrium- a texture that is not found in earlier (or later) stages.

Temperatures of erupted amphiboles in dacites are variable throughout the life of the system but have the largest range early and late. These changes in amphibole temperatures are consistent with a model that involves initially heterogeneous crust intruded by batches of magma, resulting in thermally mature crust after repeated injections. Temperatures are highest during the Polan time when single complexly zoned amphiboles indicate stirring (on a scale of ~1kbar) of the magmatic reservoir. While temperatures are consistently the highest at this stage, the temperature range is the most restricted of any group indicating a coherent and voluminous system. The high temperatures in the Polan aged samples are consistent with high Ti in zircon (Walker personal communication).

Variations in aluminum versus various cations in amphiboles have been used by various authors as indicators of intensive parameters in magma like pressure, temperature, $fO_2$ as well as composition of the melt. In this study it is borne out that aluminum alone in amphibole is not a proxy for pressure and that it is key to pair amphibole data with information from equilibrium phases, in this case plagioclase (c.f. Bachmann 2004) (Figure 32). In the case of the AVC, an assumption that Al is a proxy for pressure could lead to the assumption that the Volcan Aucanquilcha amphiboles are barometrically distinct, when in fact they appear to come from similarly shallow reservoirs, distinguished instead by differences in temperature.

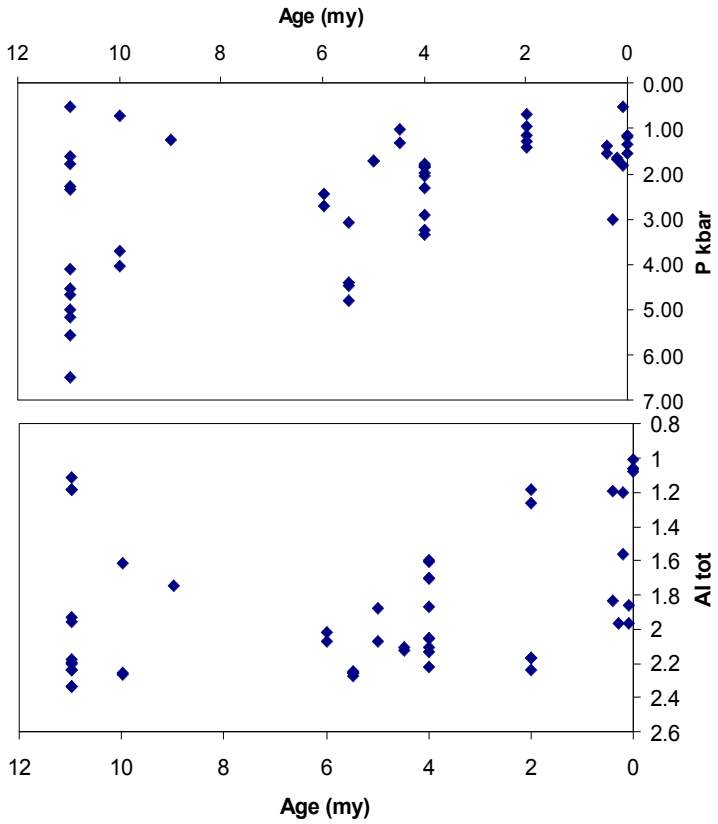


**Figure 32.**
**Aluminum total vs age combined with calculated pressure vs. age**.

In previous studies, total aluminum has been used as a proxy for pressure of amphibole formation. This dataset emphasizes the importance of using other factors to calculate the pressure associated with amphibole formation: in this case the composition of paired plagioclase was used to determine the pressure of amphibole formation. An assumption that aluminum in amphibole is a proxy for pressure of amphibole formation could lead to inaccurate interpretations regarding the pressure (and inferred depth) of amphibole formation, particularly in the youngest amphiboles from the AVC.

***Volatile Discussion:***

Volcan Aucanquilcha consistently taps a shallower reservoir than the Polan Group, and unlike the earliest Alconcha Group, amphiboles from deeper magmatic reservoirs are not erupted. Over the 11 million year history of the AVC, F increases independent of amphibole composition. The increase in F over the life of the magmatic system indicates that the same area in the crust is being tapped, and that this area is likely to be F-rich and hydrothermally altered. It appears that the top of the magmatic system, enriched in F (during the Polan time) is now at the same level in the crust as the source of the Aucanquilcha dacites, implying that they system is cannibalizing the plumbing system and surrounding crust of the precursory stages. This is supported by the presence of old (>11 million year) xenocrystic zircon crystals present in the young lavas (Walker, personal communication).

Unlike fluorine concentrations, which change temporally, chlorine and sulfur concentrations appear dependent on amphibole composition. Cl concentrations are variable, but more restricted for high aluminum amphiboles than low aluminum amphiboles. Variations in Cl from core to rim can be related to eruption dynamics. At the AVC, correlation of Cl to Mg/(Mg+Fe) in some samples indicate simultaneous degassing of Cl and crystallization, whereas in other samples, Cl and Mg# seem to be decoupled speaking to the complexity of the large-scale magmatic systems.

Like chlorine, sulfur in amphiboles seems to be tied to aluminum content, with low aluminum amphiboles having significantly less S than high aluminum amphiboles. These low sulfur samples are inferred to come from shallower depths as all low

aluminum amphiboles in this study were shallow. Despite the fact that high aluminum samples can form in either high or low pressure regimes, the samples measured on SIMS with high sulfur correspond to mineral samples with high calculated pressures (ex. AP-00-17). This is also true for samples from Volcan Aucanquilcha. Overall the amphiboles from Volcan Aucanquilcha form shallower than in other stages, however within the same rock sample, the mineral with the lower calculated pressure has lower S, than the amphibole with the higher calculated pressure (and S). This connection within a sample between calculated pressure and S content suggests the loss of S as a vapor phase as the magma ascends, or the crystallizationof an S-bearing phase as the magmas reach shallower areas within the crust.

***Stable isotope discussion:***

The calculated temperatures of amphiboles can then be used to select the likely range of isotopic values for fluids in equilibrium with the mineral phases.

The fluid in equilibrium with AP2-61 has hydrogen isotopes that range from –28 to –37 ‰ in biotite, and –39 ‰ in amphibole as measured on the TCEA. The range of δD in amphibole from AP2-61 as measured on SIMS ranges from –24 to –58 ‰. (Values measured on the TCEA commonly fall within the range of SIMS samples, most likely because the SIMS analyses are on individual grains, whereas the TCEA analyses are performed on multiple grains—of variable compositions.) These are the heaviest δD values recorded at the AVC, and imply the onset of a hydrothermal system and the

assimilation of hydrothermally altered crust. In some of the oldest samples (eg. AP-00-17), δD of fluid in equilibrium ranges from –57 to –137 ‰ reinforcing the idea that initially the magmatic system is interacting with isotopically distinct and relatively undegassed reservoirs.

Oxygen isotopes in biotites at AP2-61 range from 7.5-8.0 ‰, with a fluid in equilibrium of 10-10.5 ‰. Values for fluid in equilibrium with amphiboles in the same sample have equilibrium fluid values from 5.1 ‰ to 5.5 ‰. The calculated water in equilibrium with plagioclase is 7.1 ‰, and this sample overall has some of the heaviest $\delta^{18}O$ (and δD) for Volcan Aucanquilcha. The heavy values for oxygen isotopes reinforces the notion that the most recent volcanic activity involves the incorporation of hydrothermally altered crust, and possibly its own magmatic precursors.

**Conclusions:**

***Correspondence of amphibole texture and composition:***

Overall, it was found that there is no correlation between textural type and compositional variation of the amphibole, i.e. thin-rimmed mineral grains are not always of the same compositional type (Figure 33). Textural variations within a single sample could however be correlated to compositional variations. For example, in sample AP0017-Tuco, ‘disequilibrium’ type textures are found as compositional outliers for

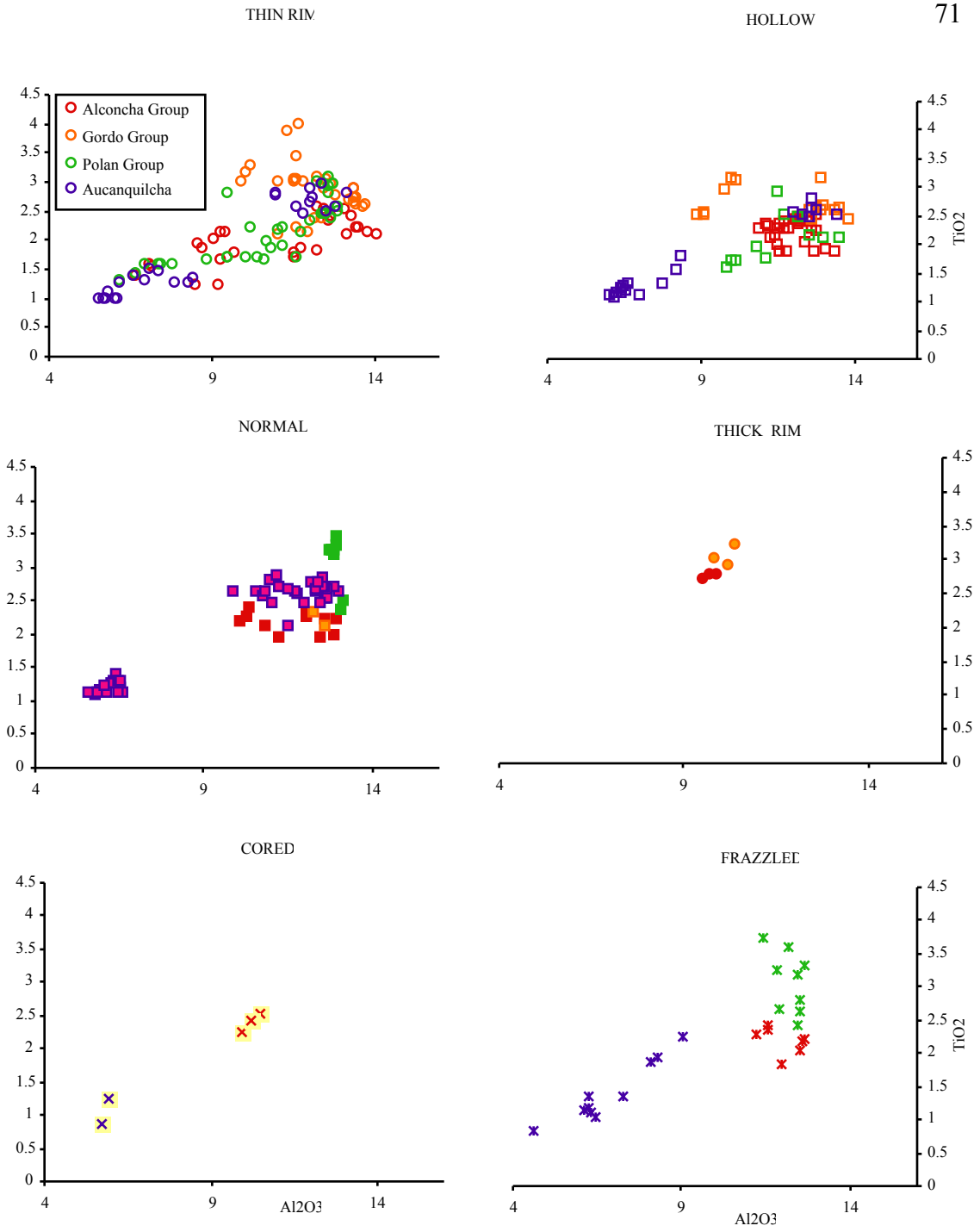


**Figure 33.**
**Compositional variety of amphibole textural types at the AVC.**
Overall there is no correlation between compositional type and compositional variation, (e.g.) amphiboles of the same textural type have wide ranges of compositions.

amphiboles within the volcanic center. This pattern is repeated in other age groups (Figure 34), where amphiboles with disequilbrium textures including thick rims and cores of other mineral phases are often compositionally distinct from equilibrium amphiboles.

***Evolution of the magmatic underpinnings of the AVC***

The changes in the amphiboles over time inform the development of the volcanic underpinnings at the AVC. An apparent lid or density cap develops over the system by the time of the Polan Group as indicated by, 1) the homogeneity in eruptive products, 2) the homogeneity in amphibole textures, and compositional zonation of the phase and 3) the generally restricted pressure and the warmer, more stable temperatures calculated for this stage.

The transition to an integrated magma system at shallow levels corresponds to an increase in the abundance and occurrence of amphiboles in dacite. Early in the evolution of the system amphiboles initiate in thermally and barometrically discrete regions. In time, coincident with an increase in the eruption rate, it appears that the magma system becomes more integrated and erupts thermally distinct yet barometrically similar amphiboles. At the final stage of volcanism, where equilibrium textures are most abundant, amphiboles in dacites form in relatively shallow reservoirs, consuming the magmatic precursors at variable temperatures.

The thermal evolution of the system is also reflected in the textrual changes in amphiboles in dacites over the 11 mllion year life of the volcanic system (Figure 35).

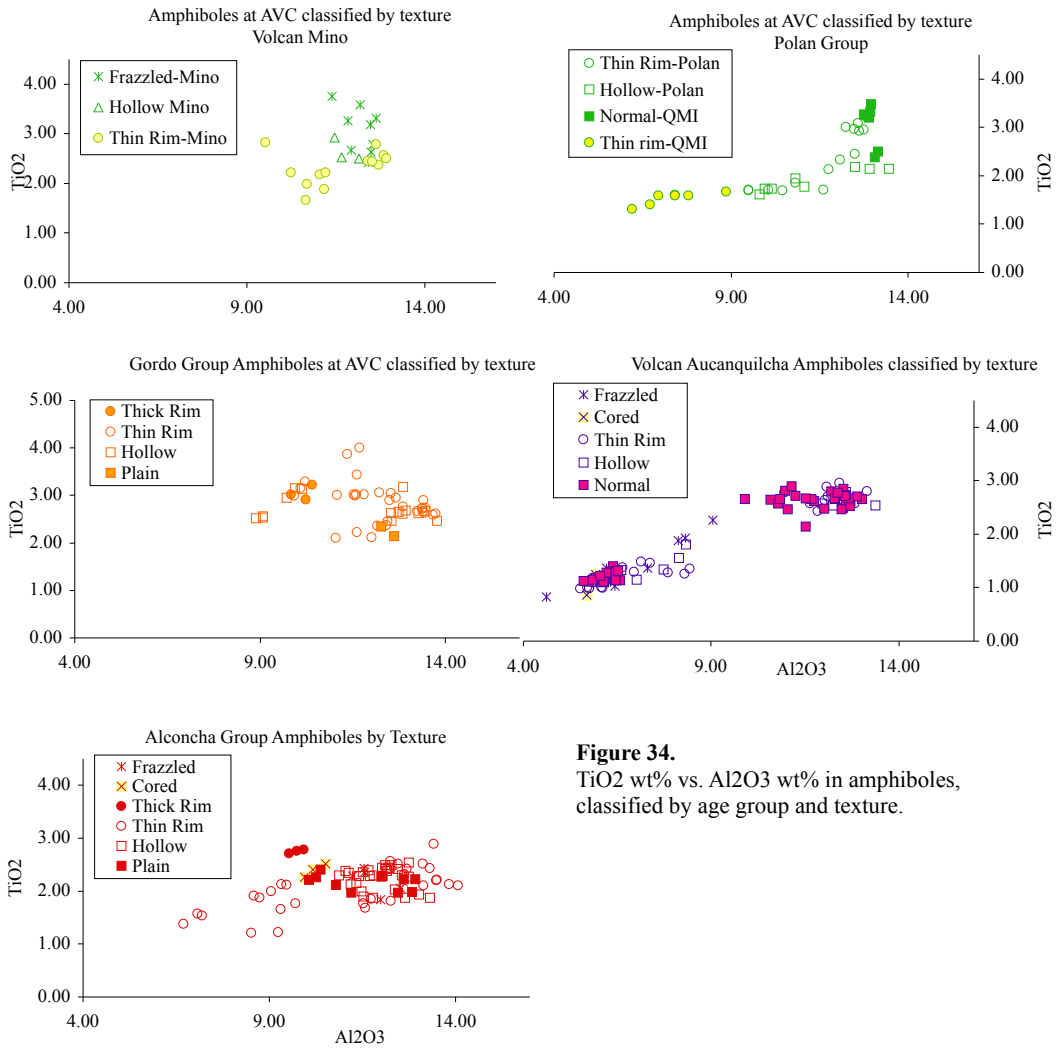


**Figure 34.**
TiO2 wt% vs. Al2O3 wt% in amphiboles, classified by age group and texture.

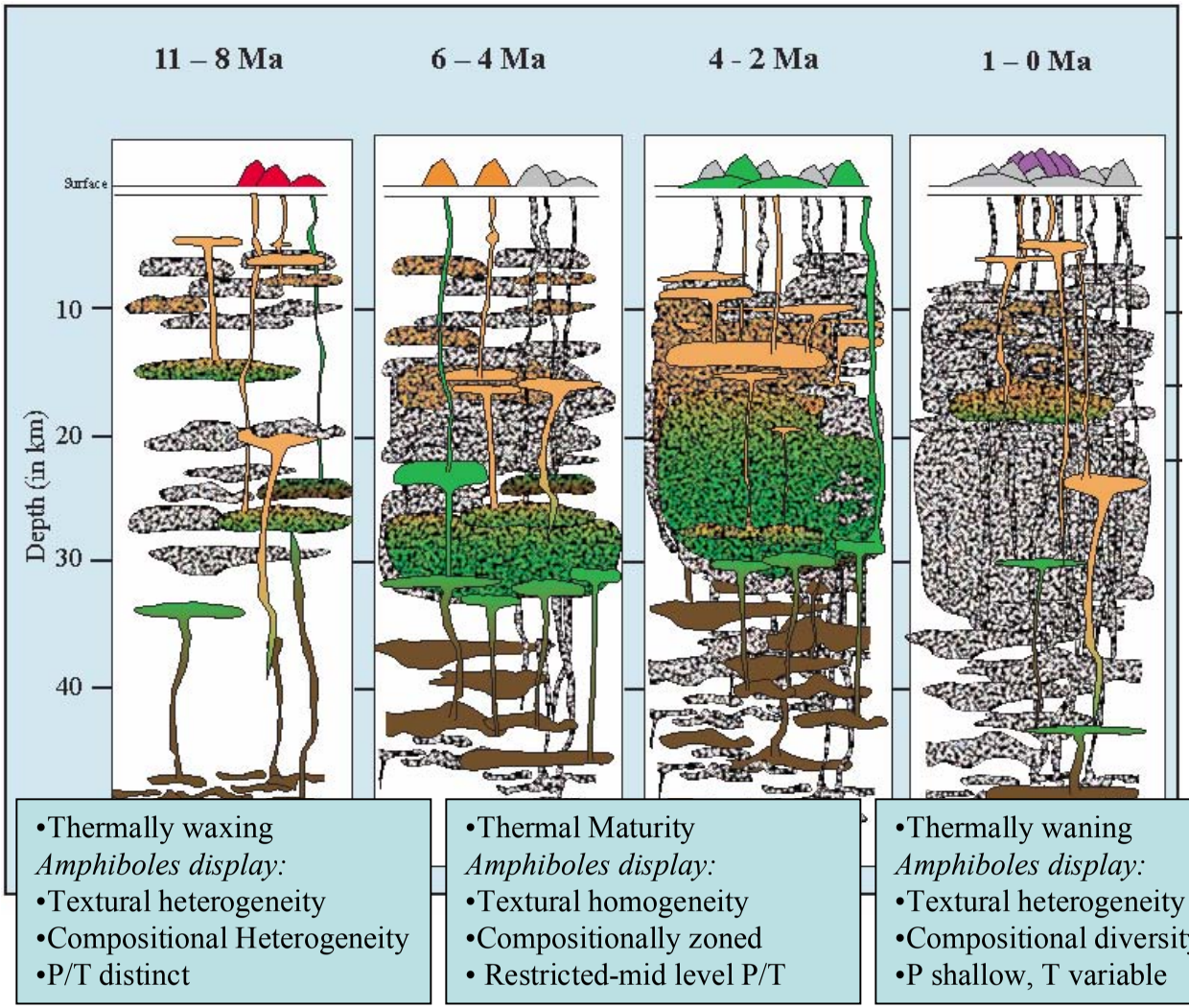


**Figure 35.**
**Model of the evolution of the AVC.**
Model of the AVC system at depth through time. F increases throughout the life of the system. Over time, the system evolves from having high thermal contrast accompanied with compositional and textural diversity in amphiboles. As the system reaches thermal maturity, amphiboles become compositionally zoned, and erupt from a similar area within the crust. At the time of Volcan Aucanquilcha, only shallow dacites are being erupted, and textural heterogeneity has returned.

Early eruptions sample diverse reservoirs with distinct pressure and temperature regimes. Over time, as the crust is heated by successive batches of magma, thermal contrast in the crust decreases and dacite bearing amphiboles erupt from a limited pressure and temperature range. These observed evolution implies either 1) the presence of a large magma chamber to feed the large volume eruptions of the Polan Group that is relatively homogeneous, or 2) a zone of mature crust-treated by repeated injections of material in which the resultant magmatic processes result in an end-product that is compositionally homogenous.

# REFERENCES


1. Anderson, J.L. and Smith, D.R. 1995. The effects of temperature and f (sub O2) on the Al-in-hornblende barometer. *American Mineralogist,* Issue 5-6, pp.559-549.

2. Bachmann, O. and Dungan, M., 2002. Temperature-induced Al-zoning in hornblendes of the Fish Canyon magma, Colorado. *American Mineralogist* v. 87, no. 8-9, pp. 1062-1076.

3. Bowring, S.A., 2001. U-Pb zircon and titantie systematics of the Fish Canyon Tuff; an assessment of high-precision U-Pb geochronology and its application to young volcanic rocks. *Geochimica et Cosmochimica Acta,* v. 65, Issue 15, pp.2571-2587.

4. Browne, B. L., 2006. The influence of magma ascent path on the texture, mineralogy, and formation of hornblende reaction rims. *Earth and Planetary Science Letters,* v.246, Issue 3-4, pp.161-176.

5. Carroll, M. R., and Wyllie, P. J., 1990. The system tonalite-$H_2O$ at 15 kbar and the genesis of calc-alkaline magmas. *American Mineralogy*, v.75, pp.345-357.

6. Coleman, D.S., Briggs, S., Glazner, A.F., and Northrup, C.J., 2003. Timing of plutonism and deformation in the White Mountains of eastern California. *GSA Bulletin,* v. 115, no. 1, p. 48-57.

7. Coleman, D.S., Gray, W., and Glazner, A.F. , 2004. Rethinking the emplacement and evolution of zoned plutons; Geochronologic evidence for incremental assembly of the Tuolumne Intrusive Suite, California. *Geology,* 32, p. 433– 436.

8. Davidson, J.P., de Silva, S., 1992. Volcanic rocks from the Bolivian Altiplano; insights into crustal structure, contamination, and magma genesis in the Central Andes. *Geology Boulder,* v.12, pp. 1130-1127.

9. Femenias, O., 2006. Calcic amphibole growth and compositions in calc-alkaline magmas; evidence from the Motru dike swarm (Southern Carpathians, Romania). *American Mineralogist*, v. 91, Issue 1, pp.73-81.

REFERENCES (Continued)

10. Gans, P. B., Mahood, G. A., and Schermer. E., 1989. Synextensional magmatism in the Basin and Range province: A case study from the eastern Great Basin. *Geol. Soc. America Special Paper* pp.233-286.

11. Giese P., Scheuber E., Schilling F., Schmitz M. and Wigger P., 1999. Crustal thickening processes in the Central Andes and the different natures of the Moho-discontinuity. *Journal of South American Earth Sciences* v.12, pp.201-220.

12. Glazner, A.F., Bartley, J.M., Coleman, D.S., Gray, W., and Taylor, R.Z., 2004. Are plutons assembled over millions of years by amalgamation from small magma chambers? *GSA Today*, Vol. 14, Issue 4-5, pp.4-11.

13. Grunder, A. L., 1995. Material and thermal roles of basalt in crustal magmatism; case study from eastern Nevada, *Geology Boulder,* v.23, pp.952-956.

14. Grunder, A.L., Klemetti, E.K., McKee, C.M., and Feeley, T.C., 2008. Eleven million years of arc volcanism at the Aucanquilcha Volcanic Cluster, northern Chilean Andes: Implications for the lifespan and emplacement of batholiths. *Transactions of the Royal Society of Edinburgh: Earth Sciences,* v. 97, p. 415-436.

15. Hammarstrom, J.M., and Zen, E. 1986. Aluminum in hornblende; an empirical igneous geobarometer. *American Mineralogist*, Issue 11-12, pp. 1313-1297.

16. Hoefs, J., 2004. Stable isotope geochemistry., Federal Republic of Germany: Springer-Verlag Berlin : Berlin, pp. 201.

17. Holland, T.J.B. and Blundy, J.D., 1994. Non-ideal interactions in calcic amphiboles and their bearing on amphibole-plagioclase thermometry. *Contributions to Mineralogy and Petrology,* v.116, pp.433-447.

18. Holtz, F., Sato, H., Lewis, J., Behrens H. and Nakada, S., 2005. Experimental Petrology of the 1991-1995 Unzen Dacite, Japan; Part I, Phase Relations, Phase Composition and Pre-eruptive conditions. *Journal of Petrology,* Vol. 46, Issue 2, pp.319-337.

REFERENCES (Continued)

19. Klemetti, E., 2005, Constraining the magmatic evolution of the Andean arc at 21S using the Volcanic and petrologic history of Volcán Aucanquilcha, Central Volcanic Zone, northern Chile. *Dissertation, Oregon State University,* pp. 169.

20. Leake, B.E., Woolley, A.R., Arps, C.E.S., Birch, W.D., Gilbert, M.C., Grice J.D., Hawthorne, F.C., Katio, A., Kisch, H.J., Krivovichev, V.G., Linthout, K., Laird, J., Mandarino, J.A., Maresch, W.V., Nickel, E.H., Rock, N.M.S., Schumacher, J.C., Smith, D.C., Stephenson, N.C.N., Ungaretti, L., Whittaker, E.J.W., Youzhi, G. 1997. Nomenclature of amphiboles: report of the subcommittee on amphiboles of the International Mineralogical Association, Commission on new minerals and mineral names. *The Canadian Mineralogist,* v. 35, pp. 219-246.

21. Lipman, P.W., 2007. Incremental assembly and prolonged consolidation of Cordilleran magma chambers: Evidence from the Southern Rocky Mountain volcanic field. *Geosphere 3,* pp. 42– 70.

22. Longo, Anthony, 2005, Evolution of volcanism and hydrothermal activity in the Yanacocha Mining District, northern Peru. *Thesis, Oregon State University.*

23. McKee, C.M., 2002, Volcanology and Petrology of Volcan Miño, Andean central volcanic zone. *Thesis Oregon State University*.

24. Naney, M.T., 1983. Phase equilibria of rock-forming ferromagnesian silicates in granitic systems. *American Journal of Science*, v.10: pp.1033-993.

25. Paterson, S.R., 1995. Bursting the bubble of ballooning plutons; a return to nested diapirs emplaced by multiple processes. *Geological Society of America Bulletin,* v.(11): p. 1380-1356.

26. Rutherford, M.J., and Devine, J.D., 1988. The May 1, 1980 eruption of Mount St. Helens: 3, Stability and chemistry of amphibole in the magma chamber. *Journal of Geophysical Research,* v. 93, no. 11, p. 949-959.

27. Sato, H., 2004. Cl/OH partitioning between hornblende and melt and its implications for the origin of oscillatory zoning of hornblende phenocrysts in Unzen dacite. *Eos, Transactions, American Geophysical Union,* v.85, Issue 47, Suppl.

REFERENCES (Continued)

28. Scaillet, B and Evans, B., 1999. The 15 June 1991 Eruption of Mount Pinatubo. I. Phase Equilibria and Pre-eruption P–T–$fO_2$–$fH_2O$ Conditions of the Dacite Magma. *Journal of Petrology* v.40, no.3, pp.381-411.

29. Sellés Mathieu, D. F., 2006. Stratigraphy, petrology, and geochemistry of Nevado de Longaví Volcano, Chilean Andes (36.2°S). *Département de Minéralogie, Genève*, v.61 pp.103.

30. Sharp, Z. D. 2001. A rapid method for determination of hydrogen and oxygen isotope ratios from water and hydrous minerals. *Chemical Geology,* v. 178, Issue 1-4, pp.197-21.

31. Woerner G, Harmon R.S., Davidson J., Moorbath S., Turner D., McMillan N., Nye C., Lopez-Escobar L., and Moreno H., 1988. The Nevados de Payachata volcanic region, *Bulletin of Volcanology,* v.50 pp.287-303.

32. Zandt, G., 1999. Crustal anisotropy inferred from P-SH conversions from the Altiplano-Puna magma body in the Central Andes. *Eos, Transactions, American Geophysical Union,* v.46, Suppl. pp. 979-978.

33. Zandt, G., Leidig, M.L., Chmielowski, J., Baumont, D., and Yuan, X., 2003. Seismic detection and characterization of the Altiplano-Puna Magma Body, Central Andes, *Pure and Applied Geophysics*, v.160, pp.789-807.

34. Zheng, Y.-F., 1993. Calculation of oxygen isotope fractionation in anhydrous silicate minerals. *Geochimica et Cosmochimica Acta,* Issue 5, pp. 1091-1079.

# APPENDICES

See included CD-ROM.